THE EFFECT OF LIQUID SURFACE TENSION

ON

WIRE MESH ENTRAINMENT SEPARATORS

BY

HERBERT F. SCHROEDER

A THESIS

PRESENTED IN PARTIAL FULFILLMENT OF

THE REQUIREMENTS FOR THE DEGREE

OF

MASTER OF SCIENCE IN CHEMICAL ENGINEERING

AT

NEWARK COLLEGE OF ENGINEERING

Newark, New Jersey
1962

APPROVAL OF THESIS

FOR

DEPARTMENT OF CHEMICAL ENGINEERING

NEWARK COLLEGE OF ENGINEERING

BY

FACULTY COMMITTEE

APPROVED: ______________________

____

____

NEWARK, NEW JERSEY

JUNE, 1962

ACKNOWLEDGEMENTS

The author wishes to express his appreciation to Prof. J. J. Salamone for his help, guidance and thoughtful encouragement throughout this entire research program. Thanks also go to Messrs. R. L. Weeks and R. W. Briant of the Esso Research and Engineering Company for lending and assembling the necessary equipment to carry out this work. A debt of gratitude is owed to Mr. E. H. Poppele of the Otto H. York Company for providing the key piece of equipment, a wire mesh entrainment separator. Thanks also to Mr. G. B. Clarke of the Atlas Chemical Company for his assistance in selecting and providing the proper surfactants. Last but not least, the author expresses deep appreciation to his Gal Friday, Mrs. H. F. Schroeder, for among other things, her many hours of tireless typing.

LIST OF TABLES

APPENDIX

LIST OF FIGURES

APPENDIX

TABLE OF CONTENTS

ABSTRACT

The effect of liquid surface tension on the capacity of a wire mesh entrainment separator was studied. An air-water system was used and the surface tension of the water was reduced through the use of surfactants.

Five test series were run, each with a different surface tension of water. The surface tensions examined covered the range of 30 dynes/cm to 70 dynes/cm. For each test run series, the effect of liquid loading was investigated. Liquid loading rates were varied between 55 and 550 $lbs/hr/ft^2$.

Entrainment separator capacity was found to vary linearly with liquid surface tension. As surface tension decreased, the demister capacity decreased. This correllation held over the entire range of liquid loading rates tested. As liquid loading increased, demister capacity decreased for all the surface tensions examined. The work of a previous investigator using an air-water system was confirmed by the data obtained in one run using plain water without surfactants.

INTRODUCTION

Wire mesh separators have long been acclaimed to be an efficient and economic technique for removing mist entrained in a moving gas stream. In the past ten years, an intensive research effort has been expanded on entrainment studies in two-phase, gas-liquid flow. Wire mist separators have also been studied with the primary objective of establishing better design criteria for demisters.

H owever, very little work has been done on determining the effect of entrained liquid properties on the performance of a demister. Several investigators have acknowledged the fact that properties such as mist droplet size, viscosity, density and surface tension of the entrained liquid, influence the capacity of a demister (1,2,3), but these points have never been pursued.

The purpose of this thesis was to determine the effect of surface tension of the entrained liquid on demister capacity. An air-water system was used for this study. The surface tension of the water was varied by employing surfactants. Five different levels of surface tension were obtained that covered a range from 30 dynes/cm to 70 dynes/cm. For each of these 5 tests the liquid loading was varied between 55 to 550 lbs/hr/ft^2.

This work represents the first step toward understanding the effect of fluid properties on entrainment separators. It is anticipated that future investigations will reveal the effect of other fluid properties and that ultimately, the capacity of a demister for any two-phase, gas-liquid system will be predictable.

REVIEW OF PRIOR WORK

Entrainment studies in two-phase, gas liquid flow have been carried out extensively in recent years. Wicks and Duckler [1] studied the entrainment and energy losses in annular two-phase flow of water and air. Similar work was carried out in England by Anderson and Mantzouranis [2]. Likewise, a fundamental study to provide basic data on flow pattern, pressure drop and liquid entrainment in a pipeline contactor was made by Alves [3].

The Russians have also worked on entrainment. Krasjakova [4] determined entrainment rates by means of a sampling probe extended into the moving gas stream. Budd [5] also employed a sampling technique for determining the amount of entrainment in an air-water system in horizontal flow. Fritzlen [6] extended Budd's work. Independently, Lane [7] and Hughes [8] postulated mechanisms for the generation of entrainment-prone droplets for a gas moving across a liquid surface.

Entrainment is an important consideration in the design of fractionating columns. Souders and Brown[9] discuss the effect of entrainment on fractionating columns. Ten other references on the effect of entrainment on the performance of fractionating columns are given by Carpenter and Othmer [10] in their paper on entrainment removal using wire-mesh separators. In fact, they list thirty-five pertinent references.

Studies aimed at determining the effect of entrainment on the performance of cyclone separators were carried out by Pollak and Work [11]. Eighty-one references are listed in their paper.

Papers written on wire-mesh separators are not as prevalent in the literature. York [12] discussed the application of the wire-mesh separator as an entrainment separator. Carpenter and Othmer [10] also studied this problem. They determined the efficiency of a demister experimentally, and they proposed a mechanism for the capture of the entrainment particles by the wires in the separator. Equations were then developed to enable optimization of the demister design.

Poppele [13] studied the effect of liquid loading on the capacity of two types of wire mesh separators. Reid [14] investigated the effect of inclining the demister at various angles to the gas stream.

Hardly any experimental work was carried out investigating the effect of fluid properties. Qualitative observations on droplet particle size were made by Dappert [15]. No references were found on the effect of surface tension on demister capacity.

THEORY

Perhaps the most popular theory on demister design is discussed both by Poppele [13] and Reid [14]. According to this theory, any demister can be characterized by its "K" factor. This factor is defined as:

$$K = \frac{V}{\sqrt{\frac{\rho_L - \rho_V}{\rho_V}}}$$

V = allowable vapor velocity for minimum entrainment

ρ_L = density of liquid

ρ_V = density of vapor

Poppele and Reid illustrated the importance of the K factor in the design of demisters. Poppele determined the effect of liquid entrainment loading on K, and Reid determined the effect of vapor impact angle on K over a wide range of liquid entrainment loads.

The K factor can be considered to be a measurement of the demister's ability to remove entrained liquid droplets. Every demister has two "K" factors. The first, K critical, is calculated using conditions at the critical point. The critical point is defined as the incipient point where the pressure drop across the demister loses its straight line relationship with air flow rate. (i.e. - a break in the curve.) K flood is defined as the incipient point of liquid break-through.

Both of the K factors must be determined experimentally. The capacity (Kfactor) of a demister is determined by the vapor velocity through the column, the liquid entrainment loading and the fluid properties. It is the purpose of this work to determine the effect of fluid surface tension on the capacity (K factor) of a demister.

The capacity of a demister depends on how well the captured liquid drains back into the test column. Flooding of the demister occurs when an insufficient amount of liquid drains back into the column. It was anticipated that lower surface tension would decrease demister capacity because the liquid would wet the surface of the wires in the demister more readily, and cling to it rather than drain back into the column. Conversely, higher surface tension would probably result in a higher capacity (K factor) because the liquid would not wet the demister as much and would drain back into the column more easily.

EQUIPMENT

An air-water system was used. Air was blown from a Spencer turbo-blower through a surge tank-cooling chamber-mixing barrel combination into a length of 4" dia. pipe containing an orifice meter. From here, the air flowed into the vertical test column that contained an 8" dia. lucite tube. This tube was transparent and contained the crinkled wire mesh entrainment seperator (demister). The system was a once through type operation; the air was not recycled to the inlet of the Spencer blower.

Water was injected into the air stream immediately upstream of the demister. A series of Spraying Systems nozzles were used. The tip of the nozzle was located 5" from the face of the demister. At this position, the spray just covered the entire face of the demister. No water was observed impinging on the side of the lucite column. The appropriate water pumps and rotameters were employed. Manometers were used to measure the pressure drop across the demister and the orifice plate.

Each of these pieces of equipment is described in detail in appendix A. However, a schematic diagram of the entire equipment arrangement is included here in Figure One. Figure Two are photographs of this equipment.

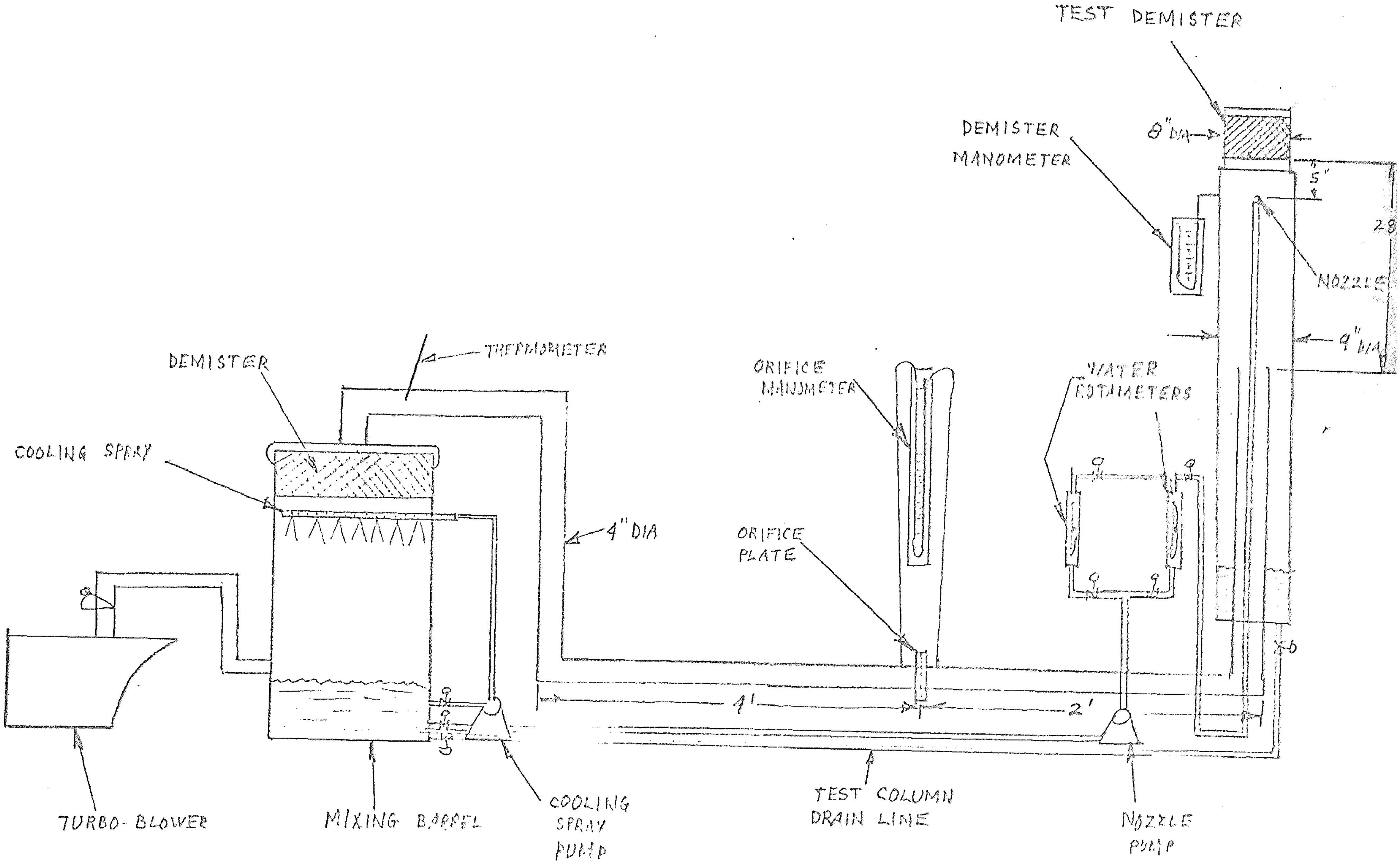

FIGURE 1

SCHEMATIC LAYOUT OF EQUIPMENT

FIGURE 2

Photographs of Equipment

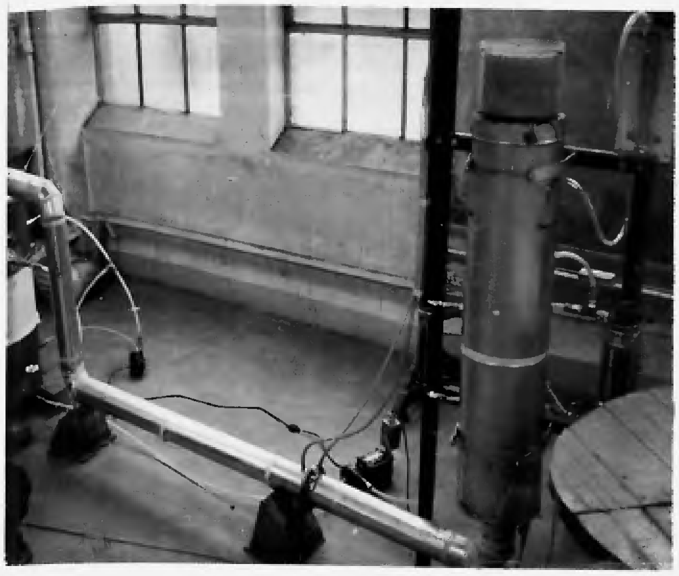

Overall view showing mixing barrel, air duct, orifice plate and test column.

Side view showing test column, orifice plate, manometer, and nozzle water pump.

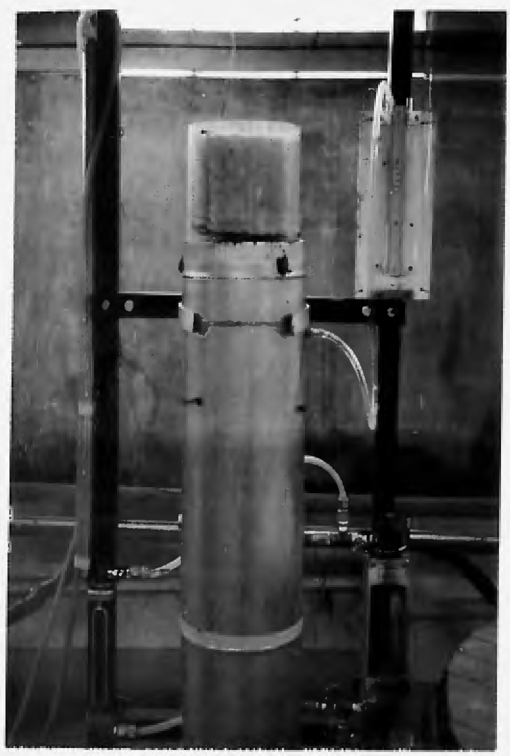

Close-up of column showing demister, demister manometer and water rotameter.

Rear view showing mixing barrel, turbo-blower and cooling water pump.

PROCEDURE

Test Water Preparation

Four of the five curves obtained in this investigation employed surfactants in the test water to lower the surface tension. Hence, the test water preparation step was a most important one.

The mixing barrel was used to prepare the various batches of test water. The maximum amount of water that could be charged into the barrel was 140 lbs., because the water level in the barrel was limited by the location of the air inlet. The surface-active agent was then added in the correct proportion to this sample of water. The concentration of the agent was usually less than 0.01 weight percent. Surface tension was always measured on the spot; before, during and after a test run. A summary of the agents used and the surface tension of the test batch of water that was prepared is shown in Table I.

Table I

Summary of Surfactants and Surface Tension

Run Numbers	Surfactant	Concentration Wt. %	Surface Tension Dynes / cm
7-18	Atlas Renex 20	0.005	47.6
19-30	None	-	69.3
31-42	Atlas Renex 20	0.010	44.8
43-50	Atlas Renex 30	0.012	31.8
51-57	Atlas Renex 20	0.002	58.5

A single batch of test water was used to determine only one curve. When all the necessary data was obtained, the remaining unused portion of the test water was dumped and the entire apparatus was disassembled and rinsed thoroughly.

Surface Tension Measurements

A Denoüy Tensiometer was used to measure the surface tension. (See appendix section A.) All the test dishes and test ring were thoroughly cleaned with a 50-50 mixture of acetone and toluene before each test. The tensiometer was then calibrated with distilled water. At least three samples of test water were taken for each surface tension determination. After the test was completed the samples were submitted to the analytical laboratories of the Esso Research and Engineering Company for a check on the surface tension reading. The laboratory results checked the experimental results very closely. For the first three series of samples, specific gravity and viscosity were also measured. These two properties did not change with the addition of a surface active agent.

Determination of Kcr

Kcr was determined by solving the classic equation,

$$K_{CR} = \frac{V_{CR}}{\sqrt{\frac{\rho_L - \rho_V}{\rho_V}}}$$

The allowable vapor velocity for minimum entrainment (Vcr) at the critical point was obtained by plotting the air flow through the demister against the pressure drop across the demister. The critical air flow is defined as the flow at which the pressure drop across the

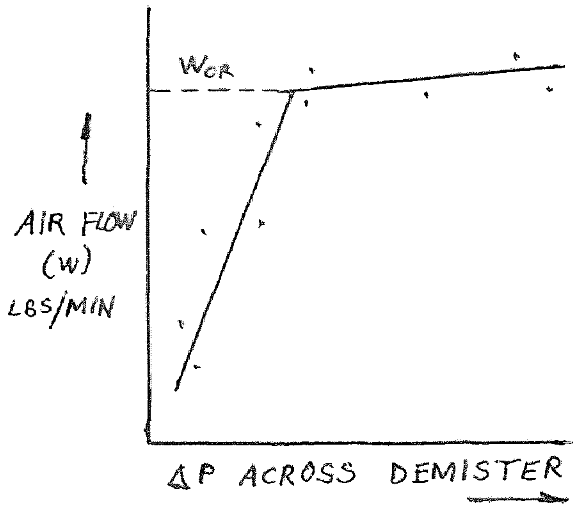

demister is no longer proportional to the air flow. (Bend in curve.) Knowing the density of both fluids, Kcr can then be calculated.

The actual running of the experiment was straight forward. The blower was turned on and the air allowed to heat up to 120°F. The cooling spray was then turned on by starting the small Eastern pump. The air temperature usually was held between 125°F and 140°F. This variation in temperature had absolutely no effect on the demister performance. The spray nozzle pump was then activated and the test was underway.

The following steps were repeated for each test batch of water:

(1) The water flow rate was set on the rotameter.

(2) Air rate was varied by the butterfly valve located in the blower discharge header.

(3) Reading of pressure drop across demister was taken.

(4) A plot of air rate vs. demister ΔP was constructed as each data point was obtained.

(5) Points were obtained at random up or down the curve. No pattern at all was followed. This technique of data collection was a test of the repeatability of the experiment. For each data point,

the ΔP across the orifice and across the demister was recorded. Air temperature and water rate were also recorded.

(6) When sufficient points were obtained to define the curve, Wcr was determined and Kcr was calculated.

Determination of K flood

While still on the same test conditions, K flood was determined. Kf was calculated from the same equation as Kcr except Vf was used instead of Vcr. The flooding velocity (air rate) was determined visually. The water level in the demister was constantly observed. As the water level approached the upper face of the demister, the pressure drop across the demister became erratic. This point was called the incipient flood point. Within a few seconds after the manometer fluid began cycling, the first few drops of liquid could be seen leaving the upper face of the demister. The air flow rate at this point was called Wf and the corresponding velocity (Vf) was used to calculate the flood point.

After determining Kcr and Kf, the water rate was changed and the entire procedure was repeated. A test run series was not completed until a sufficient number of points at different water rates was obtained to cover the range between 55 and 550 $lbs/hr/ft^2$. In some test run series, twenty points were necessary to define the line where as other series may have required only five or six points.

A plot of Kcr vs. water rate and Kf vs. water rate was made. A cross plot of Kcr and Kf vs. surface tension was then made by plotting the average valves of Kcr and Kf. From this plot, the influence of surface tension of the all important K factor for demisters was determined.

DISCUSSION OF RESULTS

The results of the experiment can be divided into three phases:

(1) Test Runs - to determine Wcr and Wf

(2) Test Run Series - made up of several test runs, all with the same surface tension, to determine effect of liquid loading on Kcr and Kf.

(3) Cross - plot of surface tension versus Kcr and Kf

Each of these phases will be discussed in order and then a final discussion on accuracy and reproducibility of the data will be presented.

Test Runs

Fifty seven runs were made. All the primary data for these runs are included in appendix section B. A sample calculation for determining Wcr and Wf is also included. For each run, a plot of air rate vs. demister ΔP was made. All these graphs also appear in appendix section B.

All the plots of W vs. demister gave sharp, clear-cut break points. Both the portion of the curve below and above this critical point gave straight lines. It was not at all difficult to draw the curve and determine the critical point. This sharp break in the curve was also observed by Poppele (13) and Reid (14). They did, however, run into smooth-flowing-type curves at low water flow rates. In this investigation, low flow rates were not examined, the lowest liquid loading employed being 55 lbs/hr/ft^2.

The data were repeatable. As mentioned in the procedure section, the curves were built with absolutely no pattern. In one run, the curve may have been built by going up in air flow rate, in other runs the opposite was true. In most of the runs, the curves were built by skipping from high to low air rates without rhyme or reason. Regardless of the manner in which the curve was built, the same curve was obtained for a given test run. In several runs, checks on the data were made after the curve was completed. All the check points fell on the original curve.

Test-Run Series

Five test run series were made. A test run series consisted of, on the average, ten or eleven test runs. Each test run series was made with a different batch of test water with a different surface tension, and covered the liquid loading range from 55 to 550 $lbs/hr/ft^2$.

The five test run series employed different batches of test water with the following surface tensions:

Series No.	Run No.	Surface Tension
1	7-18	47.6 Dynes/cm
2	19-30	69.3 Dynes/cm
3	31-42	44.8 Dynes/cm
4	43-50	31.8 Dynes/cm
5	51-57	58.5 Dynes/cm

The data from these series are plotted as Kcr vs. liquid loading in figure 3.

Series No. 2 consisted of runs using straight water. No surfactant was used and the surface tension was 69.3 dynes/cm. Since the demister used throughout this experiment was the same as Poppele used, Series No. 2 data should check his data. It did. The demister capacity (Kcr) was found to decrease as liquid loading was increased. The slope of the line was about the same and the absolute quantity of Kcr for any particular liquid loading rate was within 6% of Poppele's results. The scatter in the data was about the same spread that Poppele encountered. √

All of the other series followed the same pattern. Kcr decreased with increasing liquid loading and the data scatter was about the same. In fact, the lines plotted for each series of surface tensions were almost parallel.

The difference in surface tensions between series No. 1 (47.6 dynes/cm) and series No. 3 (44.8 dynes/cm) was not enough to yield two significantly different curves. Therefore, a single line was drawn through all these points.

The most important observation from these data is the orderly fashion the different series plotted with regard to surface tension. The series with the highest surf ce tension had the highest Kcr. (Series No. 2.) The series with the lowest surface tension had the lowest Kcr. (Series No. 4.) The other series were in between in approximately the right position.

Figure 4 is a similar plot for the flood point. The same type of results were obtained, however, the spread in the data was greater. This was caused by the visual method used to determine the flooding air rate.

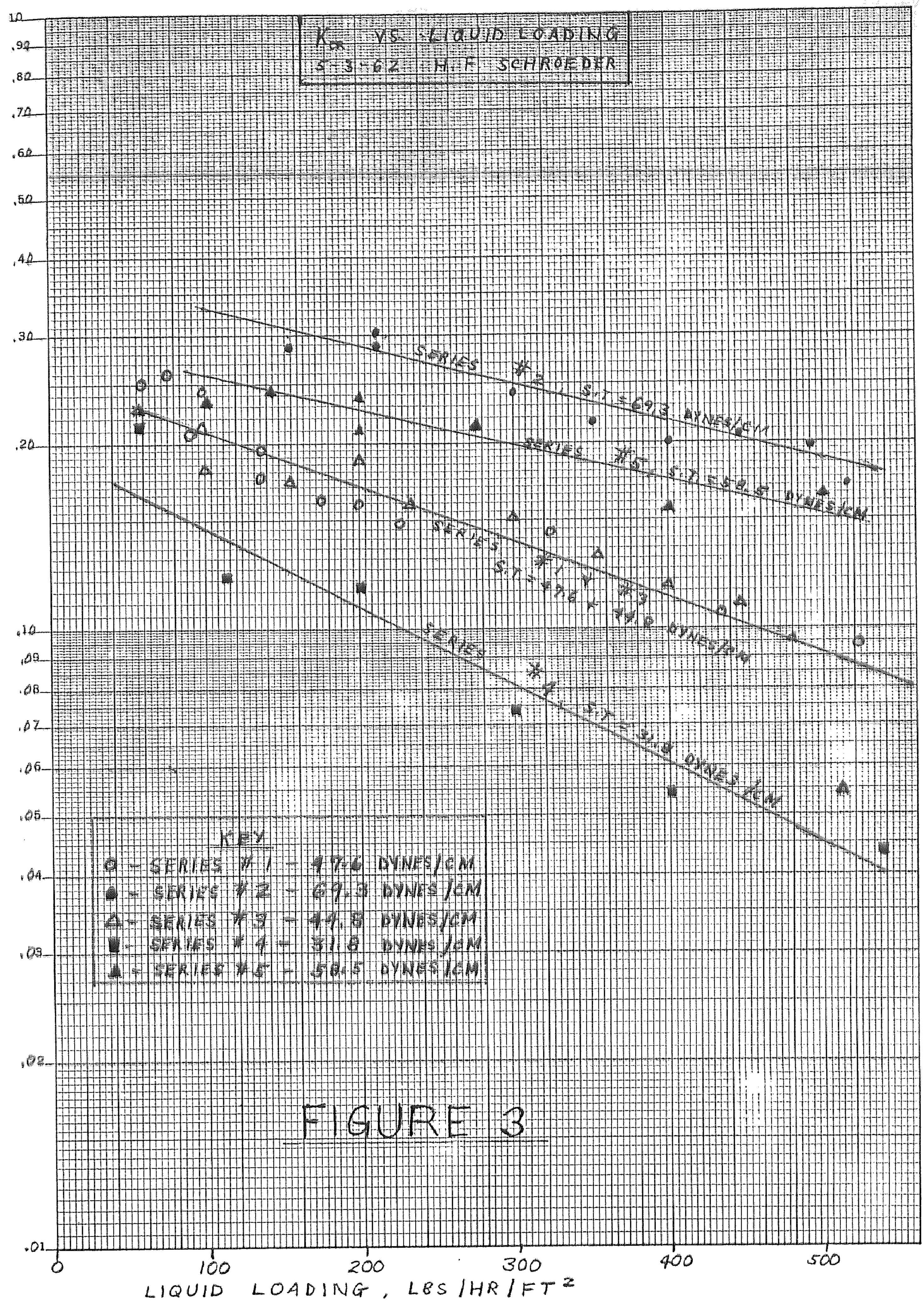

K_{ca} VS LIQUID LOADING
5-3-62 H. F. SCHROEDER
SERIES #2, S.T. = 69.3 DYNES/CM
SERIES #5, S.T. = 58.5 DYNES/CM
SERIES #1 & #3
S.T. = 47.6 & 44.8 DYNES/CM
SERIES #4, S.T. = 31.8 DYNES/CM
KEY
○ - SERIES # 1 - 47.6 DYNES/CM
● - SERIES # 2 - 69.3 DYNES/CM
△ - SERIES # 3 - 44.8 DYNES/CM
■ - SERIES # 4 - 31.8 DYNES/CM
▲ - SERIES # 5 - 58.5 DYNES/CM
1.0
.90
.80
.70
.60
.50
.40
.30
.20
.10
.09
.08
.07
.06
.05
.04
.03
.02
.01
0
100
200
300
400
500
LIQUID LOADING, LBS/HR/FT²

FIGURE 3

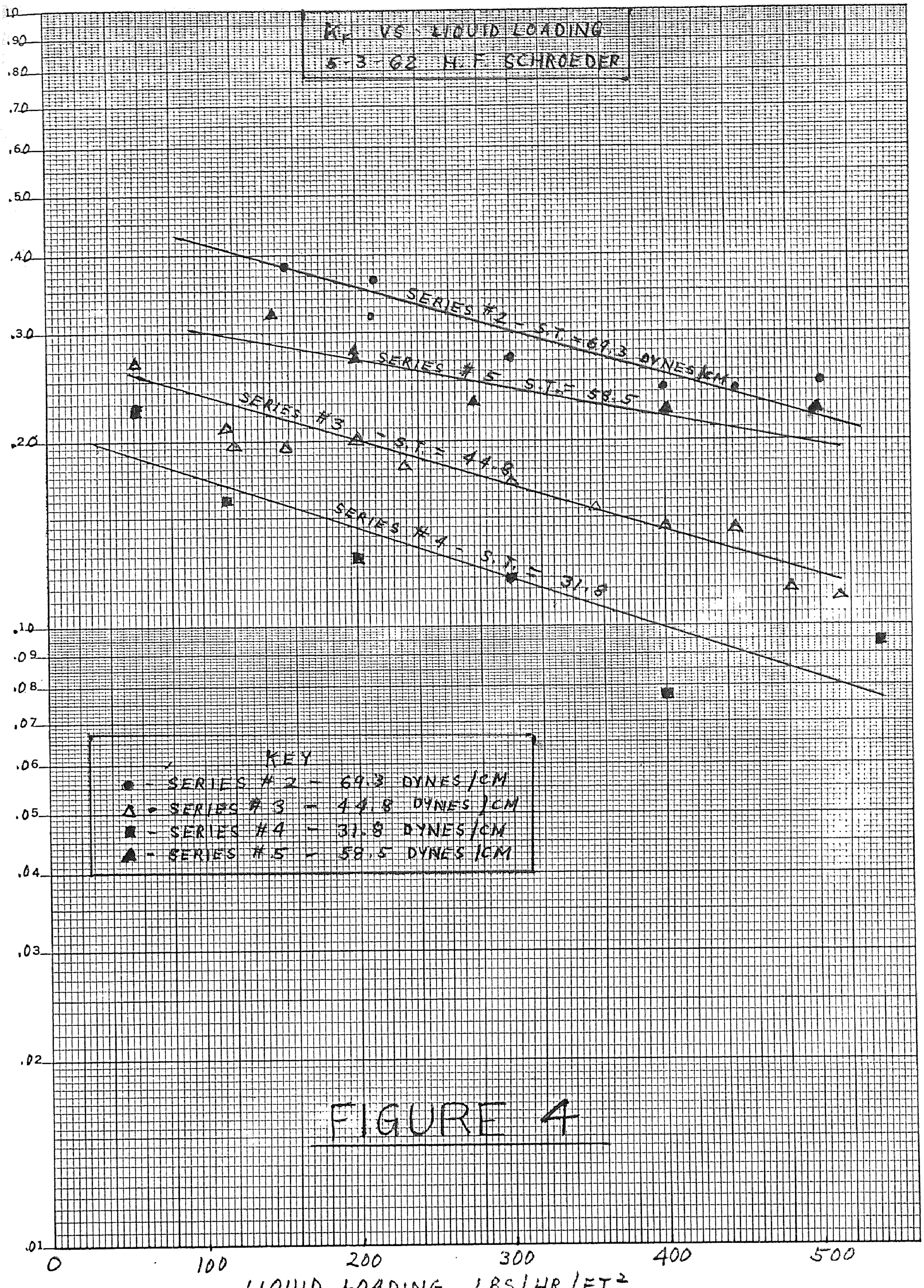
K_F VS LIQUID LOADING
5-3-62 H.F. SCHROEDER
SERIES #2 - S.T. = 69.3 DYNES/CM
SERIES #5 S.T. = 58.5
SERIES #3 - S.T. = 44.8
SERIES #4 - S.T. = 31.8
KEY
● - SERIES #2 - 69.3 DYNES/CM
△ - SERIES #3 - 44.8 DYNES/CM
■ - SERIES #4 - 31.8 DYNES/CM
▲ - SERIES #5 - 58.5 DYNES/CM
1.0
.90
.80
.70
.60
.50
.40
.30
.20
.10
.09
.08
.07
.06
.05
.04
.03
.02
.01
0
100
200
300
400
500
LIQUID LOADING, LBS/HR/FT²

FIGURE 4

Cross-Plot of Surface Tension vs. K

The results presented in figure 3 were cross-plotted against surface tension to determine the effect of surface tension on the demister Kcr factor. To construct this plot, the average line drawn through the points in figure 3 was used to read Kcr for each of three liquid loading rates. Surface tension was then plotted against Kcr for each of the three liquid loading conditions.

This plot can be seen in figure 5. Once again, a straight line function is apparent over the range of surface tension tested. All three of the liquid loading rates displayed this trend. As surface tension decreased, Kcr decreased. The results in figure 4 (Kf vs. liquid loading), were also cross-plotted against surface tension. The resulting plot (figure 6) displayed the same trends as figure 5 except there was wider scatter in the data.

The straight lines of figures 5 and 6 give the following equation:

$$K=m\sigma+b$$, where

K is the demister characterization factor

σ is the surface tension of the water, dynes/cm

m and b are constants for the straight line

The values of the constants m and b for each of the three liquid loading rates for both the critical and flood points are presented in Table II.

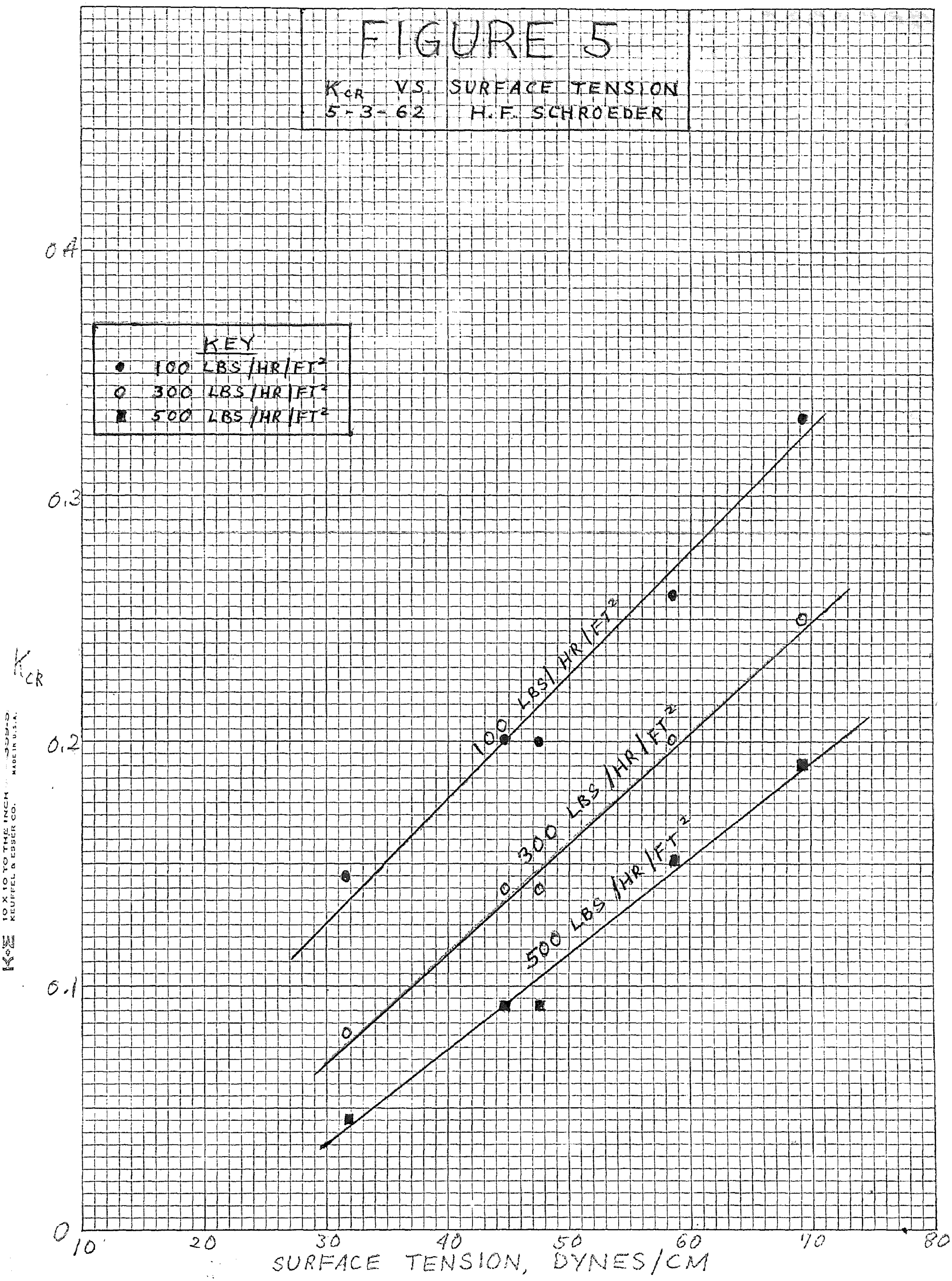
FIGURE 5
K_{CR} VS. SURFACE TENSION
5-3-62 H.F. SCHROEDER
KEY
100 LBS/HR/FT²
300 LBS/HR/FT²
500 LBS/HR/FT²
100 LBS/HR/FT²
300 LBS/HR/FT²
500 LBS/HR/FT²
K_{CR}
0
0.1
0.2
0.3
0.4
10
20
30
40
50
60
70
80
SURFACE TENSION, DYNES/CM
10 X 10 TO THE INCH
KEUFFEL & ESSER CO.
MADE IN U.S.A.

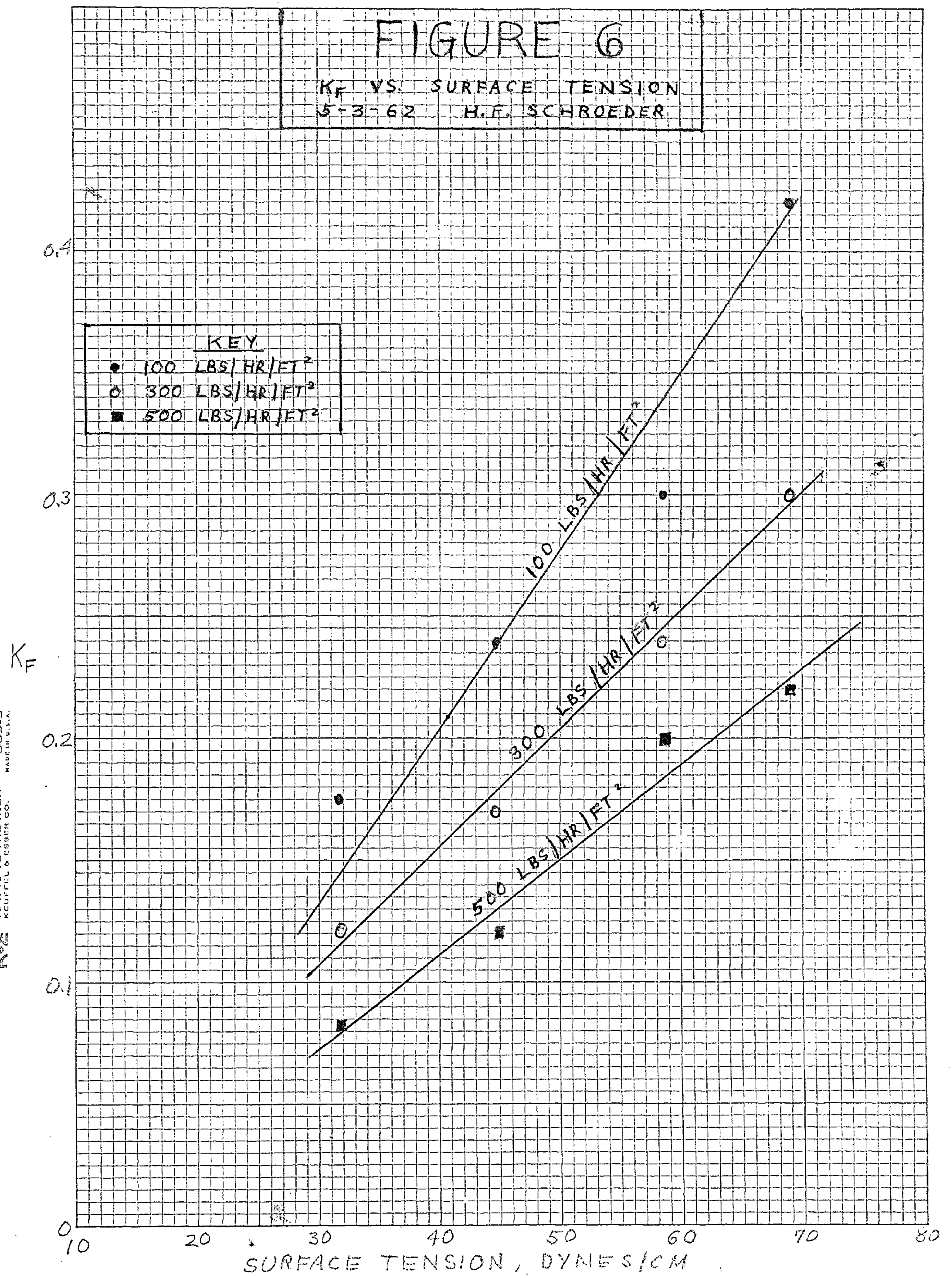
FIGURE 6
K_F VS. SURFACE TENSION
5-3-62 H.F. SCHROEDER
KEY
● 100 LBS/HR/FT²
○ 300 LBS/HR/FT²
■ 500 LBS/HR/FT²
100 LBS/HR/FT²
300 LBS/HR/FT²
500 LBS/HR/FT²
K_F
0.4
0.3
0.2
0.1
0
10
20
30
40
50
60
70
80
SURFACE TENSION, DYNES/CM

Table II

Summary of Constants Determined for Equations of K vs. Surface Tension

Liquid Loading Rate	Critical Point		Flood Point	
$lbs/hr/ft^2$	m	b	m	b
100	0.00504	0.025	0.00731	-0.012
300	0.00446	-0.018	0.00480	0.012
500	0.00386	-0.042	0.00388	-0.005

Accuracy and Reproducibility of Data

In the detailed description of equipment in appendix section A, it is mentioned that the accuracy of the orifice meter is $\pm$ 2% because of the short straight run of pipe on both sides of the orifice plates. This $\pm$ 2% accuracy represents the maximum error in the experiment. The water rates were extremely accurate and the reading of pressure drop across the demister was very consistent. (Except at point of incipient flooding.)

The reproducibility of the test data was checked by attempting to duplicate several individual test runs. For example, in series No. 2 the test run at 210 $lbs/hr/ft^2$ was repeated. Kcr's of 0.29 and 0.30 were obtained. The percent error is $\frac{0.30-0.29}{0.30} \times 100 = 3.33\%$. Since this error is within the $\pm$ 2% accuracy of the orifice calibration, the data was considered to be reproducible.

In the last test series (No. 5), the scatter in the data seemed to be greater than usual. The same type of reproducibility test was run and the discrepancy was found to be 12% which is much greater than the $\pm$ 2% accuracy of the orifice. These data were therefore not considered exactly reproducible. It is noted in figure 3 that the series No. 5 line is the only one that is not parallel. One explanation for these slightly poorer results, is that the demister was contaminated with other surfactants for this last test, even though all the equipment was thoroughly rinsed with clean water. For maximum reproducibility of the data, the equipment should be cleaned with an appropriate solvent.

CONCLUSIONS

Based on these results the following conclusions are reached:

(1) The work of Poppele has been confirmed for York style No. 421 demister.

(2) K decreases as liquid loading is increased for all surface tensions examined (30 to 70 dynes/cm.)

(3) K decreases at the same rate for increased liquid loading for all surface tensions examined.

(4) K varies linearly with liquid surface tension, as surface tension decreases, K decreases.

RECOMMENDATIONS

This investigation represents a step toward understanding the effect of fluid properties on the performance of wire mesh entrainment separators. A lot more work needs to be done. The effect of surface tension should be explored even further. Exotic surfactants capable of reducing the surface tension of water below 20 dynes/cm should be sought out. A much wider range of surface tensions could thus be examined using an air-water system. At the time of this writing, an agent was discovered in the literature that is capable of reducing the surface tension of water to about 15 dynes/cm. It was developed by the Minnesota Mining and Manufacturing Company and is their new "fluorochemical surfactant".

The next step toward understanding the effect of surface tension would be to examine two-phase systems other than air and water. It may turn out, for example, that the interfacial tension between a vapor and its entrained liquid is an important variable.

After surface tension has really been pinned down, fluid viscosity should be studied. Mist droplet size must then be examined. Perhaps a spinning-disc atomizer could be employed to give uniform particle size. [16, 17] A magnetically vibrated wire placed over the opening of a capillary was found to produce uniform droplets by Parker and Grosh. [18] This paper contained a bibliography on droplet formation and measurement.

Finally, a correlation must be found between all these variables and their effects on demister capacity. The correlation should be supported by a set of experiments designed by statistical techniques. Perhaps, a factorial or latin-square type experiment would suffice.

Only when this work is accomplished; will the all-important K factor for demisters be predictable from an equation rather than determined empiracally.

APPENDIX A

DETAILED DESCRIPTION OF EQUIPMENT

Turbo-Blower

A Spencer Turbo-Compressor model No. 5010-H was used. It had a maximum output of 250 scfm against a head of 80 oz/in^2. The motor driving the blower was rated at 10 horsepower at 3500 RPM. The unique feature of this Spencer blower was the linear relationship between the amperes drawn by the motor and the volume of air delivered. As the control valve was opened allowing more air to be delivered, the amperage increased. If for any reason the output of the blower exceeded the rated 250 scfm (leaks in the system or not enough back pressure), the circuit breaker tripped and protected the motor against excessively high amperage. In order to prevent blower shut-downs, the seams of all the sheet metal pipe were taped.

Surge Tank - Cooling Chamber - Mixing Barrel Combination

A 55 gal. drum served three purposes:

1) Air surge tank

2) Air cooling chamber

3) Liquid mixing and storage tank

The air surge tank was needed to smooth out the delivery of high volume air. All vibrations and flow pulsations were entirely eliminated with this tank. The manometerfluid in the orifice manometer was usually always steady. Flow readings were therefore easily and accurately obtained.

The cooling chamber was used to cool and humidify the air being blown through the system. A water sprayer located directly above the air inlet consisted of two 2 ft. lengths of stainless steel tubing with 1/32" diameter holes drilled in the bottom. These "shower heads" were mounted horizontally in the barrel 90° apart.

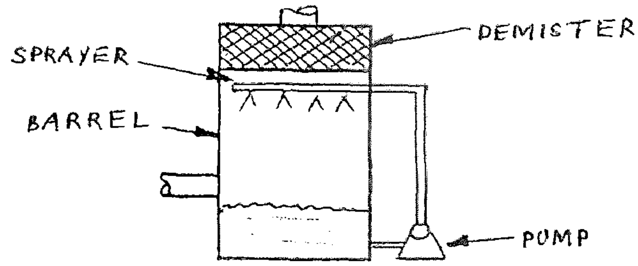

Water was pumped from the bottom of the barrel to the sprayer by an Eastern Industries pump model No. 8-1 Type 150. The spray from both shower heads appeared to completely fill the barrel. Unfortunately, 100% saturated air could never be obtained because of the high temperature of the air. However, 50% relative humidity was usually obtained. A York demister 22" in diameter and 6" thick was installed at the top of the barrel to remove any liquid that may have become entrained by the violently mixing air and water streams. See figure A-3 of this appendix section.

The third feature of this important piece of equipment is the storage and mixing facilities it affords. The water used in the test was usually mixed with a surfactant in this tank. The test fluid was also stored in the tank and used as needed. The tank had a maximum storage capacity of 140 lbs. because of the location of the air inlet.

<u>Orifice Plates</u>

The orifice plates used were made and installed in accordance with the standards set forth in "Use of Orifice Meters", Process Engineering Department, Standard Oil Development Company, Report No. PE 2M44.

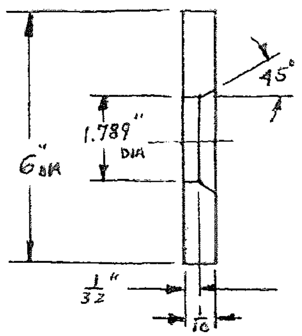

SMALL ORIFICE

$\beta = 0.446$

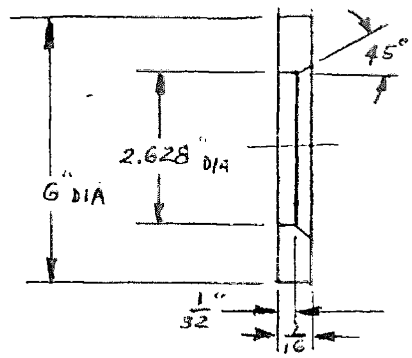

LARGE ORIFICE

$\beta = 0.657$

The orifice diameters were calculated using the classic flow equation in Perry's Handbook. Two plates were required because of the wide range of flow rates anticipated. A final check indicated $0.20 < \beta < 0.75$, so these diameters were acceptable. The small orifice is particularly suited for low air flow measuring since $0.20 < \beta < 0.50$. The discharge coefficients were obtained from the same Esso manual using flange taps.

The plate thickness of 1/16" is the minimum recommended thickness for pipe sizes up to 4" diameter. The leading edge thickness also conforms with the specs since it does not exceed 1/50 of the internal pipe diameter, 1/8 of the orifice diameter, or 1/4 of the dam height.

Flange taps were used primarily to eliminate the necessity of applying a correction factor for the mislocation of vena contracta taps when the orifice plates were changed. They are also easier to install and are less subject to errors of installation. The center of the upstream tap is located exactly 1" from the upstream face of the plate, and the center of the downstream tap is located 1" from the downstream face.

Unfortunately, the required length of straight pipe upstream of the orifice for maximum accuracy was impractical. (50 internal pipe diameter.) However, since ± 2% accuracy was acceptable, it was decided to use the shorter lengths set forth by the minimum requirements of the standards (without straightening vanes.) The minimum distance upstream and downstream from the orifice for an elbow, tee or cross is a function of β, the ratio of orifice diameter to pipe diameter. The limiting β was for the large orifice. For $\beta = 0.5$, the minimum required distance upstream is 6.8 pipe diameters. (for flange taps.) For a 4" diameter pipe, this minimum distance is 28". Actually, the upstream elbow is 48" from the orifice. The minimum required distance to a downstream elbow is 3.6 diameters or 14.5" from the orifice. Once again, the orifice is installed well within the limits for ± 2% accuracy since the distance to the downstream elbow is 24".

The orifice calibration curves are included as figures A-1 and A-2 of this Appendix Section.

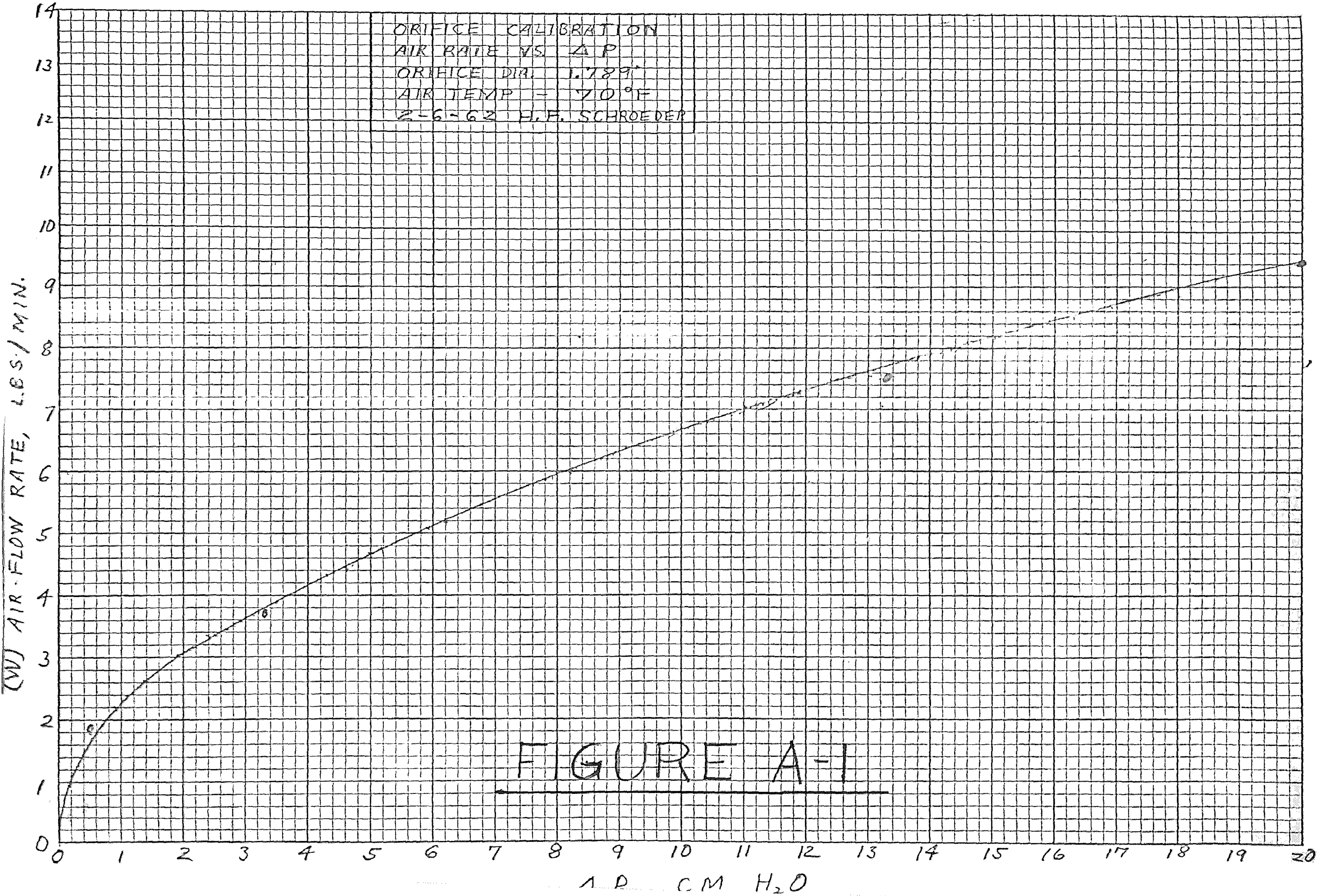
ORIFICE CALIBRATION
AIR RATE VS. ΔP
ORIFICE DIA. 1.789"
AIR TEMP - 70°F
2-6-62 H.H. SCHROEDER
(VV) AIR·FLOW RATE, LBS/MIN.
ΔP CM H2O
0
1
2
3
4
5
6
7
8
9
10
11
12
13
14
15
16
17
18
19
20

FIGURE A-1

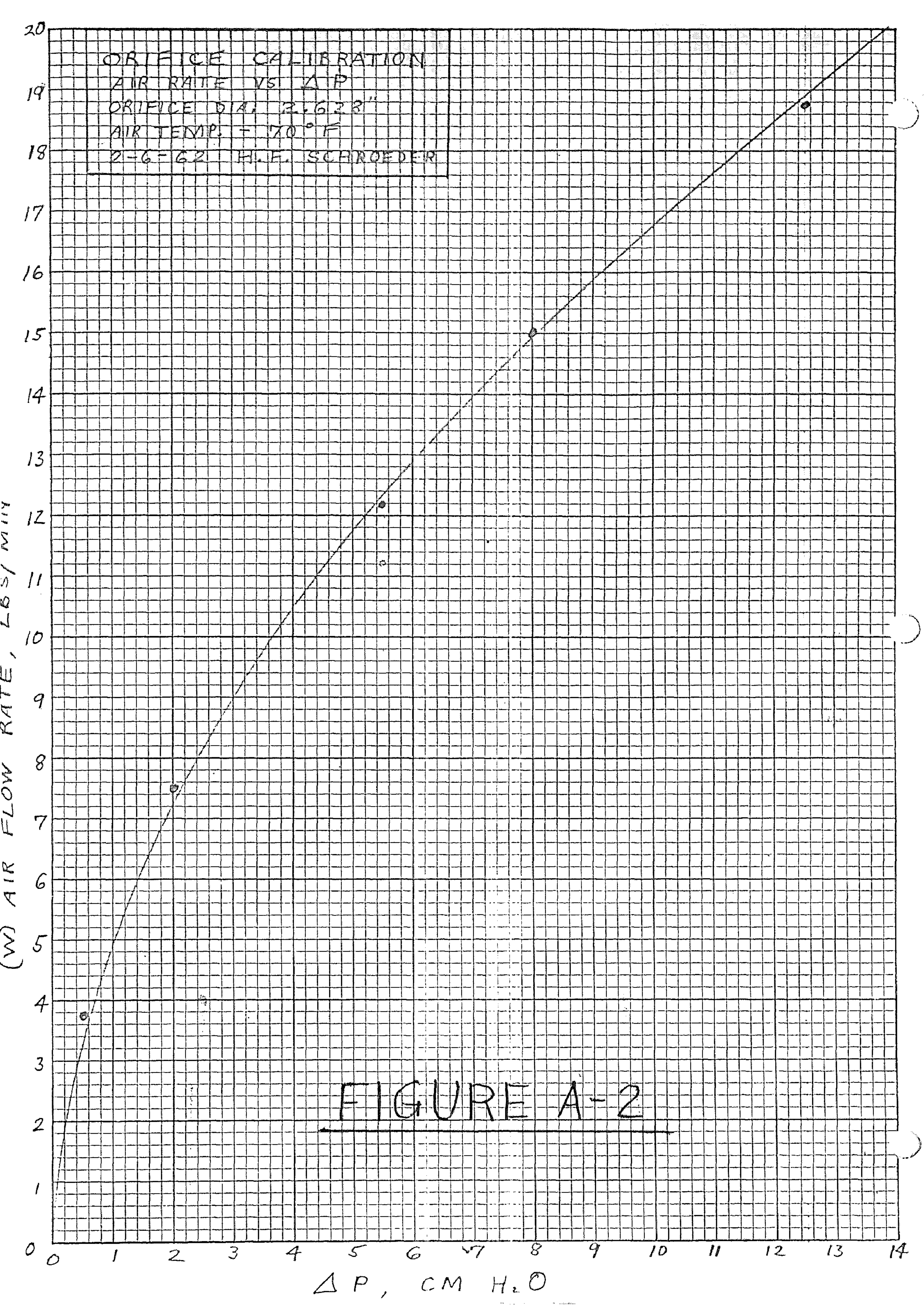
ORIFICE CALIBRATION
AIR RATE VS ΔP
ORIFICE DIA. 2.628"
AIR TEMP. = 70° F
2-6-62 H.F. SCHROEDER
(W) AIR FLOW RATE, LBS/MIN
ΔP, CM H_2O
0
1
2
3
4
5
6
7
8
9
10
11
12
13
14
15
16
17
18
19
20

FIGURE A-2

Test Demister

A York demister, model No. 421 was used for the test. It has a mesh density of 12.0 lbs/ft^3 and a wire surface area of 132 ft^2/ft^3. This demister is exactly the same style as used by Poppele in his investigations. The demister was 8" in diameter by 6" thick. See figure A-3.

Water Handling Equipment

Nozzles made by the Spraying Systems Co. were used to spray the test water into the moving air stream. The nozzles were located 5" below the bottom face of the demister. At this position, the spray was observed to completely cover the demister without impinging off the side of the lucite test column. The nozzle was axial

Nozzle	Range of Flow Rate
AN-8	55 to 135 $lbs/hr/ft^2$
AN-14	100 to 220 $lbs/hr/ft^2$
G-3	220 to 550 $lbs/hr/ft^2$

to the flow of air and centered in the air stream.

An Eastern Industries pump model No. D-11, type 100 was used to pump the test water from the mixing barrel to the nozzle. The capacity of this pump was about 20 gph against a head of 15 psig.

Two rotameters connected in parallel were used to cover the range of flow rates. The smaller rotameter was capable of measuring water rates from 50 to 90 $lbs/hr/ft^2$. It was a 1/4" Fischer-Porter instrument, tube No. 2F - 1/4 - 25 - 5/70 with a sapphire float. The larger rotameter covered a range of 100 to 550 $lbs/hr/ft^2$. (Only 50% of

FIGURE A-3

Photograph of Demisters

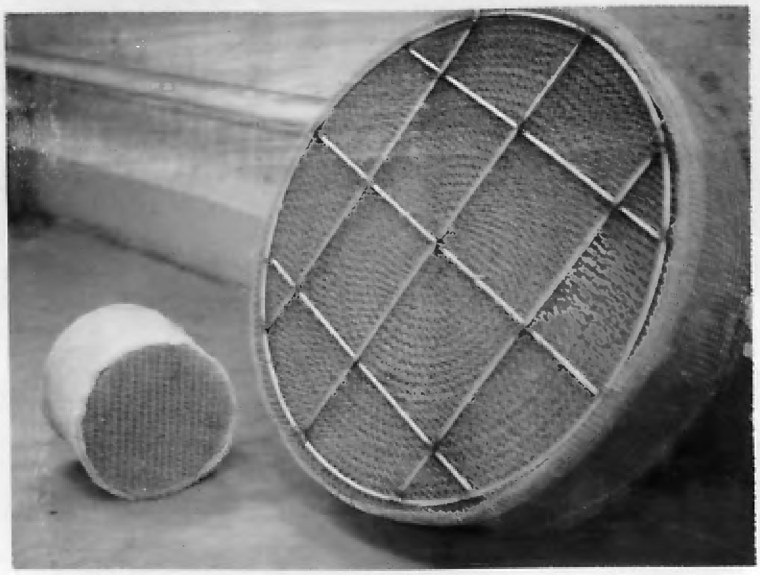

Left - Test Demister, 8" Dia. X 6"

Right - Mixing Barrel Demister 22" Dia. X 6"

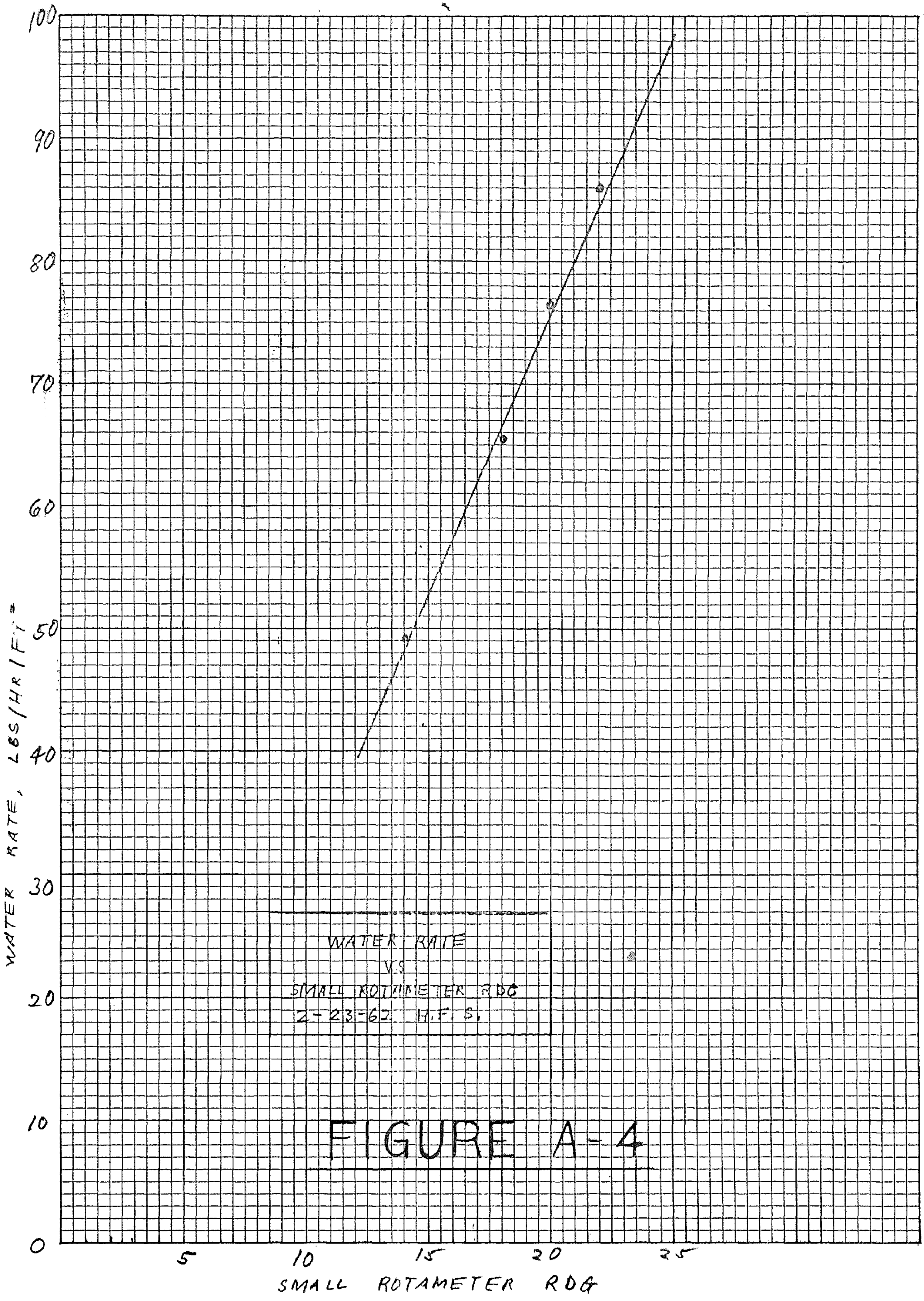
WATER RATE, LBS/HR/FT²
SMALL ROTAMETER RDG
0
10
20
30
40
50
60
70
80
90
100
5
10
15
20
25
WATER RATE
VS
SMALL ROTAMETER RDG
2-23-62 H.F.S.

FIGURE A-4

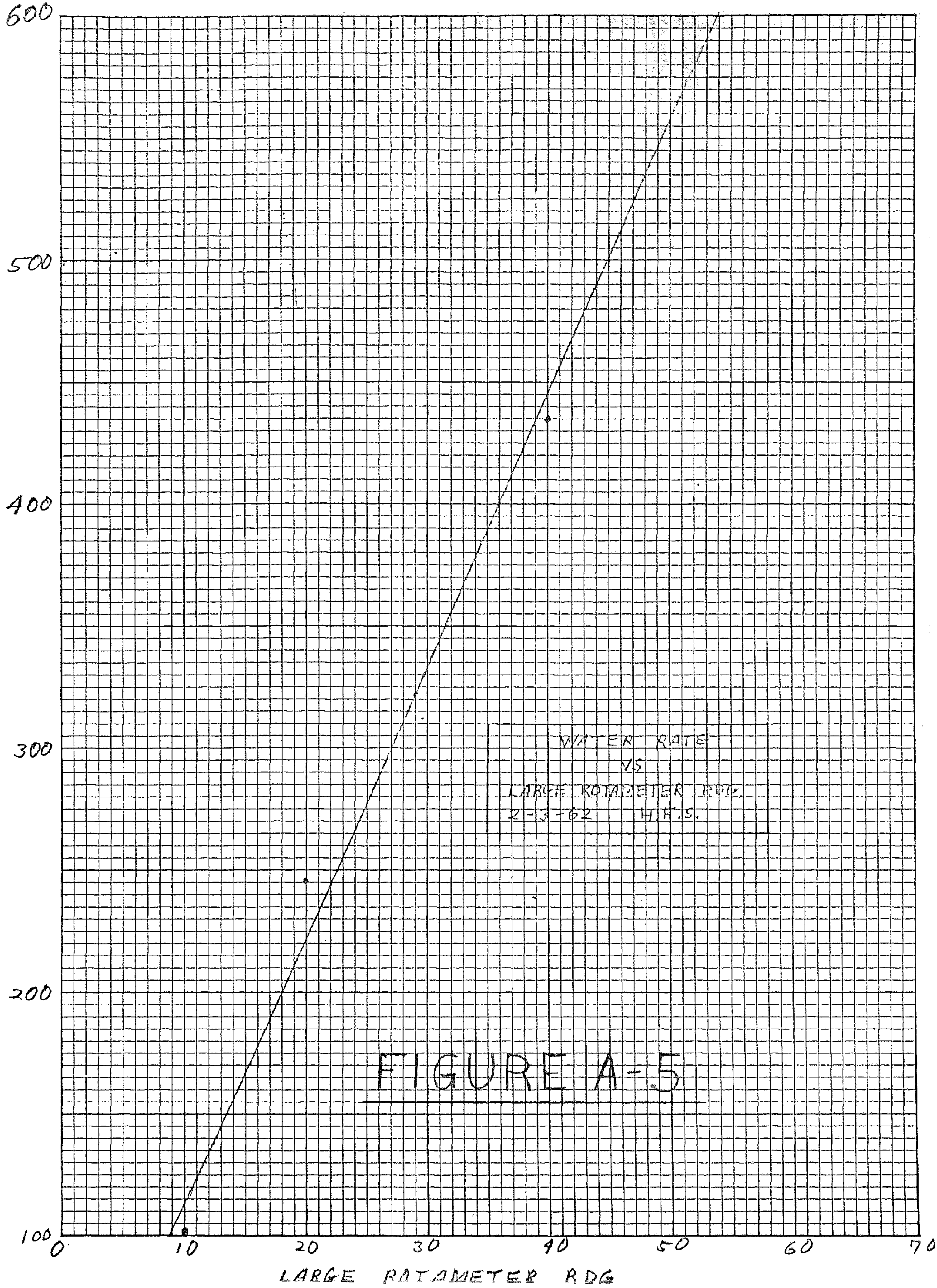

600
500
400
300
200
100
0
10
20
30
40
50
60
70
LARGE ROTAMETER RDG
WATER RATE
VS
LARGE ROTAMETER RDG.
2-3-62 H.F.S.

FIGURE A-5

rotameter capacity needed.) This rotameter consisted of Fischer-Porter tube No. B4-27-5/77 with a stainless steel float.

Tensiometer

Surface tension measurements were made with a Denoüy Interfacial Tensiometer. This precision direct reading model (model No. 70545) measures surface and interfacial tension by the ring method. The ring was model No. 70542 made of platinum. It had a mean circumference of 5.991 cm and an R/r of 54. Both the tensiometer and the ring was cleaned immediately before a test with a 50-50 mixture of acetone and toluene. A photograph of this equipment can be seen in figure A-6.

FIGURE A-6

Photograph of Tensiometer

APPENDIX B

PRIMARY DATA TABLES AND TEST RUN PLOTS OF AIR RATE VS. DEMISTER ΔP

Symbols Used in Tables

Po - Pressure drop across orifice, cm H_2O.

Ps - Static pressure upstream of orifice, cm H_2O.

T - Air temperature upstream of orifice, $^{\circ}F$.

Po - Pressure drop across demister, cm H_2O.

F - Flood point

Run No.	- 7
Nozzle	- AN - 8
Water Rate	- 60 lbs/hr/ft^2
Surface Tension	- 47.6 Dynes/cm
Orifice	- 2.628" Dia.

Δ Po	Ps	T	W	Δ Pd
1.4	1036	110	5.78	0.5
3.3	1038	110	9.08	0.8
6.8	1048	118	13.33	6.7
3.7	1039	124	9.15	1.3
3.0	1038	124	8.58	0.9
2.0	1037	122	6.98	0.5
5.0	1041	122	11.31	1.7
3.6	1039	122	9.45	1.2
4.8	1041	124	11.00	1.9
4.0	1039	122	10.03	1.4
4.5	1040	126	10.61	1.8
5.7	1044	126	12.08	4.0
5.1	1042	130	11.32	3.3
6.0	1045	130	12.30	4.8

Sample Calculation

Wcr = 10.8 lbs/min

$$\rho = 0.075 \times \frac{530}{585} \times \frac{1040}{1034} = 0.0684 \frac{\text{lbs}}{\text{ft}^3}$$

$$V = \frac{10.8}{.0684 \times 20.88} = 7.56 \text{ ft/sec}$$

$$K = \frac{V}{\sqrt{\frac{\rho_l - \rho_v}{\rho_v}}} = \frac{7.56}{\sqrt{\frac{62.4 - .0684}{.0684}}} = 0.250$$

Run No. - 8
Nozzle - AN - 8
Water Rate - 77 lbs/hr/ft^2
Surface Tension - 47.6 Dynes/cm
Orifice - 2.628" Dia.

ΔPo	Ps	T	W	ΔPd
2.8	1038	122	8.29	0.8
3.7	1039	122	9.65	1.0
5.0	1041	126	11.31	1.9
4.5	1040	128	10.60	1.5
4.0	1039	128	9.96	1.4
5.6	1045	128	11.90	5.6
5.4	1043	128	11.69	3.2
4.8	1041	128	11.11	2.4

Run No. - 9
Nozzle - AN - 8
Water Rate - 99 lbs/hr/ft^2
Surface Tension - 47.6 Dynes/cm
Orifice - 2.628" Dia.

ΔPo	Ps	T	W	ΔPd
2.0	1037	118	6.90	0.6
2.7	1038	118	8.15	0.8
3.3	1038	120	9.04	1.0
4.4	1040	124	10.52	1.6
5.6	1044	126	11.90	4.0
4.9	1044	128	11.12	5.5
4.4	1041	128	10.52	2.6
5.6	1043	128	11.88	3.3
4.7	1042	128	10.92	3.4

Run No. - 10
Nozzle - AN - 8
Water Rate - 135 lbs/hr/ft^2
Surface Tension - 47.6 Dynes/cm
Orifice - 2.628" Dia.

ΔPo	Ps	T	W	ΔPd
2.4	1037	126	7.63	0.8
3.3	1040	122	9.05	2.8
2.3	1038	124	7.44	1.2
2.8	1040	124	8.25	2.7
2.6	1038	124	7.96	1.4
3.4	1041	124	9.19	3.8
1.1	1036	128	4.95	0.5
2.2	1037	124	7.25	0.7
1.4	1036	122	5.64	0.6
3.0	1040	122	8.63	3.1

Run No. - 11
Nozzle - AN - 14
Water Rate - 90 lbs/hr/ft^2
Surface Tension - 47.6 Dynes/cm
Orifice - 1.789" Dia.

ΔPo	Ps	T	W	ΔPd
8.3	1043	118	5.94	0.5
10.8	1045	118	6.67	0.6
13.9	1049	117	7.63	0.7
16.2	1051	121	8.20	0.8
18.0	1053	124	8.66	0.9
20.1	1055	124	9.15	1.0
22.4	1060	126	9.66	3.7
21.4	1060	126	9.46	4.8
19.8	1057	126	9.06	2.8
19.4	1055	126	8.99	1.7
19.6	1055	125	9.06	1.7
20.4	1056	124	9.26	2.0
21.8	1059	125	9.56	2.9
20.9	1058	126	9.38	3.0

Run No. - 12
Nozzle - AN - 14
Water Rate - 135 lbs/hr/ft^2
Surface Tension - 47.6 Dynes/cm
Orifice - 1.789" Dia.

ΔPo	Ps	T	W	ΔPd
11.7	1046	122	6.91	0.7
14.6	1049	122	7.76	0.8
16.3	1051	124	8.20	0.9
19.4	1054	124	8.96	1.0
20.1	1057	126	9.16	2.4
20.9	1058	128	9.34	3.5
19.0	1055	128	8.86	1.8
19.0	1055	128	8.86	1.6
18.4	1053	128	8.75	1.4
17.4	1053	128	8.46	1.3
16.7	1052	126	8.29	1.3

Run No. - 13
Nozzle - AN - 14
Water Rate - 175 lbs/hr/ft^2
Surface Tension - 47.6 Dynes/cm
Orifice - 1.789" Dia.

ΔPo	Ps	T	W	ΔPd
11.2	1046	124	6.74	0.6
15.0	1050	124	7.90	0.8
17.0	1055	124	8.41	3.5
14.6	1051	127	7.50	2.1
13.6	1049	126	7.49	1.4
12.4	1048	126	7.12	1.2
8.0	1043	124	6.11	0.6
10.0	1045	124	6.36	0.6
12.0	1047	122	7.04	0.8

Run No. - 14
Nozzle - AN - 14
Water Rate - 200 lbs/hr/ft^2
Surface Tension - 47.6 Dynes/cm
Orifice - 1.789" Dia.

ΔPo	Ps	T	W	ΔPd
8.0	1042	124	5.74	0.4
12.0	1047	124	7.03	0.8
13.0	1050	130	7.27	3.0
12.2	1047	128	7.10	1.2
11.0	1046	128	6.71	1.0
12.1	1048	128	7.08	1.5
13.5	1050	128	7.49	2.9
12.0	1049	129	7.28	1.7
4.0	1038	130	3.98	0.4
6.0	1041	128	4.93	0.5
10.3	1045	123	6.54	0.7

Run - 15
Nozzle - G - 3
Water Rate - 225 lbs/hr/ft^2
Surface Tension - 47.6 Dynes/cm
Orifice - 1.789" Dia.

ΔPo	Ps	T	W	ΔPd
4.0	1039	100	4.09	0.6
8.2	1043	112	5.81	0.7
9.3	1044	114	6.21	0.9
11.1	1047	122	6.74	1.7
10.5	1046	128	6.54	1.2
11.2	1048	130	6.76	2.7
10.4	1046	130	6.50	1.4
5.1	1040	130	4.47	0.6

Run No. - 16
Nozzle - G - 3
Water Rate - 325 lbs/hr/ft^2
Surface Tension - 47.6 Dynes/cm
Orifice - 1.789" Dia.

ΔP_o	P_s	T	W	ΔP_d
2.5	1037	126	3.18	0.3
10.0	1047	120	6.37	2.7
8.8	1045	132	5.94	1.8
7.2	1043	134	5.34	1.5
6.3	1042	132	5.00	1.4
4.0	1039	132	3.98	0.9
9.0	1045	130	6.00	2.1
10.1	1048	132	6.40	3.9
10.8	1052	134	6.61	7.6

Run No. - 17
Nozzle - G - 3
Water Rate - 435 lbs/hr/ft^2
Surface Tension - 47.6 Dynes/cm
Orifice - 1.739" Dia.

ΔP_o	P_s	T	W	ΔP_d
6.0	1044	130	4.87	3.8
5.4	1042	130	4.62	2.2
5.0	1041	132	4.45	1.8
4.4	1040	136	4.16	1.5
4.0	1039	138	3.96	1.4
0.9	1036	138	1.98	0.9
2.0	1037	138	2.90	0.8
8.0	1045	136	5.67	3.1

Run No. - 18
Nozzle - G - 3
Water Rate - 523 lbs/hr/ft^2
Surface Tension - 47.6 Dynes/cm
Orifice - 1.789" Dia.

ΔP_o	P_s	T	W	ΔP_d
4.6	1041	144	4.19	1.9
1.4	1037	144	2.44	1.2
0.4	1036	144	1.37	1.1
1.2	1036	138	2.26	1.1
2.4	1038	140	3.11	1.4
4.0	1040	136	3.96	2.0
5.4	1042	138	4.56	2.7
7.0	1049	144	5.37	7.5
5.1	1043	150	4.42	3.4
6.0	1045	152	4.81	5.0
7.6	1048	154	5.44	6.3

Run No. - 19
Nozzle - aN - 8
Water Rate - 57 lbs/hr/ft^2
Surface Tension - 69.3 Dynes/cm
Orifice - 2.628" Dia.

ΔP_o	P_s	T	W	ΔP_d
7.7	1044	130	13.90	1.8
5.2	1040	130	11.41	1.2
8.9	1045	130	15.09	2.1
11.0	1048	130	16.80	2.6
12.4	1049	130	18.00	2.9

Reached max. cap. of blower without obtaining critical V

14.0	1051	130	19.28	3.4
16.3	1054	130	21.15	3.8

Overload protection shut off motor on blower

Run No. - 20
Nozzle - AN - 8
Water Rate - 115 lbs/hr/ft^2
Surface Tension - 69.3 Dynes/cm
Orifice - 2.628" Dia.

ΔPo	Ps	T	W	ΔPd
4.2	1039	124	10.26	1.1
6.2	1042	124	12.56	2.1
7.8	1044	124	14.20	2.6
10.2	1048	130	16.19	3.3
12.2	1051	130	17.81	4.5
14.2	1053	130	19.45	5.0
16.1	1057	130	20.95	6.5

Max. cap. of blower reached without obtaining critical V

Run No. - 21
Nozzle - AN - 14
Water Rate - 210 lbs/hr/ft^2
Surface Tension - 69.3 Dynes/cm
Orifice - 2.628" Dia.

ΔPo	Ps	T	W	ΔPd
4.7	1042	124	10.89	3.5
8.0	1048	126	14.40	6.0
6.0	1045	128	12.38	4.7
2.2	1037	128	7.61	0.8
10.2	1054	145	16.28	10.0
8.1	1049	130	14.40	7.0
7.2	1046	130	13.50	5.2
7.8	1048	130	14.10	6.0
8.9	1050	130	15.06	7.2
9.9	1052	130	16.00	8.0
9.2	1051	130	15.40	8.2
9.7	1053	129	15.84	9.2 F

Run No. - 22
Nozzle - AN - 14
Water Rate - 155 lbs/hr/ft^2
Surface Tension - 69.3 Dynes/cm
Orifice - 2.628" Dia.

ΔPo	Ps	T	W	ΔPd
4.7	1041	126	10.89	2.3
6.0	1043	126	12.34	3.0
8.1	1048	128	14.40	5.4
7.0	1046	130	13.39	4.8
6.6	1045	130	12.92	4.8
8.9	1047	130	15.10	6.2
9.8	1051	131	15.90	7.0
10.8	1053	130	16.80	7.7
10.6	1055	130	16.60	10.0 F
7.0	1046	130	13.36	5.1
2.8	1038	128	8.25	1.4
4.9	1041	124	11.11	2.5

Run No. - 23
Nozzle - AN - 14
Water Rate - 95 lbs/hr/ft^2
Surface Tension - 69.3 Dynes/cm
Orifice - 2.628" Dia.

ΔPo	Ps	T	W	ΔPd
4.9	1041	128	11.00	1.9
7.2	1044	130	13.50	2.3
9.1	1046	131	15.22	2.7
11.6	1050	132	17.38	3.9
14.5	1054	134	19.75	5.0

Max. cap. of blower reached without obtaining Vcr.

Run No. - 24
Nozzle - G - 3
Water Rate - 210 lbs/hr/ft^2
Surface Tension - 69.3 Dynes/cm
Orifice - 2.628" Dia.

ΔPo	Ps	T	W	ΔPd
2.7	1038	124	8.06	1.5
4.1	1040	120	10.20	2.0
5.0	1042	126	11.24	2.5
6.1	1044	128	12.46	3.4
7.5	1046	130	13.80	4.5
9.0	1058	130	15.13	F
7.3	1051	131	13.68	F
6.8	1045	130	13.19	3.8
7.2	1045	128	13.54	4.0
8.1	1048	128	14.39	6.0

Run No. - 25
Nozzle - G-3
Water Rate - 300 lbs/hr/ft^2
Surface Tension - 69.3 Dynes/cm
Orifice - 2.628" Dia.

ΔPo	Ps	T	W	ΔPd
2.9	1038	126	8.39	1.4
4.1	1041	122	10.18	2.7
3.5	1040	124	9.31	2.0
1.6	1036	124	6.10	0.6
4.5	1042	122	10.68	3.0
5.6	1047	128	11.89	7.0 F
3.3	1040	130	8.95	2.2
4.9	1043	128	11.10	4.0

Run No. - 26
Nozzle - G-3
Water Rate - 350 lbs/hr/ft^2
Surface Tension - 69.3 Dynes/cm
Orifice - 1.789" Dia.

ΔPo	Ps	T	W	ΔPd
13.1	1048	110	7.28	1.2
18.8	1055	112	8.79	1.8
22.1	1060	120	9.54	3.5
24.5	1063	124	10.09	4.0
20.1	1057	126	9.06	2,6
8.2	1043	126	5.54	0.6
18.5	1055	122	8.70	2.0
25.6	1063	124	10.18	3.7
28.2	1067	128	10.60	4.3
33.3	1075	128	11.41	8.0 F
27.2	1068	126	10.42	7.0 F

Run No. - 27
Nozzle - G - 3
Water Rate - 400 lbs/hr/ft^2
Surface Tension - 69.3 Dynes/cm
Orifice - 1.789" Dia.

ΔPo	Ps	T	W	ΔPd
6.2	1041	124	4.81	0.5
10.4	1046	118	6.52	1.2
14.6	1050	116	7.71	1.8
18.2	1055	120	8.66	2.3
22.1	1060	122	9.54	3.7
25.8	1064	126	10.18	4.2
29.1	1067	126	10.77	5.5 F

Run No. - 28
Nozzle - G - 3
Water Rate - 445 lbs/hr/ft^2
Surface Tension - 69.3 Dynes/cm
Orifice - 1.789" Dia.

ΔPo	Ps	T	W	ΔPd
9.2	1044	122	5.99	0.9
14.5	1060	118	7.64	1.5
18.8	1055	118	8.75	2.6
23.6	1061	124	9.80	3.4
28.0	1067	124	10.56	5.3 F

Run No. - 29
Nozzle - G - 3
Water Rate - 490 lbs/hr/ft^2
Surface Tension - 69.3 Dynes/cm
Orifice - 1.789" Dia.

ΔPo	Ps	T	W	ΔPd
14.2	1050	124	7.59	1.8
17.9	1055	120	8.71	2.7
29.5	1069	122	10.90	6.0F
23.6	1063	126	9.81	5.0
20.9	1058	126	9.20	3.5
6.4	1041	124	4.88	0.5

Run No. - 30
Nozzle - G - 3
Water Rate - 516 lbs/hr/ft^2
Surface Tension - 69.3 Dynes/cm
Orifice - 1.789" Dia.

ΔPo	Ps	T	W	ΔPd
6.4	1041	116	4.91	0.5
14.0	1050	114	7.51	1.8
18.1	1055	120	7.89	2.5
22.2	1061	122	9.46	4.4
26.4	1067	124	10.34	6.7

Run No. - 31
Nozzle - G - 3
Water Rate - 511 lbs/hr/ft^2
Surface Tension - 44.8 Dynes/cm
Orifice - 1.789" Dia.

ΔPo	Ps	T	W	ΔPd
2.7	1037	100	3.36	2.3
2.2	1039	102	3.22	3.2
1.2	1036	103	2.34	0.6
0.3	1035	102	1.22	0.2
2.1	1038	101	3.02	2.2
1.3	1037	98	2.49	1.9
0.9	1036	100	1.86	1.2
0.2	1034	102	0.97	0.2
0.6	1035	99	1.76	0.4
2.8	1039	100	3.41	2.3
3.5	1041	102	3.82	3.2
4.6	1043	114	4.29	4.4
5.9	1046	120	4.90	6.1 F

Run No. - 32
Nozzle - G - 3
Water Rate - 480 lbs/hr/ft^2
Surface Tension - 44.8 Dynes/cm
Orifice - 1.789" Dia.

ΔPo	Ps	T	W	ΔPd
0.9	1035	122	2.10	0.3
0.2	1034	121	0.91	0.1
2.4	1038	118	3.16	1.6
4.6	1043	112	4.31	4.5
5.8	1047	114	4.85	6.8 F
3.2	1039	128	3.52	2.0
5.2	1044	134	4.51	4.3
4.8	1043	138	4.36	3.8
4.2	1043	148	4.14	2.4
2.2	1038	146	3.08	1.7
1.2	1036	144	2.25	0.5
1.8	1036	138	2.80	0.5

Run No. - 33
Nozzle - G - 3
Water Rate - 445 lbs/hr/ft^2
Surface Tension - 44.8 Dynes/cm
Orifice - 1.789" Dia.

ΔPo	Ps	T	W	ΔPd
1.8	1036	138	2.78	0.6
0.7	1035	138	1.89	0.2
4.2	1039	134	4.06	1.1
6.0	1042	122	4.97	1.8
8.2	1047	118	5.78	5.0
6.8	1046	124	5.18	4.8
6.2	1044	126	4.99	3.7
9.1		126	6.18	F

Run No. - 34
Nozzle - G - 3
Water Rate - 400 lbs/hr/ft^2
Surface Tension - 44.8 Dynes/cm
Orifice - 1.789" Dia.

ΔPo	Ps	T	W	ΔPs
2.5	1038	122	3.24	1.9
4.3	1043	118	4.14	2.3
6.2	1043	116	5.02	3.0
8.2	1048	120	5.78	5.3
7.2	1045	124	5.38	3.4
8.8	1048	124	5.96	5.3
9.9	1054	124	6.36	F

Run No. - 35
Nozzle - G - 3
Water Rate - 355 lbs/hr/ft^2
Surface Tension - 44.8 Dynes/cm
Orifice - 1.789" Dia.

ΔPo	Ps	T	W	ΔPd
3.0	1037	124	3.43	0.8
5.8	1041	118	4.80	1.3
8.9	1048	118	6.05	4.7
8.1	1044	122	5.76	2.3
8.7	1046	124	5.95	2.8
11.1	1053	124	6.76	8.3 F

Run No. - 36
Nozzle - G - 3
Water Rate - 300 lbs/hr/ft^2
Surface Tension - 44.8 Dynes/cm
Orifice - 1.789" Dia.

ΔPo	Ps	T	W	ΔPd
1.7	1037	122	2.77	0.9
3.8	1039	118	3.86	1.0
5.9	1041	111	4.94	1.4
6.9	1043	118	5.30	1.6
8.0	1043	120	5.78	1.3
11.1	1047	122	6.74	2.2
11.3	1048	124	6.79	2.7
12.7	1053	126	7.45	6.7
11.4	1051	126	6.85	5.7
13.7	1056	126	7.56	F

Run No. - 37
Nozzle - G - 3
Water Rate - 232 lbs/hr/ft^2
Surface Tension - 44.8 Dynes/cm
Orifice - 1.789" Dia.

ΔPo	Ps	T	W	ΔPd
6.2	1041	124	4.98	1.0
7.8	1043	120	5.63	0.7
11.9	1049	120	7.04	3.3
13.8	1054	124	7.55	6.3
10.4	1047	126	6.47	2.3
8.7	1043	124	5.95	0.7
15.1	1059	122	7.91	9.5 F
12.9	1055	126	7.33	8.4
11.8	1048	124	6.94	2.5

Run No. - 38
Nozzle - AN - 14
Water Rate - 155 lbs/hr/ft^2
Surface Tension - 44.8 Dynes/cm
Orifice - 1.789" Dia.

ΔPo	Ps	T	W	ΔPd
2.7	1037	88	3.40	0.2
5.9	1040	90	5.04	0.4
10.0	1045	96	6.57	0.6
14.0	1049	112	7.65	0.7
14.3	1051	124	7.70	3.0
16.2	1054	122	8.24	4.2
16.9	1059	122	8.42	8.2
17.9	1060+	124	8.69	F

Run No. - 39
Nozzle - AN - 14
Water Rate - 200 lbs/hr/ft^2
Surface Tension - 44.8 Dynes/cm
Orifice - 1.789" Dia.

ΔPo	Ps	T	W	ΔPd
7.9	1042	120	5.58	0.6
11.8	1047	118	7.00	0.8
15.1	1052	120	7.94	3.3
14.0	1050	124	7.62	2.3
15.9	1055	122	8.14	5.2
16.5	1062	124	8.34	9.3 F

Run No. - 40
Nozzle - AN - 14
Water Rate - 95 lbs/hr/ft^2
Surface Tension - 44.8 Dynes/cm
Orifice - 2.628" Dia.

Δ Po	Ps	T	W	Δ Pd
0.8	1035	100	4.19	0.2
1.8	1036	98	6.70	0.6
2.9	1038	104	8.55	0.8
4.0	1041	124	10.08	3.3
3.4	1045	124	9.21	7.3 F
3.1	1042	124	8.71	5.0
2.4	1037	122	7.64	0.8
3.0	1048	120	8.60	0.9
3.5	1040	120	9.34	2.2

Run No. - 41
Nozzle - AN - 8
Water Rate - 100 lbs/hr/ft^2
Surface Tension - 44.8 Dynes/cm
Orifice - 2.628" Dia.

Δ Po	Ps	T	W	Δ Pd
1.2	1036	98	5.26	0.4
3.0	1045	132	8.58	8.0 F
2.8	1042	124	8.34	5.2
2.6	1039	119	7.95	2.3
2.2	1037	118	7.29	0.8
6.7	1035	118	3.83	0.2

Run No. - 42
Nozzle - AN - 8
Water Rate - 57 lbs/hr/ft^2
Surface Tension - 44.8 Dynes/cm
Orifice - 2.628" Dia.

Δ Po	Ps	T	W	Δ Pd
0.6	1035	110	3.57	0.2
2.2	1037	109	7.69	0.6
4.0	1040	114	10.07	2.4
5.2	1048	126	11.53	9.2 F
4.7	1046	128	10.92	7.7
4.2	1046	126	10.58	7.3
3.8	1042	124	9.79	4.6
3.4	1039	124	9.15	2.0
2.8	1038	122	8.26	1.1

Run No. - 43
Nozzle - AN - 2
Water Rate - 57 lbs/hr/ft^2
Surface Tension - 31.8 Dynes/cm
Orifice - 2.628" Dia.

Δ Po	Ps	T	W	Δ Pd
1.6	1036	94	6.28	0.4
3.6	1044	102	9.69	6.2
2.7	1039	120	8.14	1.9
2.2	1038	122	7.25	1.3
0.7	1035	122	3.86	0.2
1.3	1036	120	5.45	0.4
3.4	1040	118	9.24	2.8
3.7	1045	130	9.61	7.7 F

Run No. - 44
Nozzle - AN - 8
Water Rate - 115 $lbs/hr/ft^2$
Surface Tension - 31.8 Dynes/cm
Orifice - 2.628" Dia.

ΔPo	Ps	T	W	ΔPd
1.1	1036	124	4.85	0.4
2.1	1043	124	7.15	6.8 F
1.3	1037	132	5.40	1.9
0.2	1035	130	1.71	0.4
0.8	1036	124	4.19	0.8
1.7	1039	126	6.29	3.2

Run No. - 47
Nozzle - G - 3
Water Rate - 535 $lbs/hr/ft^2$
Surface Tension - 31.8 Dynes/cm
Orifice - 1.789" Dia.

ΔPo	Ps	T	W	ΔPd
3.1	1037+	72	3.70	F
1.1	1038	80	2.40	3.2
0.5	1038	88	1.68	1.0
0.2	1034	86	0.99	0.1
1.9	1041	86	2.96	4.8
3.1	1037+	90	3.64	F
0.6	1036	98	1.76	1.5
0.3	1035	112	1.21	0.6

Run No. - 48
Nozzle - G - 3
Water Rate - 300 $lbs/hr/ft^2$
Surface Tension - 31.8 Dynes/cm
Orifice - 1.789" Dia.

ΔPo	Ps	T	W	ΔPd
0.3	1035	105	1.26	0.4
1.9	1038	106	2.92	1.8
4.1	1043	106	4.09	4.5
1.3	1036	118	2.45	1.0
0.7	1035	120	1.82	0.5
2.8	1038	118	3.36	1.6
3.4	1040	114	3.72	2.5
5.4	1045	123	4.68	5.4
6.8	1041+	128	5.21	F
6.1	1047	134	4.94	6.2

Run No. - 49
Nozzle - G - 3
Water Rate - 400 $lbs/hr/ft^2$
Surface Tension - 31.8 Dynes/cm
Orifice - 1.789" Dia.

ΔPo	Ps	T	W	ΔPd
1.1	1036	134	2.28	1.3
0.4	1035	132	1.33	0.3
1.9	1037	128	2.86	1.1
3.8	1038+	120	3.86	F
2.3	1041	120	3.00	4.8
1.7	1038	124	2.77	3.0
2.7	1042	118	3.30	5.5 F

Run No. - 50
Nozzle - G - 3
Water Rate - 200 lbs/hr/ft^2
Surface Tension - 31.8 Dynes/cm
Orifice - 1.789" Dia.

ΔPo	Ps	T	W	ΔPd
0.2	1035	112	0.96	0.4
3.7	1040	112	3.86	2.4
6.0	1041	104	4.98	2.7
7.6	1046	120	5.59	4.4
9.2	1044+	132	6.11	F
8.0	1042+	134	5.70	F

Run No. - 51
Nozzle - G - 3
Water Rate - 500 lbs/hr/ft^2
Surface Tension - 58.5 Dynes/cm
Orifice - 1.789" Dia.

ΔPo	Ps	T	W	ΔPd
3.3	1038	100	3.68	0.8
7.6	1043	108	5.64	1.3
9.9	1046	116	6.40	2.0
11.7	1048	122	6.94	2.4
14.0	1051	124	7.61	2.9
17.0	1055	128	8.40	4.0
17.8	1057	130	8.56	5.0
18.6	1059	131	8.75	6.4
21.2	1063	132	9.43	8.0
23.6	1065	132	9.85	F
18.2	1057	132	8.62	5.0
12.0	1048	130	6.99	2.4

Run No. - 52
Nozzle - G - 3
Water Rate - 277 lbs/hr/ft^2
Surface Tension - 58.5 Dynes/cm
Orifice - 1.789" Dia.

ΔPo	Ps	T	W	ΔPd
26.0	1071	134	10.08	8.9 F
22.5	1061	132	9.81	4.2
20.0	1057	132	9.06	2.8
16.3	1052	132	8.19	2.0
12.7	1048	130	7.19	1.0
9.3	1044	130	6.11	0.7
5.6	1040	128	4.71	0.4
1.7	1036	126	2.72	0.1

Run No. - 53
Nozzle - G - 3
Water Rate - 400 lbs/hr/ft^2
Surface Tension - 58.5 Dynes/cm
Orifice - 1.789" Dia.

ΔPo	Ps	T	W	ΔPd
1.6	1036	112	2.70	0.1
14.0	1050	130	7.57	2.4
17.7	1055	132	8.54	3.4
21.5	1057	138	9.36	5.0
25.0	1067	142	9.75	F
12.0	1048	140	6.91	1.6
7.7	1043	136	5.54	0.8
4.0	1038	132	3.98	0.4

Run No. - 54
Nozzle - AN - 14
Water Rate - 200 lbs/hr/ft^2
Surface Tension - 58.5 Dynes/cm
Orifice - 2.628" Dia.

ΔPo	Ps	T	W	ΔPd
2.4	1037	112	7.70	0.5
3.5	1041	120	9.34	3.5
2.7	1038	126	8.10	1.5
1.6	1036	130	6.06	0.6
0.8	1035	130	4.13	0.3
3.2	1040	128	8.89	2.4
4.6	1046	132	10.73	7.4
5.2	1048	140	10.40	8.8
5.6	1049	140	11.84	F

Run No. - 55
Nozzle - AN - 14
Water Rate - 100 lbs/hr/ft^2
Surface Tension - 58.5 Dynes/cm
Orifice - 2.628" Dia.

ΔPo	Ps	T	W	ΔPd
5.8	1043	138	12.01	3.4
7.6	1046	138	13.86	4.3
9.4	1049	140	15.40	5.7
5.8	1043	138	12.01	3.1
1.2	1036	136	5.10	0.4
4.6	1041	128	10.70	2.4
3.6	1039	134	9.39	1.4
8.8	1047	134	15.00	4.6
10.7	1051	140	16.60	6.6
11.7	1053	136	17.40	7.4

Run No. - 56
Nozzle - AN - 14
Water Rate - 145 lbs/hr/ft^2
Surface Tension - 58.5 Dynes/cm
Orifice - 2.628" Dia.

ΔPo	Ps	T	W	ΔPd
2.6	1037	118	7.95	0.7
3.5	1039	114	9.36	1.0
5.5	1045	122	11.79	5.0
7.6	1053	128	14.04	F
6.4	1049	132	12.70	9.0
6.0	1048	134	12.30	7.8
4.8	1043	134	10.98	3.7
4.0	1040	134	9.96	1.7
1.4	1036	133	5.61	0.4

Run No. - 57
Nozzle - AN - 14
Water Rate - 200 lbs/hr/ft^2
Surface Tension - 58.5 Dynes/cm
Orifice - 2.628" Dia.

ΔPo	Ps	T	W	ΔPd
1.3	1036	130	5.35	0.5
3.6	1041	130	9.44	3.1
5.8	1049	138	12.08	9.0
4.9	1045	142	11.00	5.6
4.2	1042	142	10.20	4.0
3.8	1041	142	9.65	3.0
3.4	1040	140	9.06	2.2
2.6	1038	138	7.84	1.2
2.1	1037	138	7.08	0.8
6.4	1050	134	12.72	10.0 F
5.6	1050	142	11.80	9.9 F

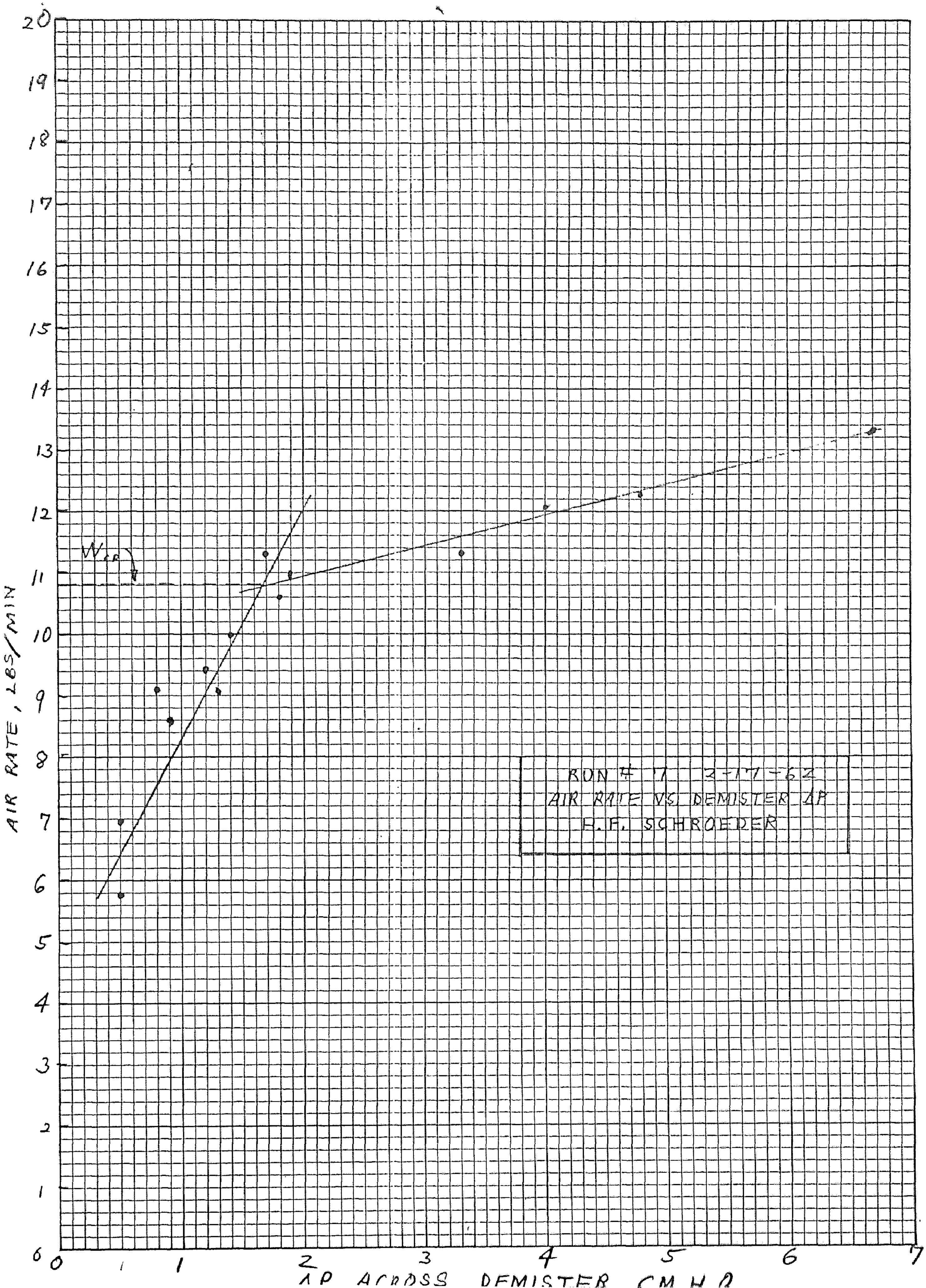

RUN # 7 2-17-62
AIR RATE VS DEMISTER ΔP
H.F. SCHROEDER
AIR RATE, LBS/MIN
ΔP ACROSS DEMISTER CM H_2O
W_{CR}
20
19
18
17
16
15
14
13
12
11
10
9
8
7
6
5
4
3
2
1
0
1
2
3
4
5
6
7

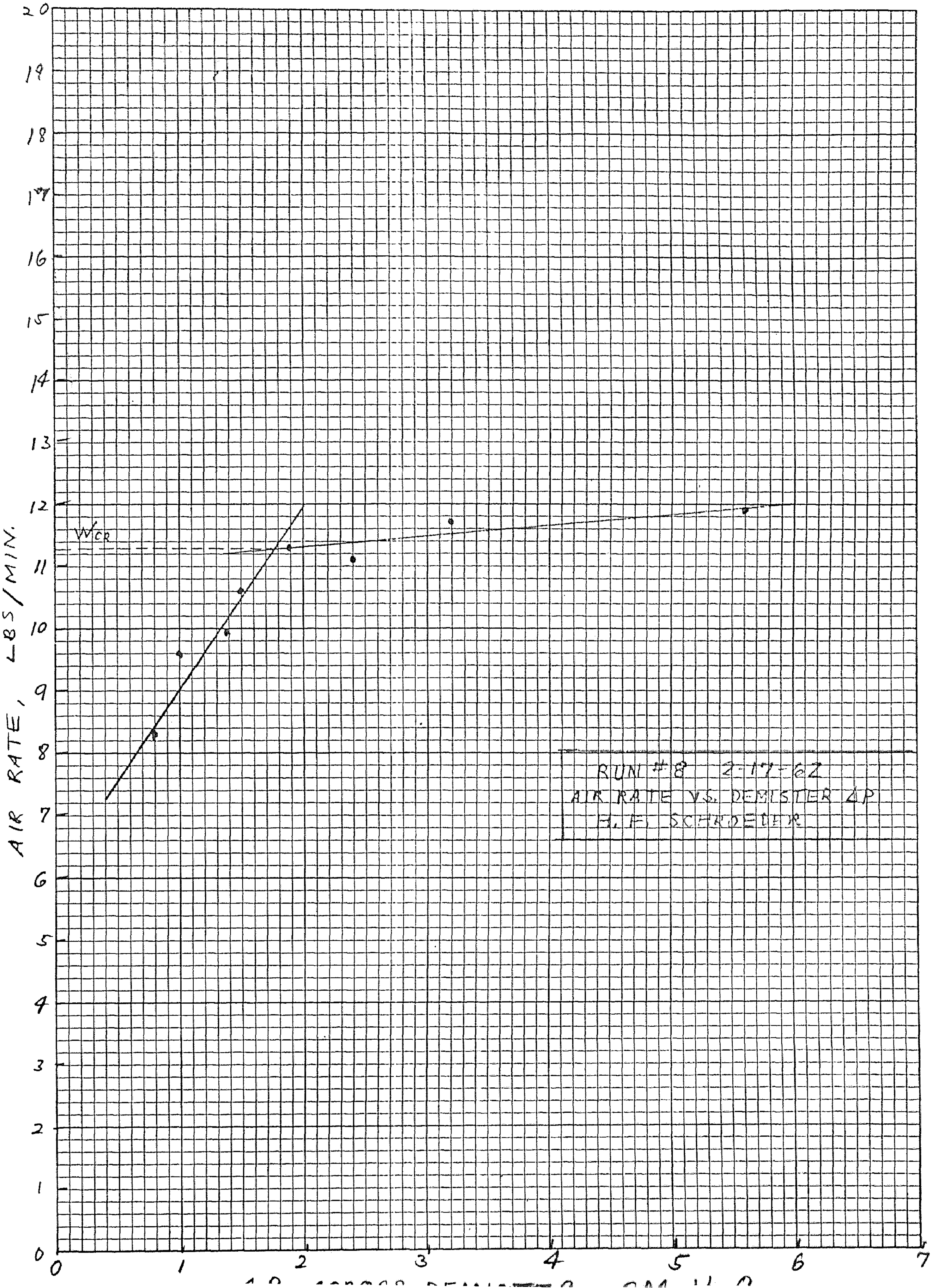
20
19
18
17
16
15
14
13
12
11
10
9
8
7
6
5
4
3
2
1
0
AIR RATE, LBS/MIN.
W_CR
0
1
2
3
4
5
6
7
RUN #8 2-17-62
AIR RATE VS. DEMISTER ΔP
H.F. SCHROEDER

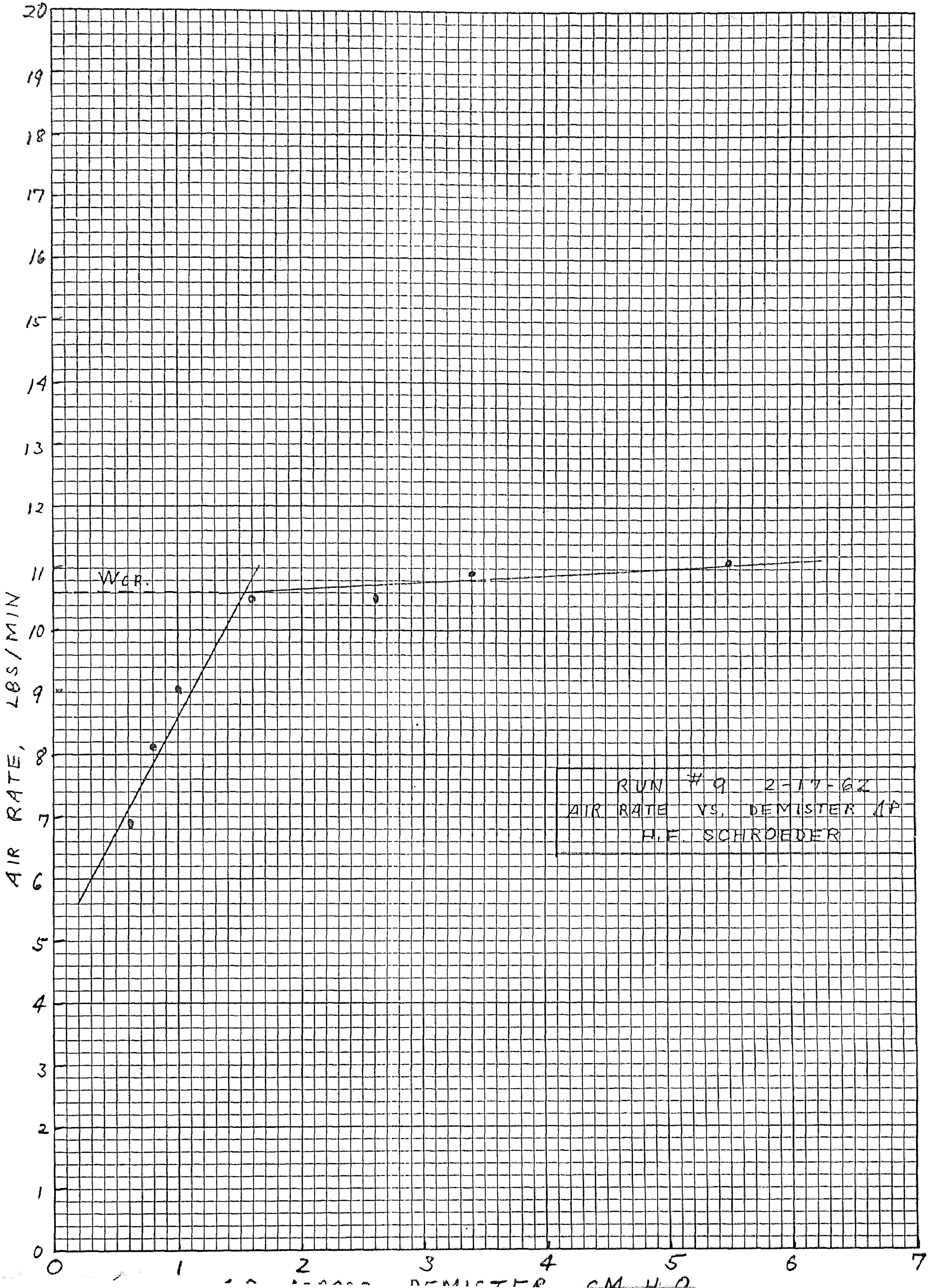
AIR RATE, LBS/MIN
Wcr.
RUN #9 2-17-62
AIR RATE VS. DEMISTER ΔP
H.E. SCHROEDER

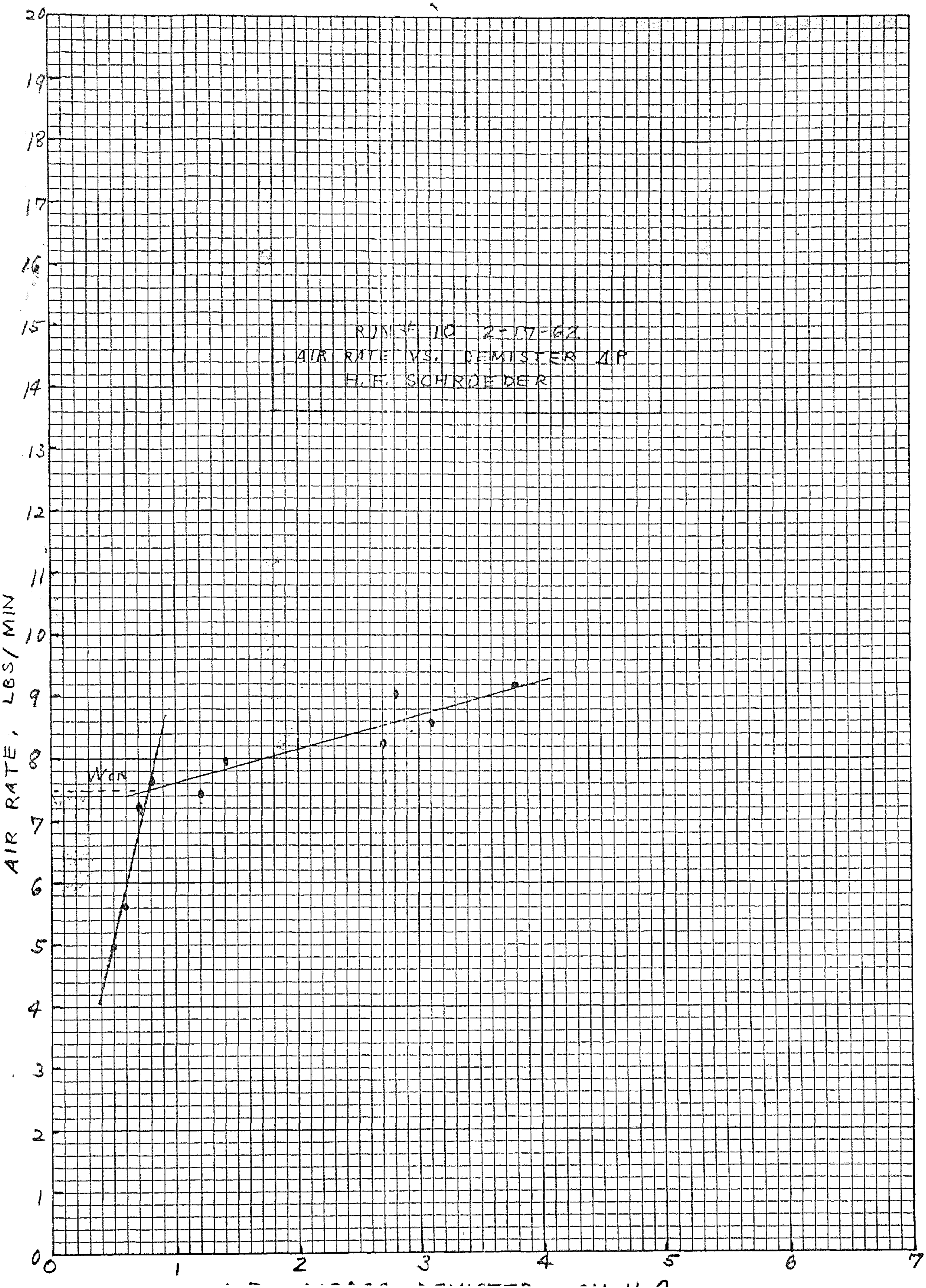
RUN # 10 2-17-62
AIR RATE VS. DEMISTER ΔP
H.F. SCHROEDER
AIR RATE, LBS/MIN
W_cr
20
19
18
17
16
15
14
13
12
11
10
9
8
7
6
5
4
3
2
1
0
0
1
2
3
4
5
6
7

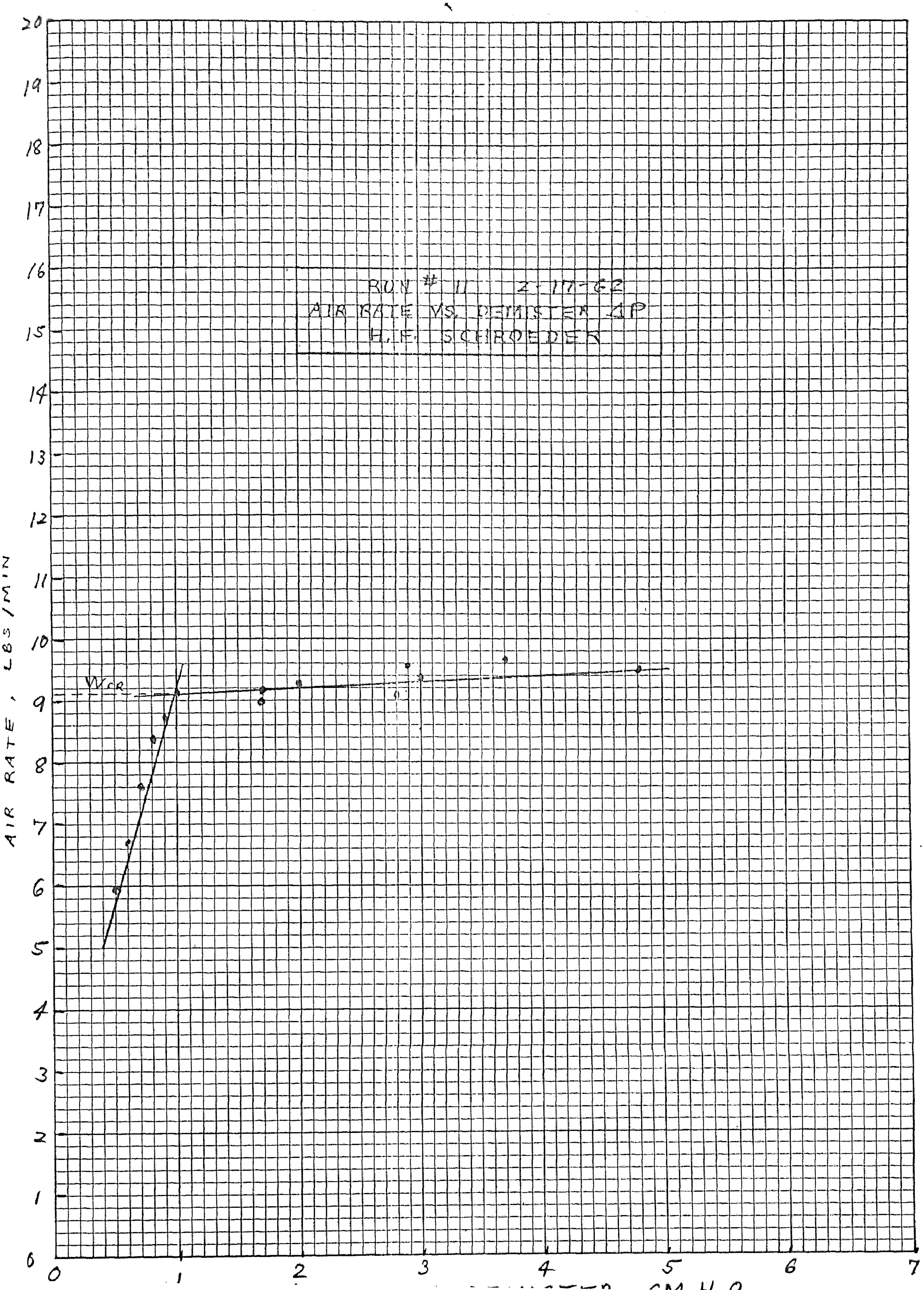
RUN # 11 2-17-62
AIR RATE VS. DEMISTER ΔP
H.F. SCHROEDER
AIR RATE, LBS/MIN
W_{CR}
0
1
2
3
4
5
6
7
8
9
10
11
12
13
14
15
16
17
18
19
20
0
1
2
3
4
5
6
7
DEMISTER, CM H_2O

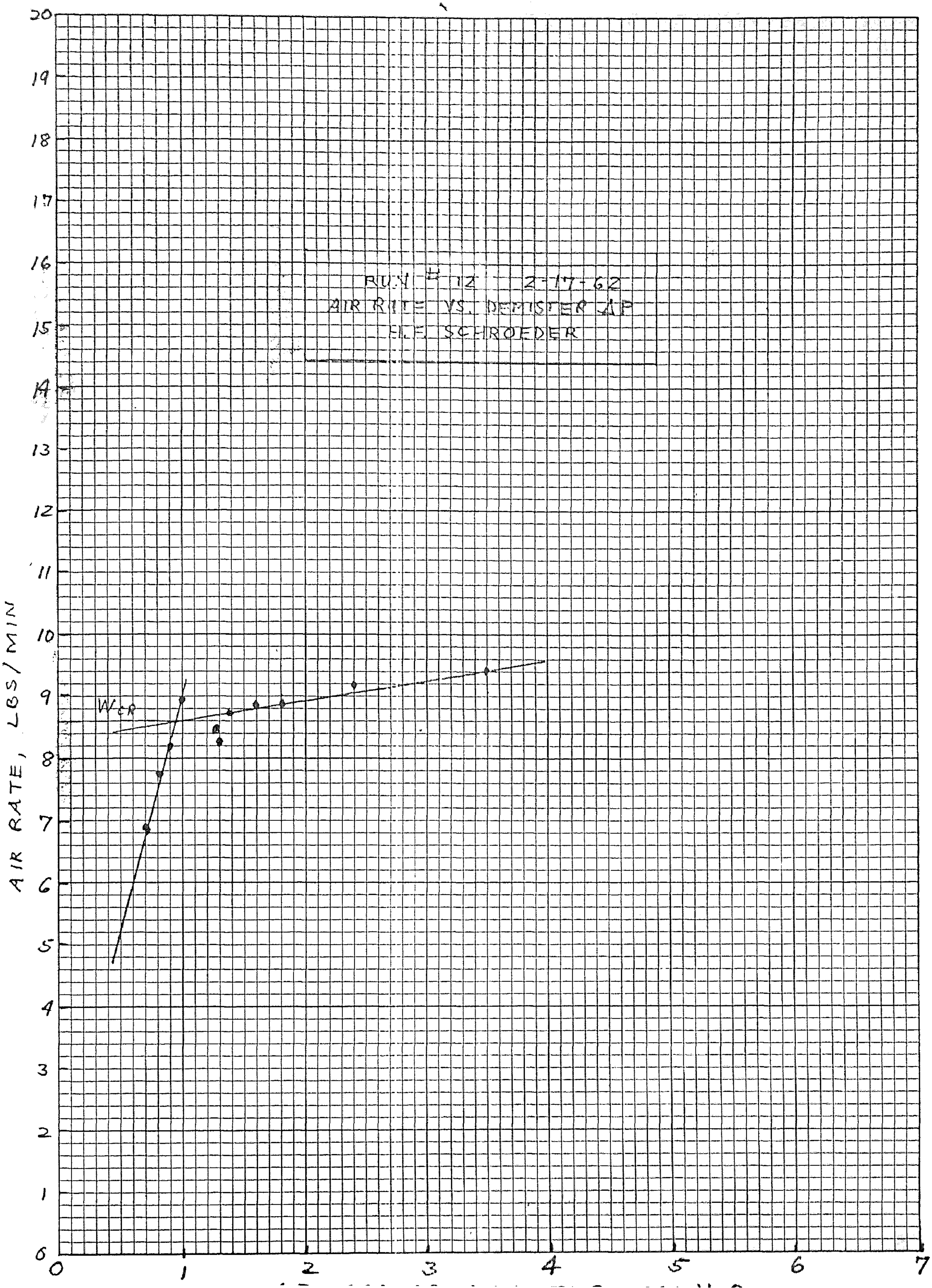

RUN # 12 2-17-62
AIR RATE VS. DEMISTER ΔP
E.L.F. SCHROEDER
AIR RATE, LBS/MIN
W_{CR}
0 1 2 3 4 5 6 7
0 1 2 3 4 5 6 7 8 9 10 11 12 13 14 15 16 17 18 19 20

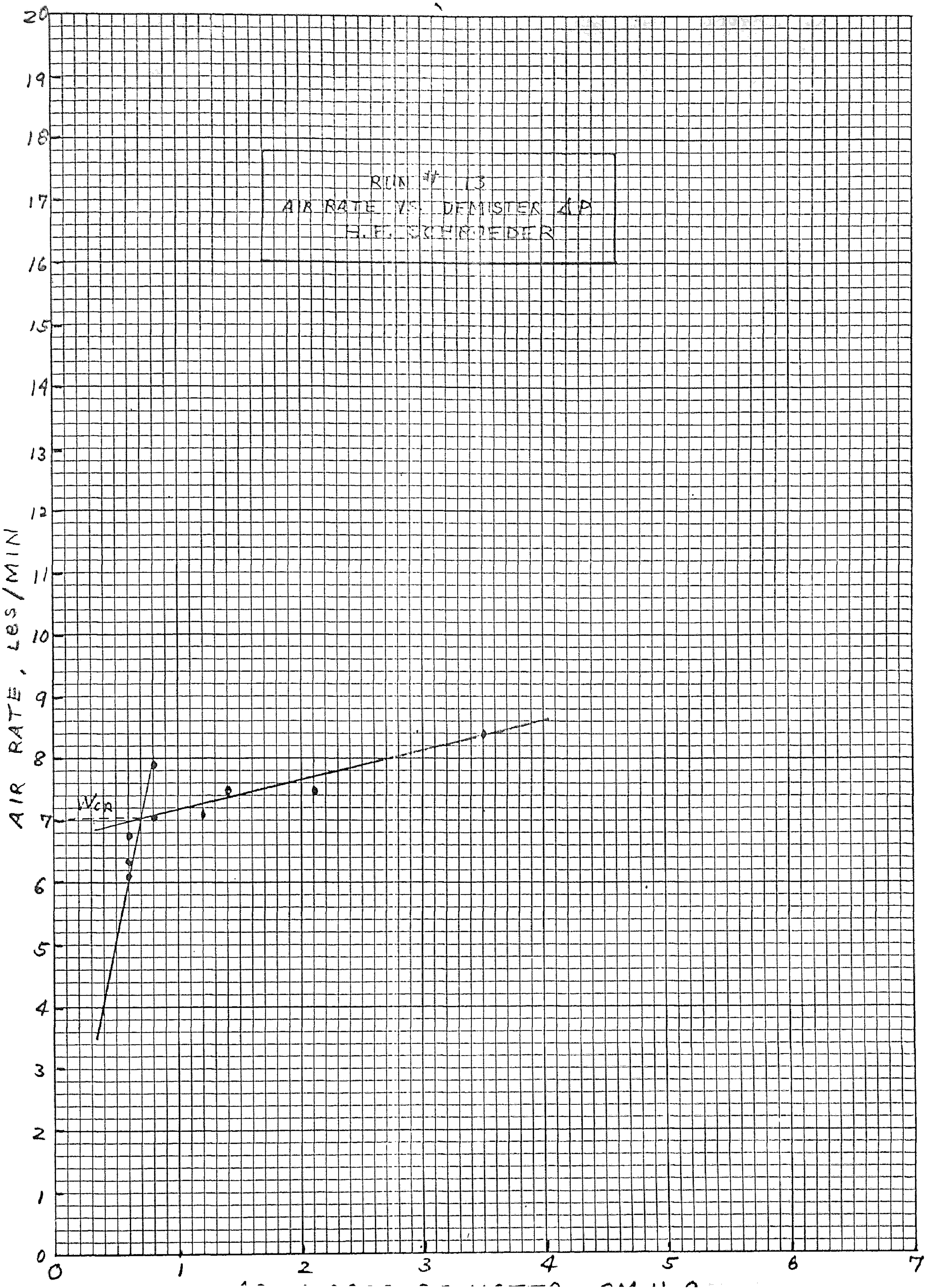
RUN # 13
AIR RATE VS. DEMISTER ΔP
B.E. SCHROEDER
AIR RATE, LBS/MIN
W_{CR}
0
1
2
3
4
5
6
7
8
9
10
11
12
13
14
15
16
17
18
19
20

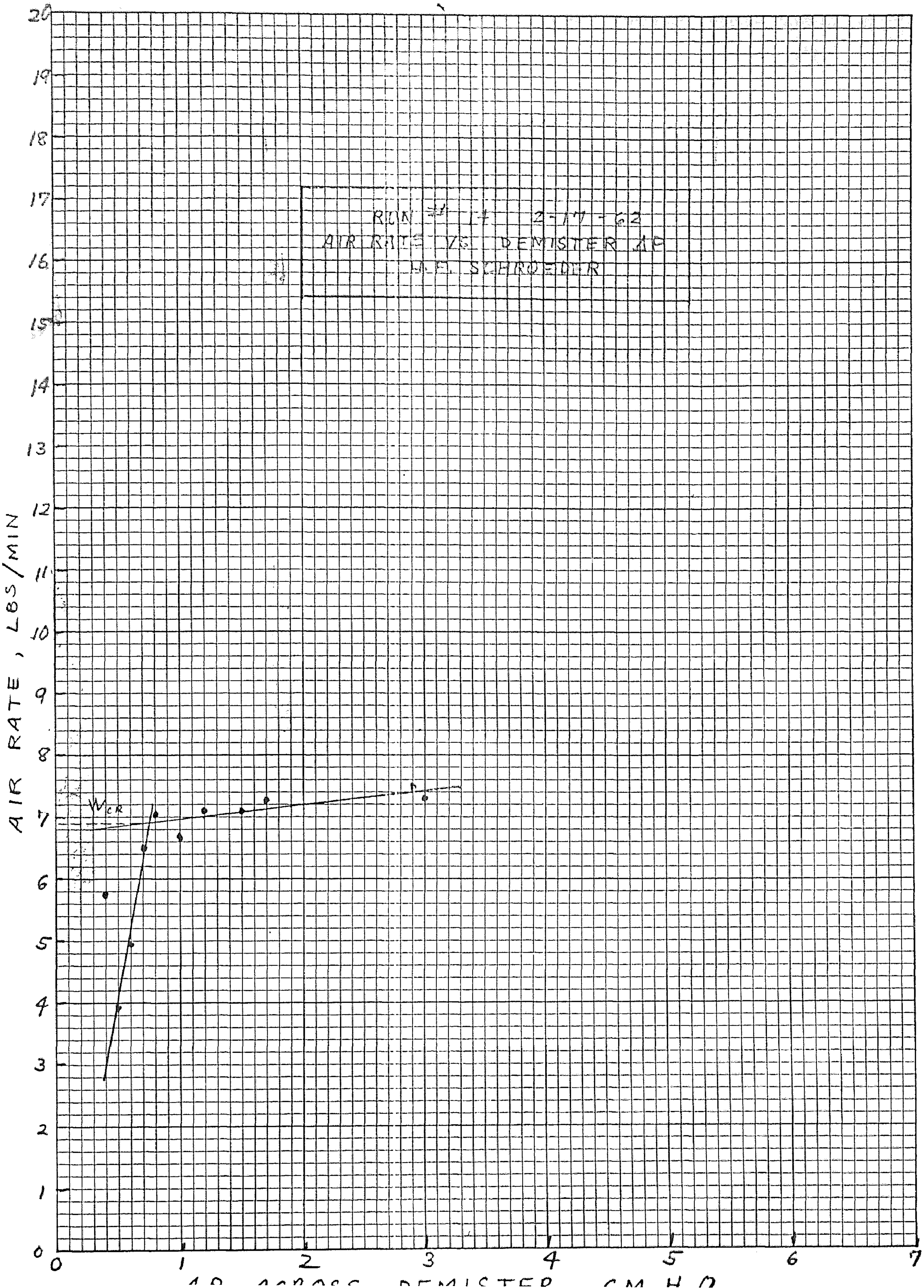
RUN # 14 2-17-62
AIR RATE VS DEMISTER ΔP
H.E. SCHROEDER
AIR RATE, LBS/MIN
W_{CR}
0 1 2 3 4 5 6 7 8 9 10 11 12 13 14 15 16 17 18 19 20
0 1 2 3 4 5 6 7

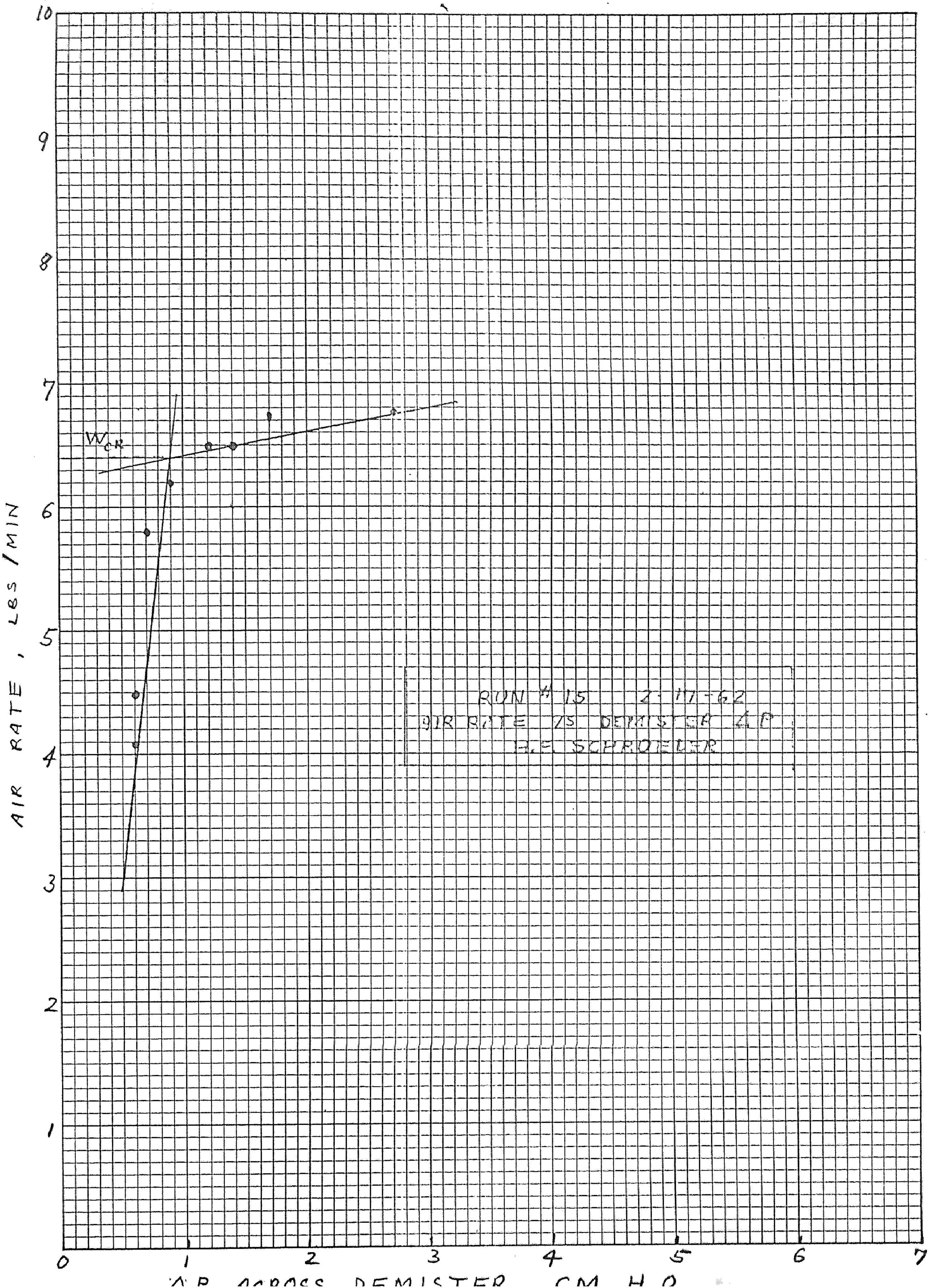
10
9
8
7
6
5
4
3
2
1
0
1
2
3
4
5
6
7
W_{CR}
AIR RATE, LBS/MIN
ΔP ACROSS DEMISTER CM H2O
RUN # 15 2-17-62
AIR RATE VS DEMISTER ΔP
B.E. SCHROEDER

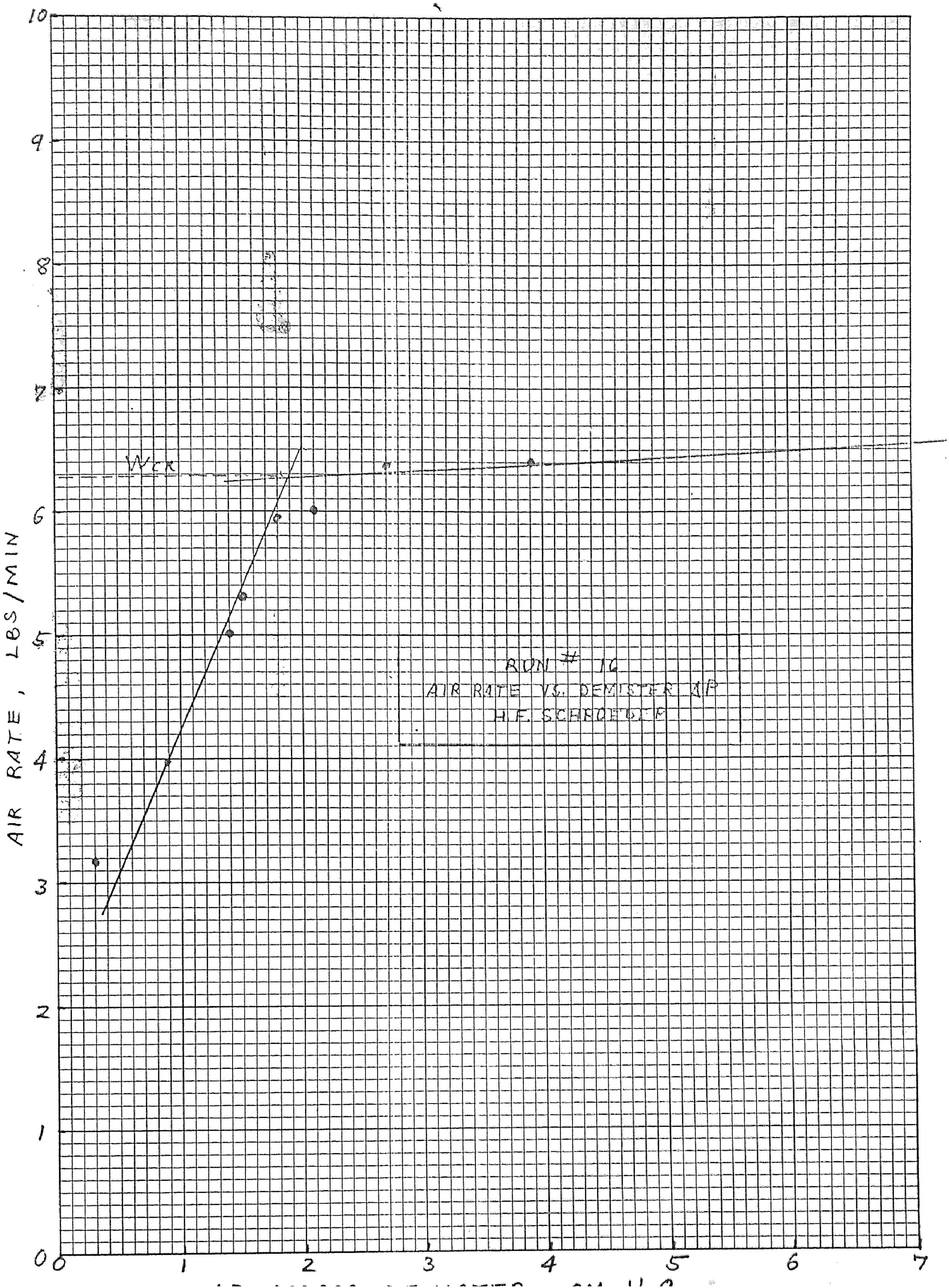

10
9
8
7
6
5
4
3
2
1
0
0
1
2
3
4
5
6
7
AIR RATE, LBS/MIN
W_{CR}
RUN # 16
AIR RATE VS. DEMISTER ΔP
H.F. SCHROEDER

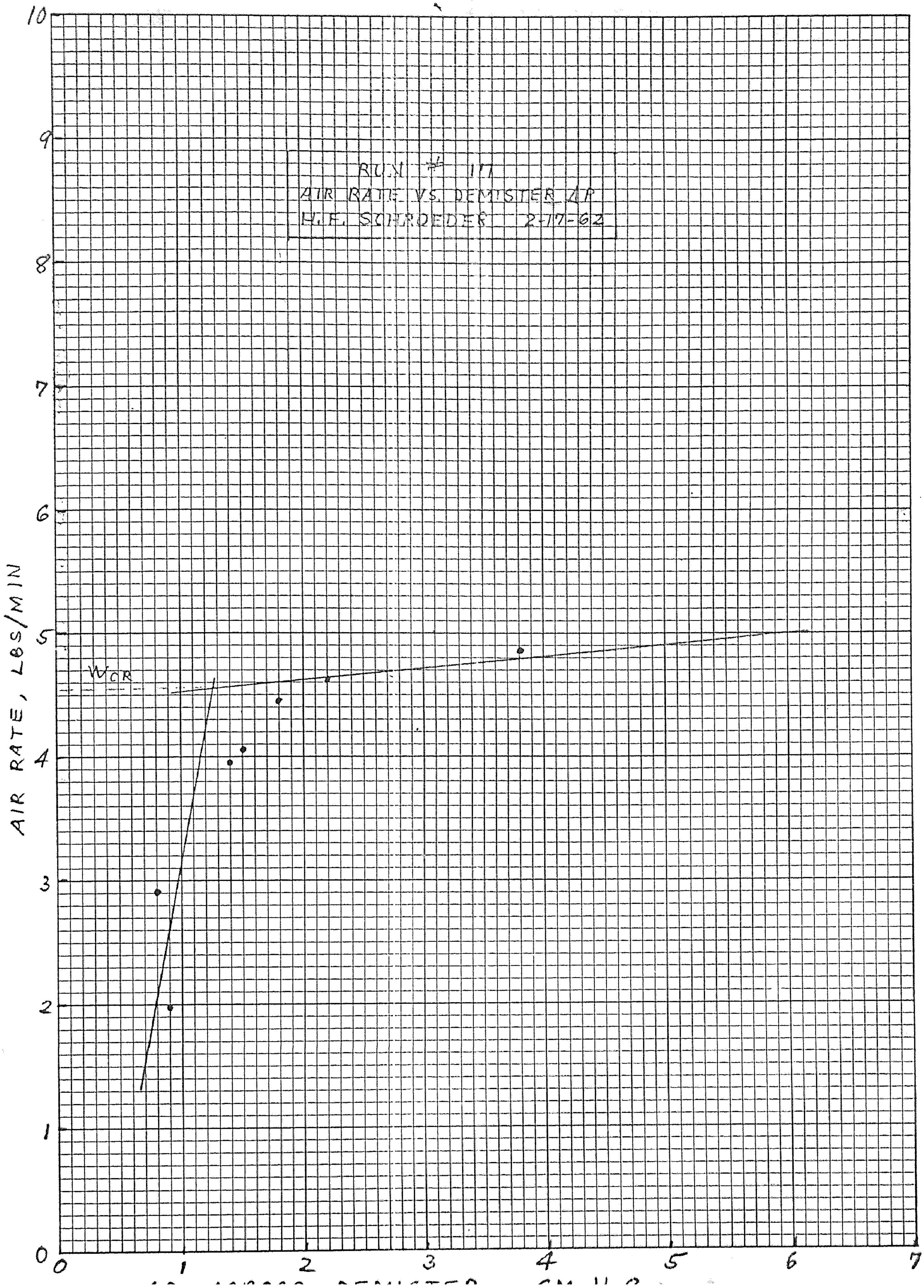
RUN # 17
AIR RATE VS. DEMISTER ΔP
H.F. SCHROEDER 2-17-62
AIR RATE, LBS/MIN
WCR
0
1
2
3
4
5
6
7
8
9
10

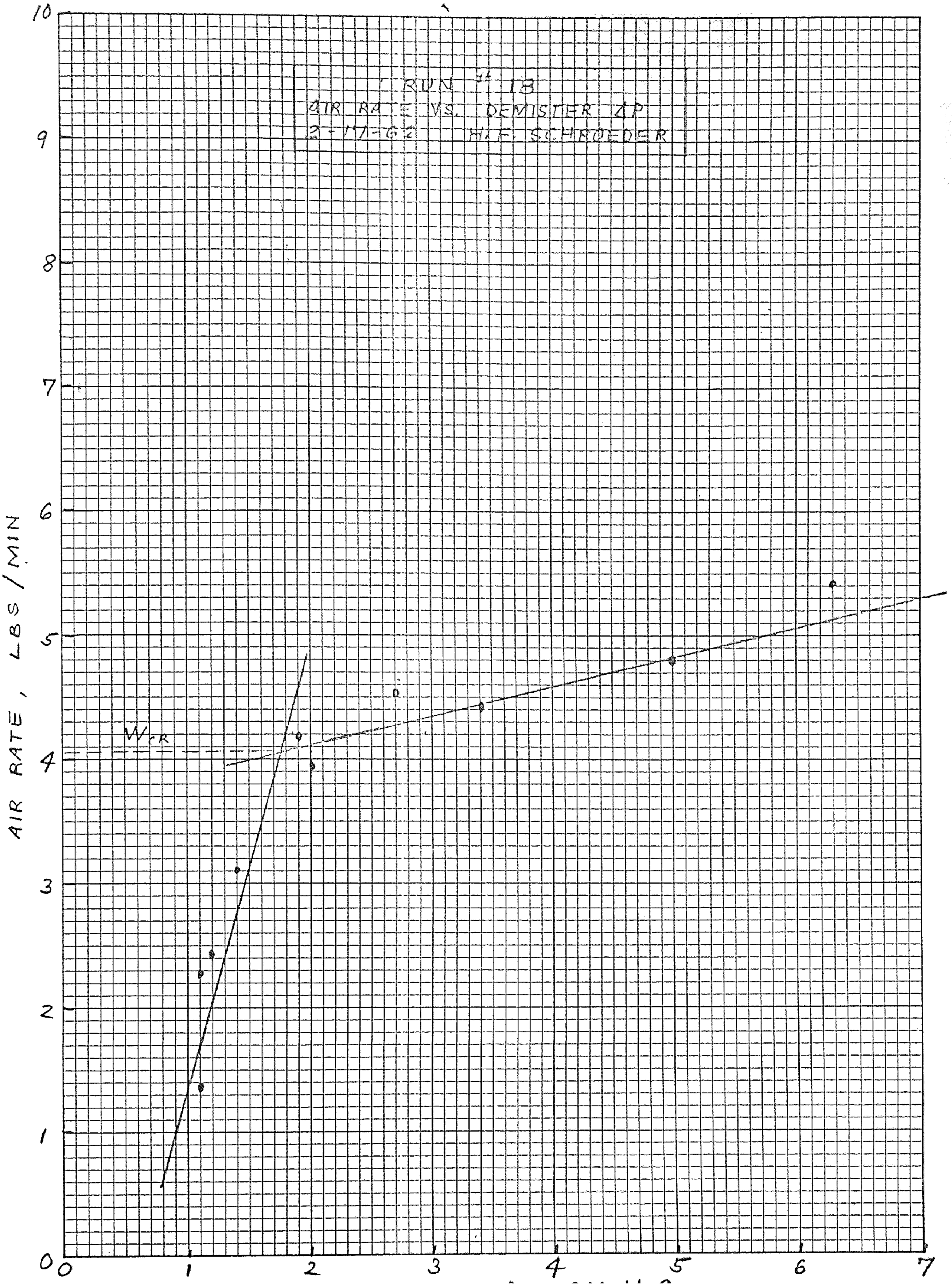
RUN # 18
AIR RATE VS. DEMISTER ΔP
2-17-62 H.F. SCHROEDER
AIR RATE, LBS/MIN
W_CR
0
1
2
3
4
5
6
7
8
9
10

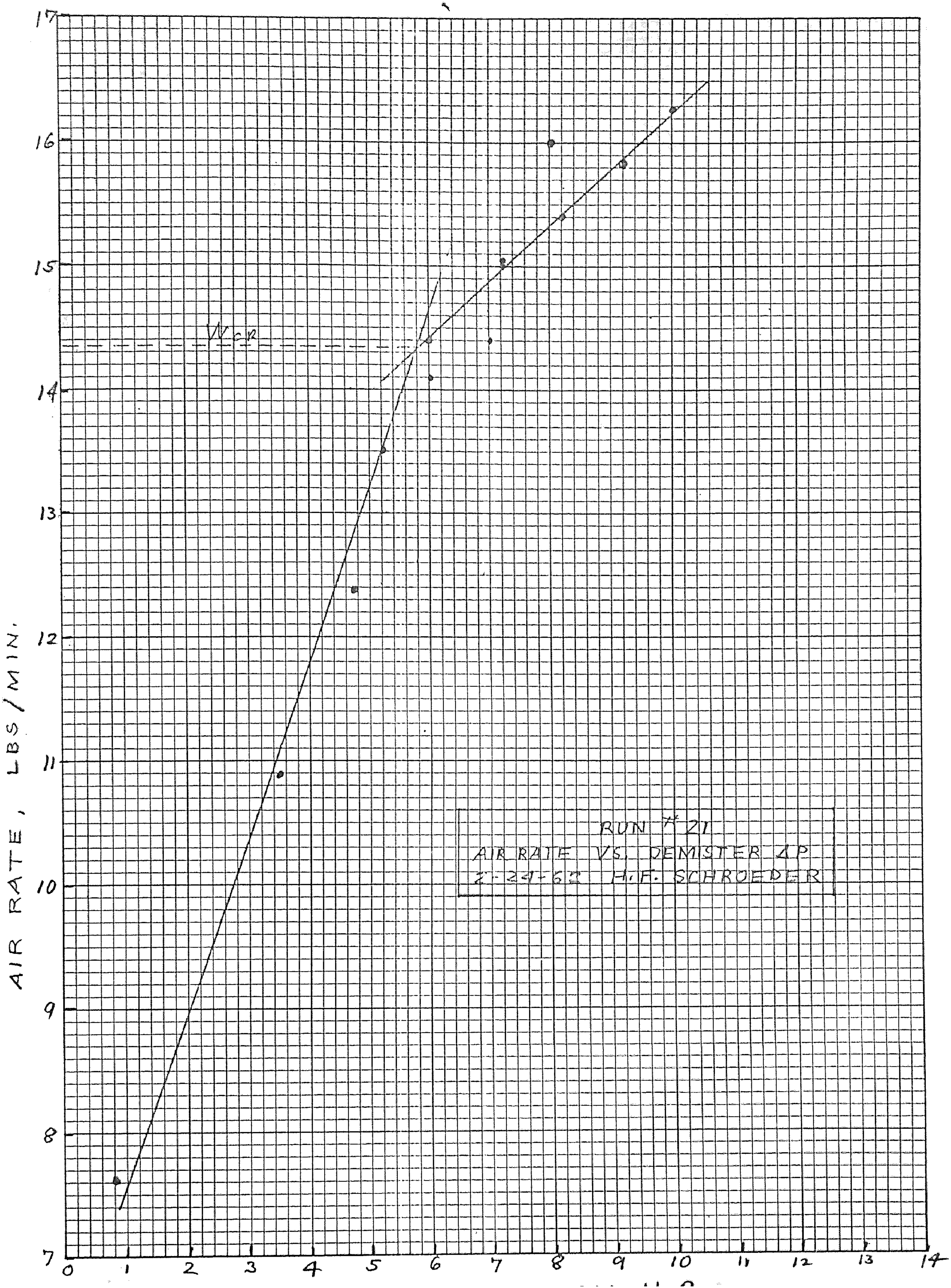
AIR RATE, LBS/MIN.
17
16
15
14
13
12
11
10
9
8
7
0
1
2
3
4
5
6
7
8
9
10
11
12
13
14
W_{CR}
RUN # 21
AIR RATE VS. DEMISTER ΔP
2-24-62 H.F. SCHROEDER

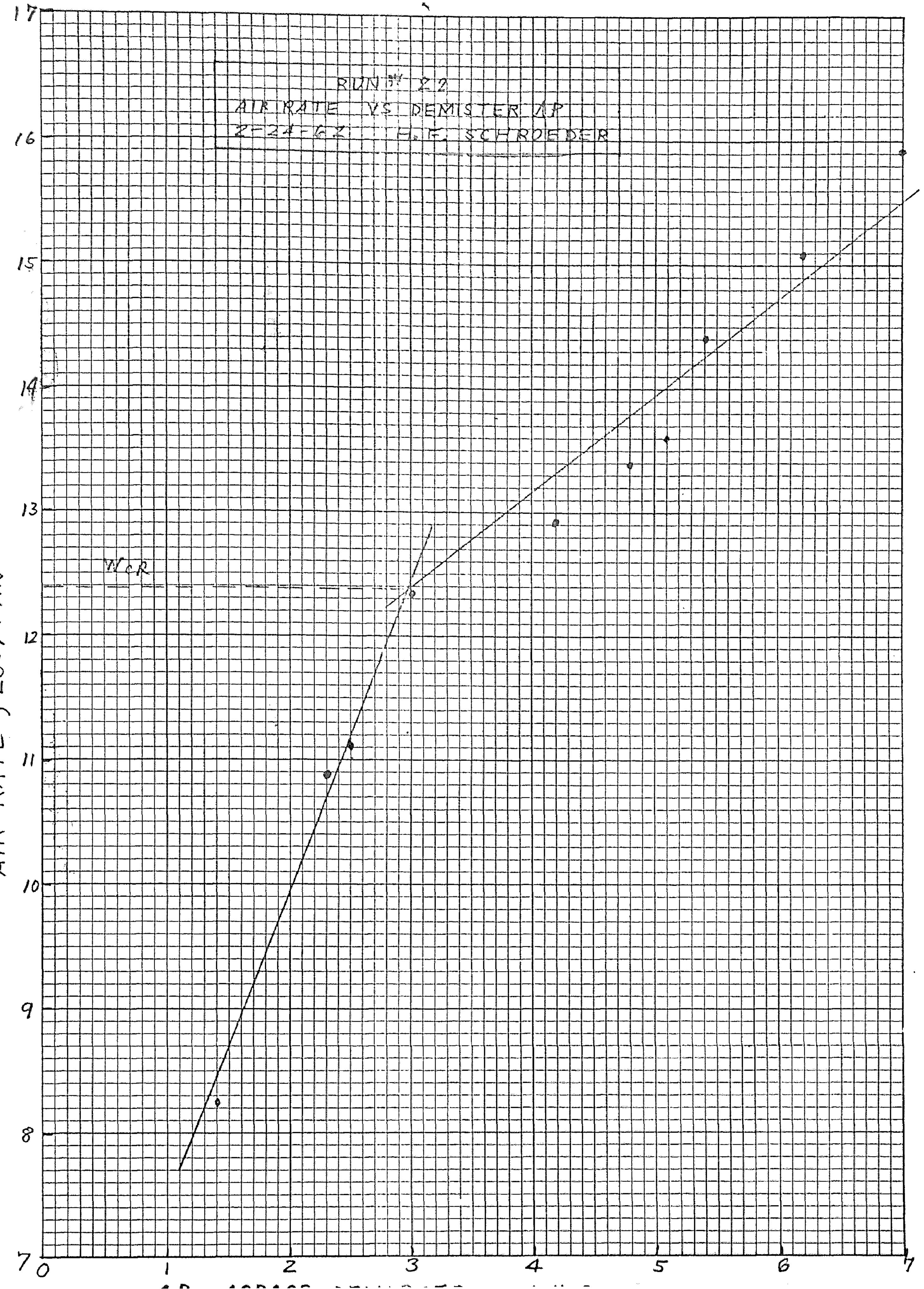
RUN # 22
AIR RATE VS DEMISTER ΔP
2-24-62 H.E. SCHROEDER
17
16
15
14
13
12
11
10
9
8
7
0
1
2
3
4
5
6
7
W_{CR}
AIR RATE, LBS/MIN

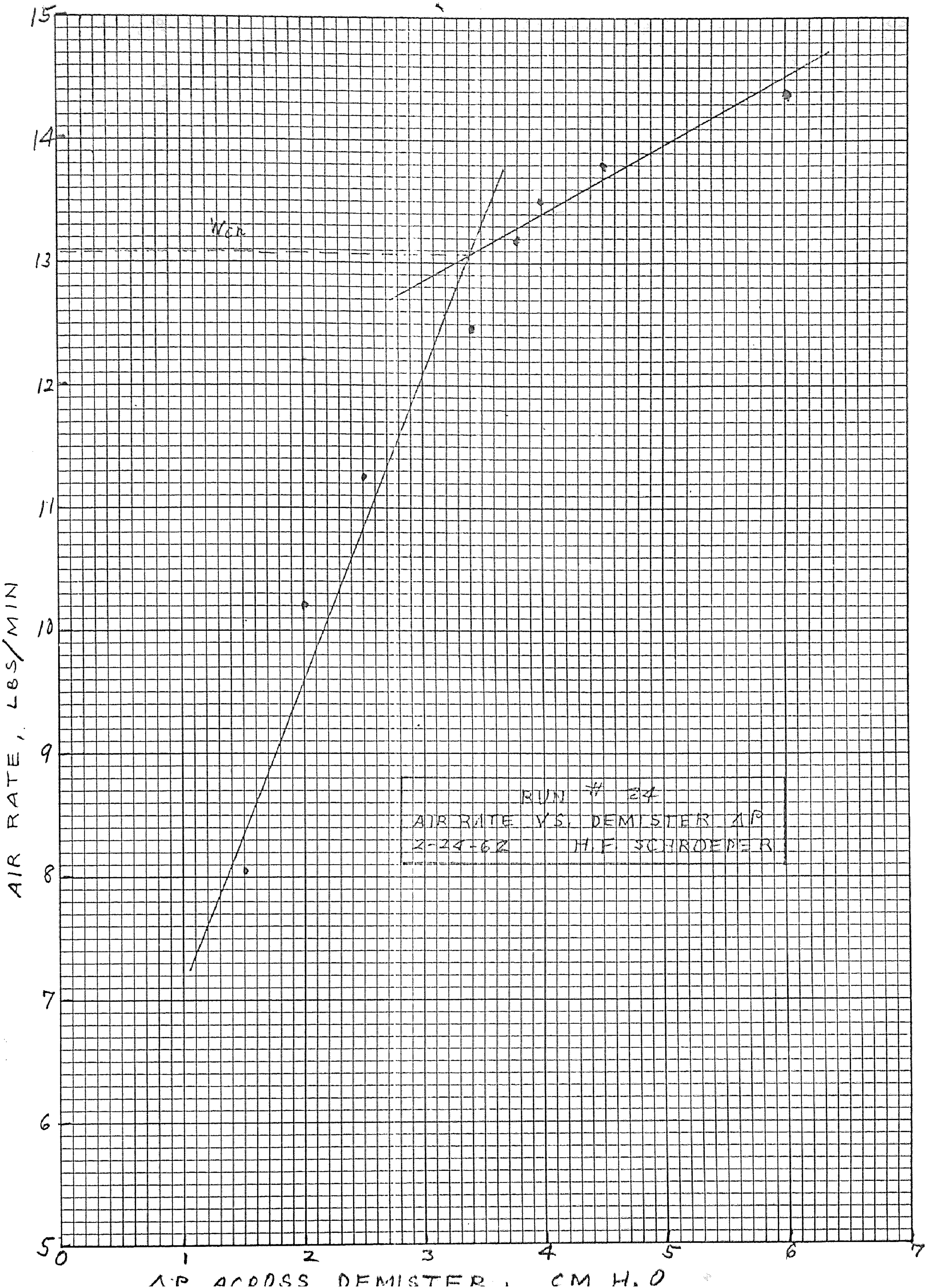
15
14
13
12
11
10
9
8
7
6
5
0
1
2
3
4
5
6
7
W_{CR}
RUN # 24
AIR RATE VS. DEMISTER ΔP
2-24-62 H.F. SCHROEDER
AIR RATE, LBS/MIN
ΔP ACROSS DEMISTER, CM H_2O

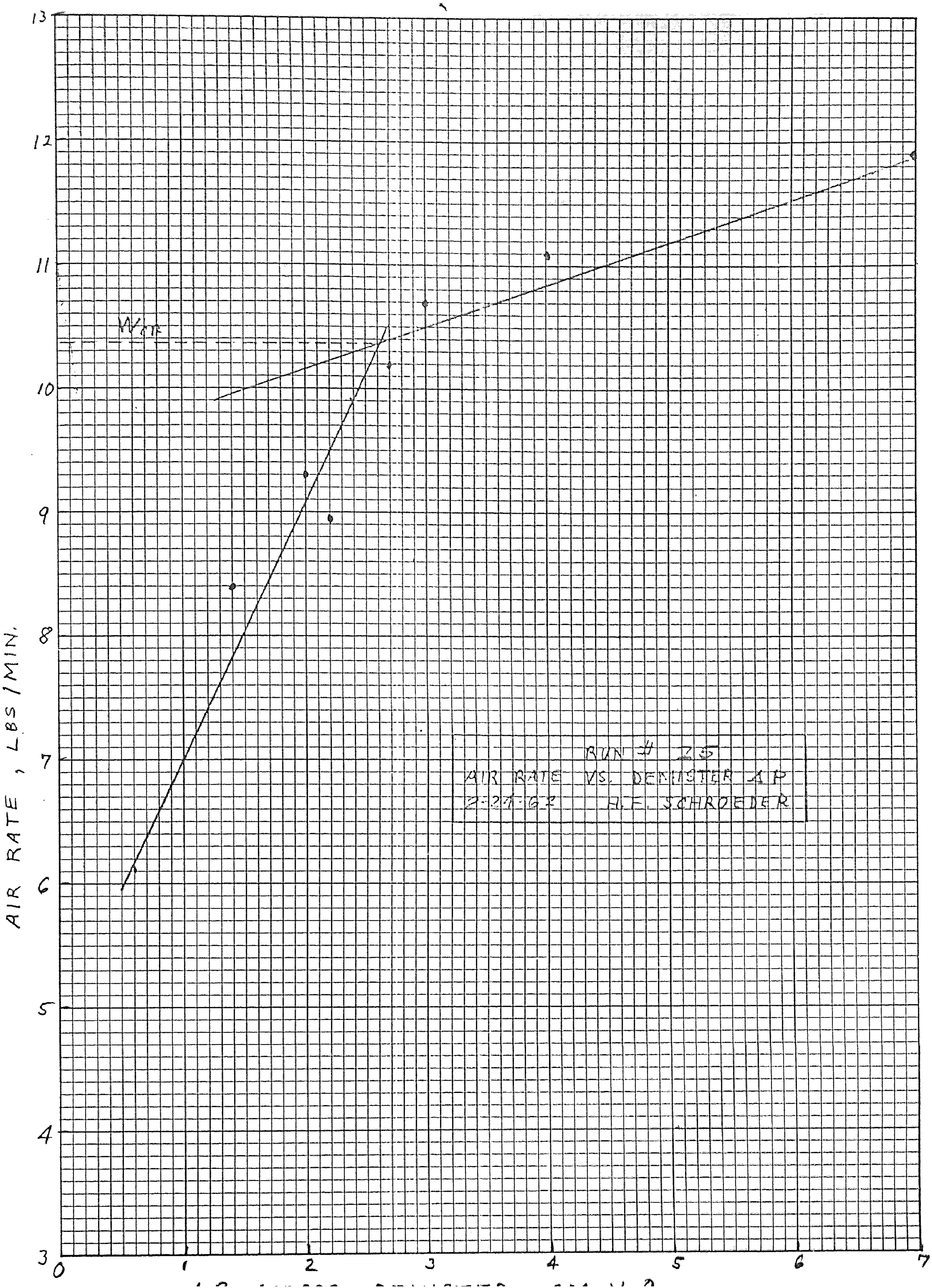
RUN # 25
AIR RATE VS. DEMISTER ΔP
2-27-67 H.F. SCHROEDER
AIR RATE, LBS/MIN.
W
13
12
11
10
9
8
7
6
5
4
3
0
1
2
3
4
5
6
7

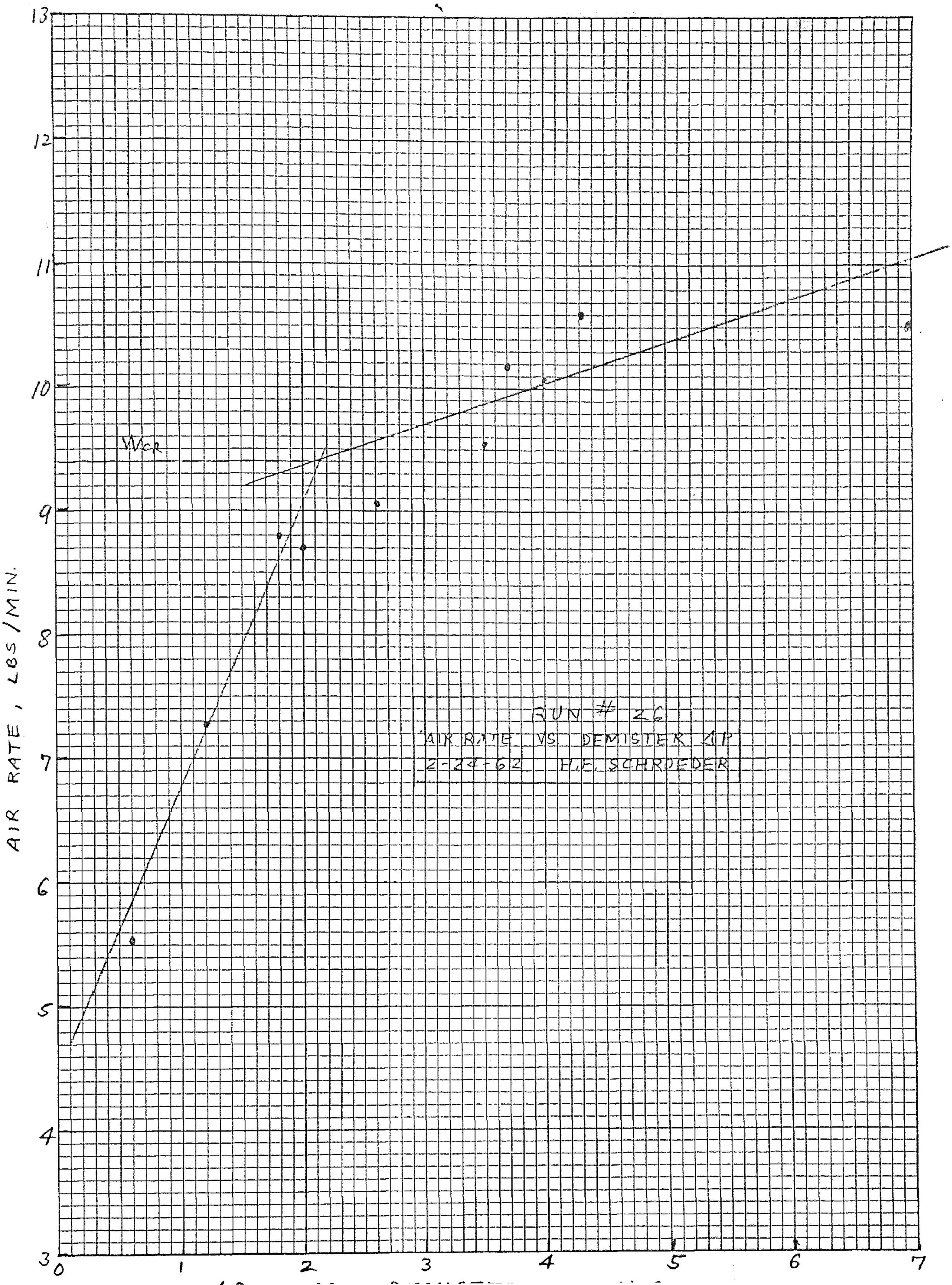
RUN # 26
AIR RATE VS DEMISTER ΔP
2-24-62 H.F. SCHROEDER
AIR RATE, LBS/MIN.
W_{CR}
13
12
11
10
9
8
7
6
5
4
3
0
1
2
3
4
5
6
7

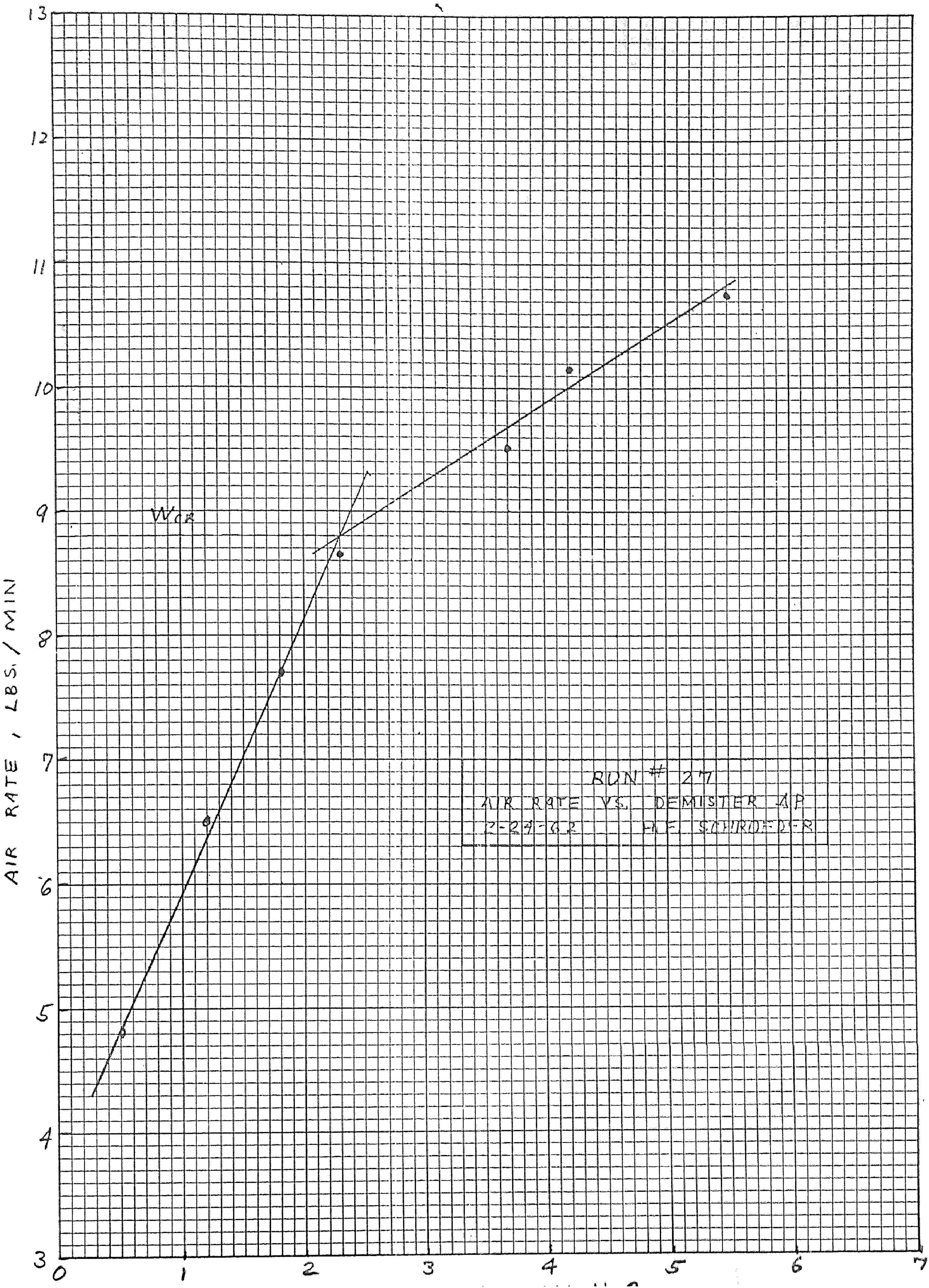

AIR RATE, LBS./MIN
13
12
11
10
9
8
7
6
5
4
3
0
1
2
3
4
5
6
7
Wcr
RUN # 27
AIR RATE VS. DEMISTER ΔP
2-24-62 H.E. SCHROEDER

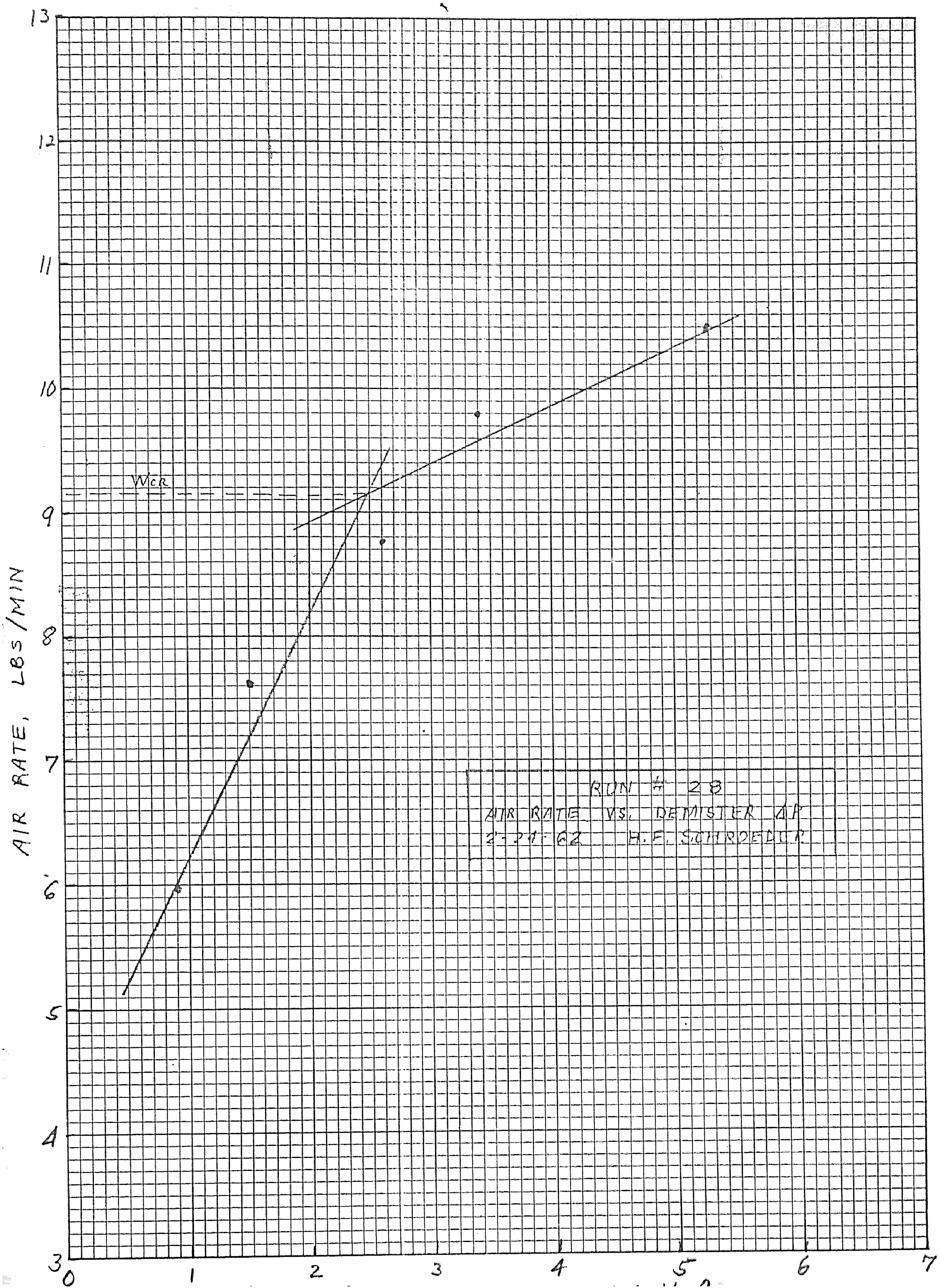
RUN # 28
AIR RATE VS. DEMISTER ΔP
2-21-62 H.F. SCHROEDER
AIR RATE, LBS/MIN
W_{CR}
13
12
11
10
9
8
7
6
5
4
3
0
1
2
3
4
5
6
7

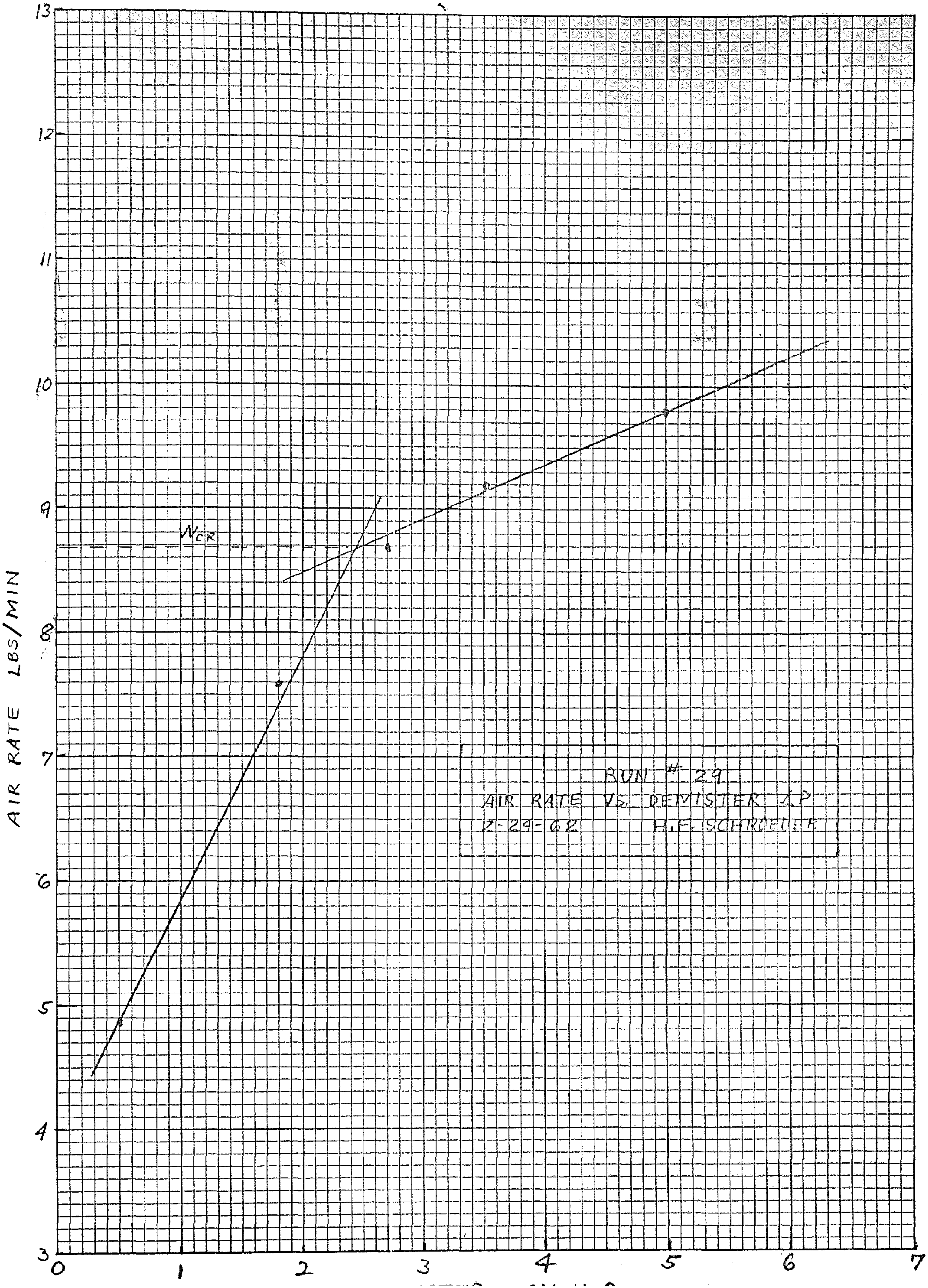
13
12
11
10
9
8
7
6
5
4
3
0
1
2
3
4
5
6
7
AIR RATE LBS/MIN
W CR
RUN # 29
AIR RATE VS. DEMISTER ΔP
2-29-62
H.F. SCHROEDER

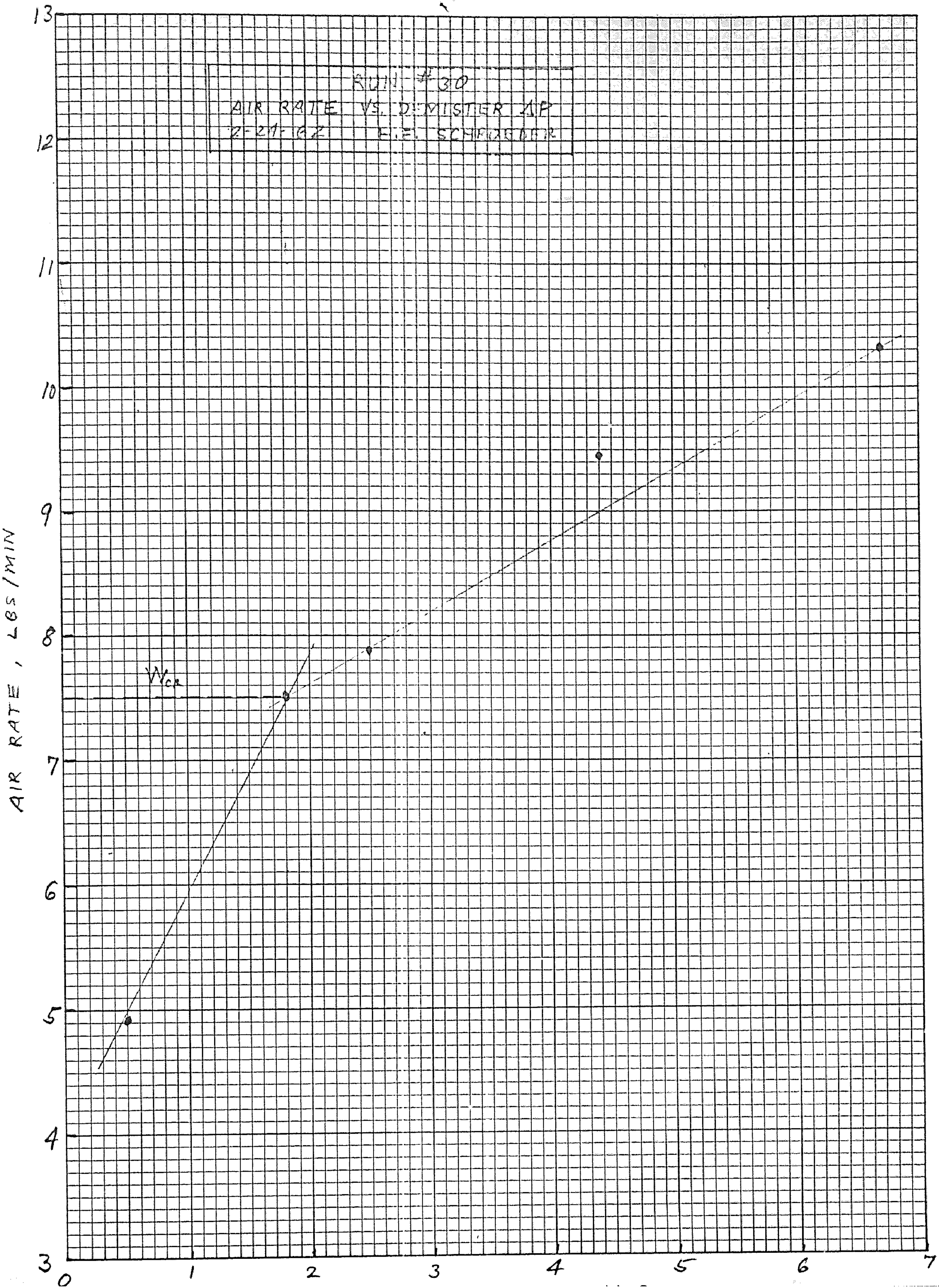
RUN # 30
AIR RATE VS. DEMISTER ΔP
2-21-62
AIR RATE, LBS/MIN
W_{cr}
13
12
11
10
9
8
7
6
5
4
3
0
1
2
3
4
5
6
7

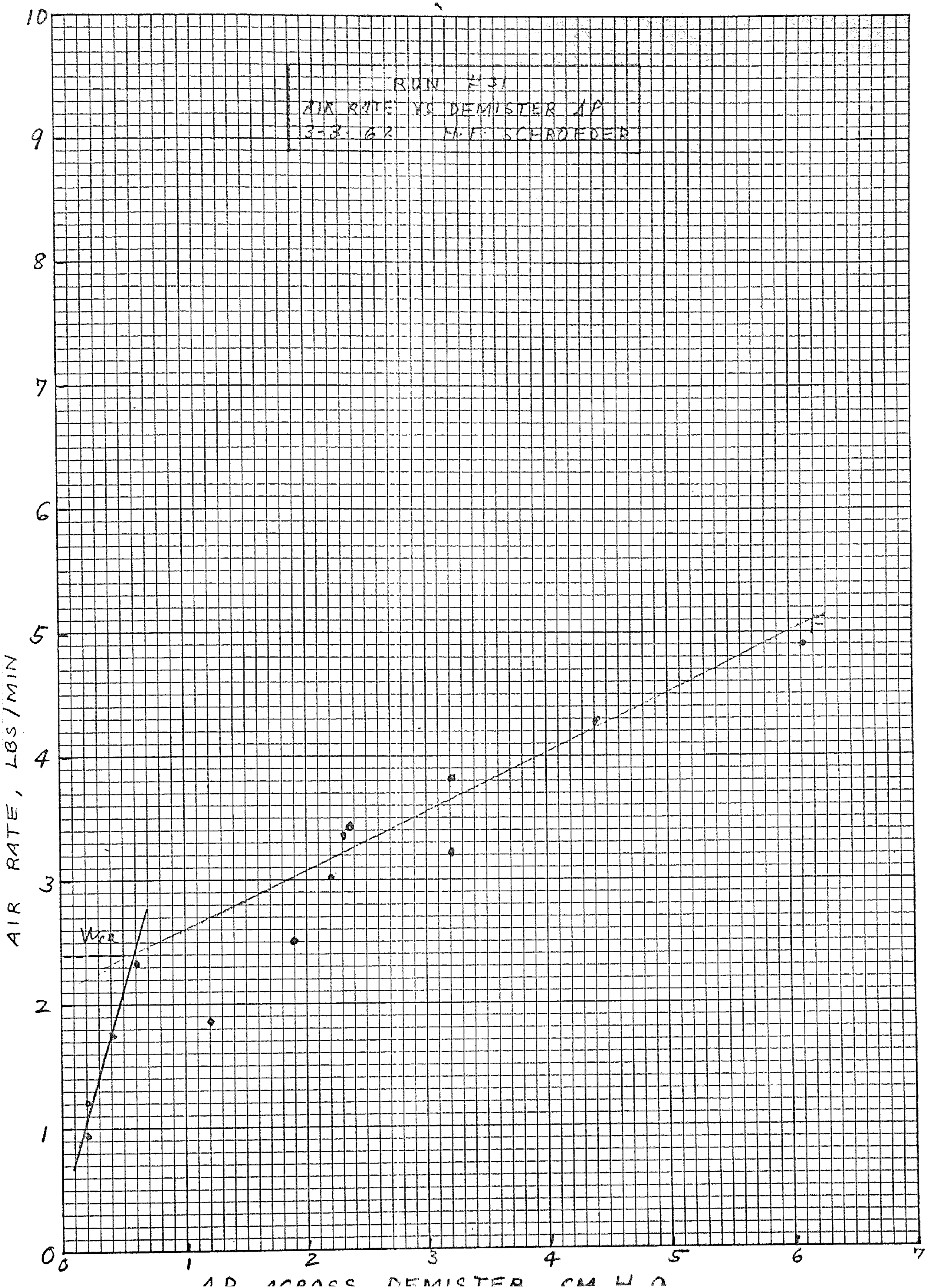

RUN #31
AIR RATE VS DEMISTER ΔP
3-3-62 H.F. SCHROEDER
AIR RATE, LBS/MIN
ΔP ACROSS DEMISTER, CM H_2O
W_{CR}
0
1
2
3
4
5
6
7
8
9
10

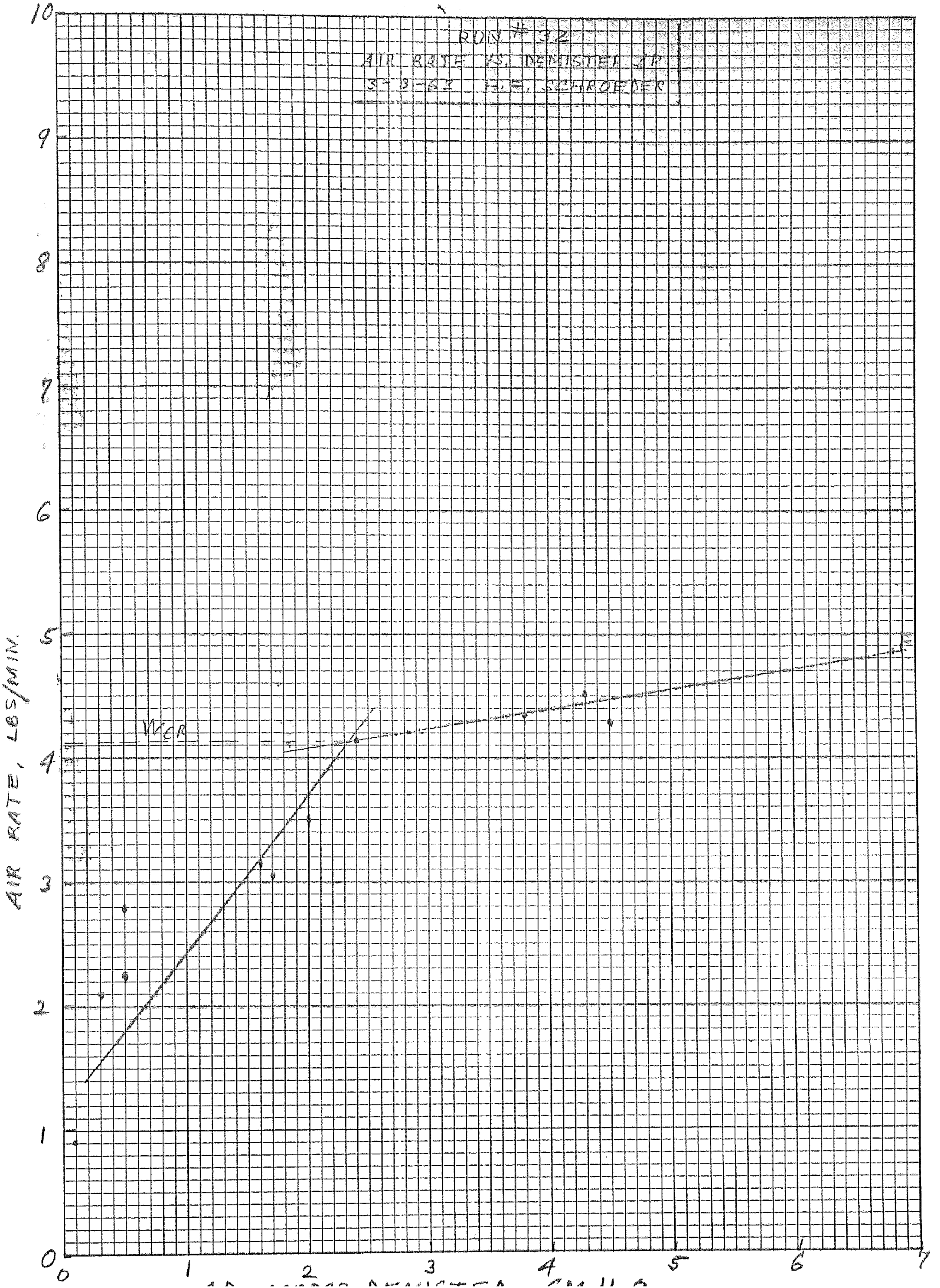
RUN # 32
AIR RATE VS. DEMISTER ΔP
3-3-62 H.E. SCHROEDER
AIR RATE, LBS/MIN.
WER
0
1
2
3
4
5
6
7
8
9
10
0
1
2
3
4
5
6
7

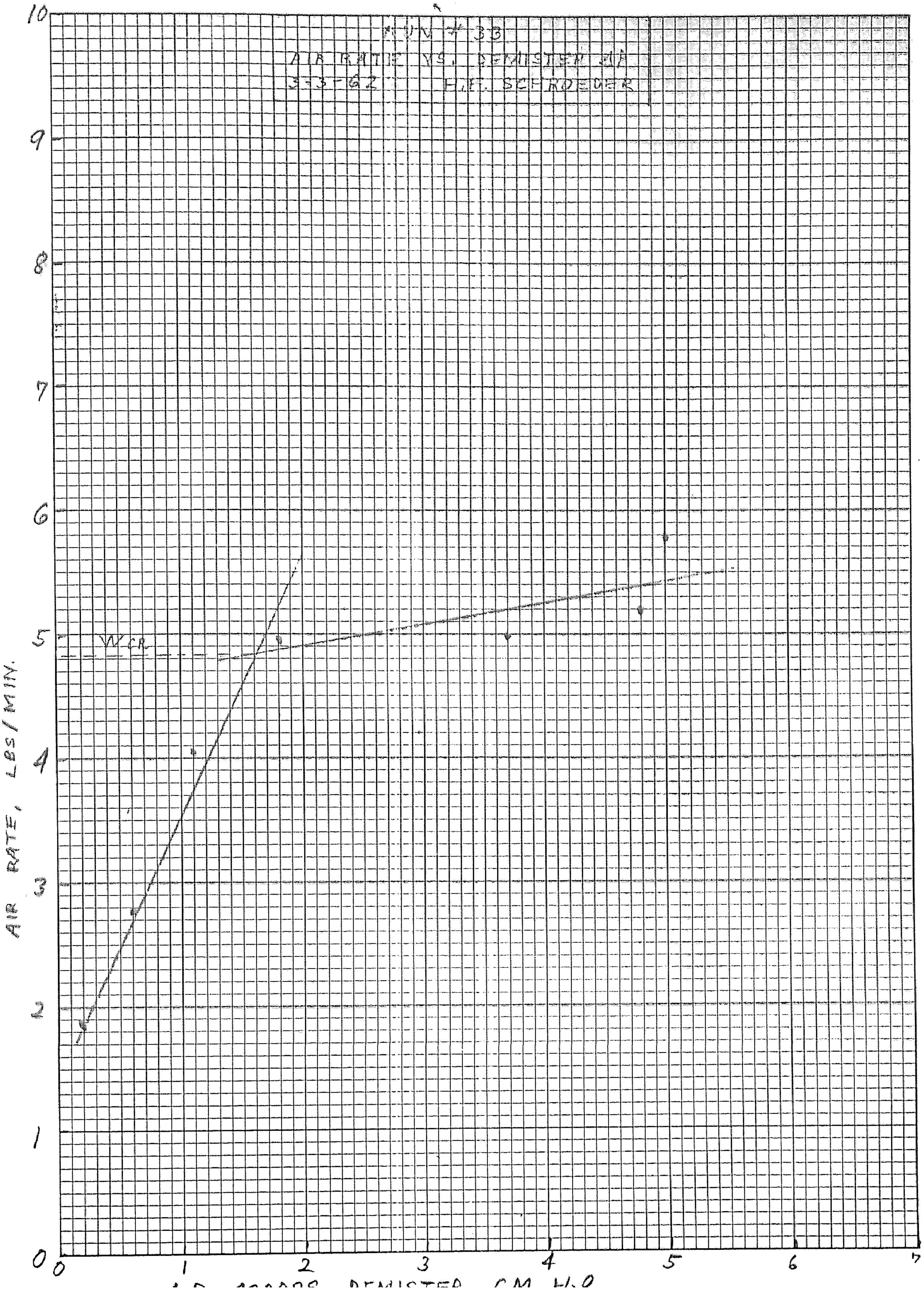
RUN # 33
AIR RATE VS. DEMISTER ΔP
3-3-62
SCHROEDER
AIR RATE, LBS/MIN.
W_{CR}
0
1
2
3
4
5
6
7
8
9
10
0
1
2
3
4
5
6
7

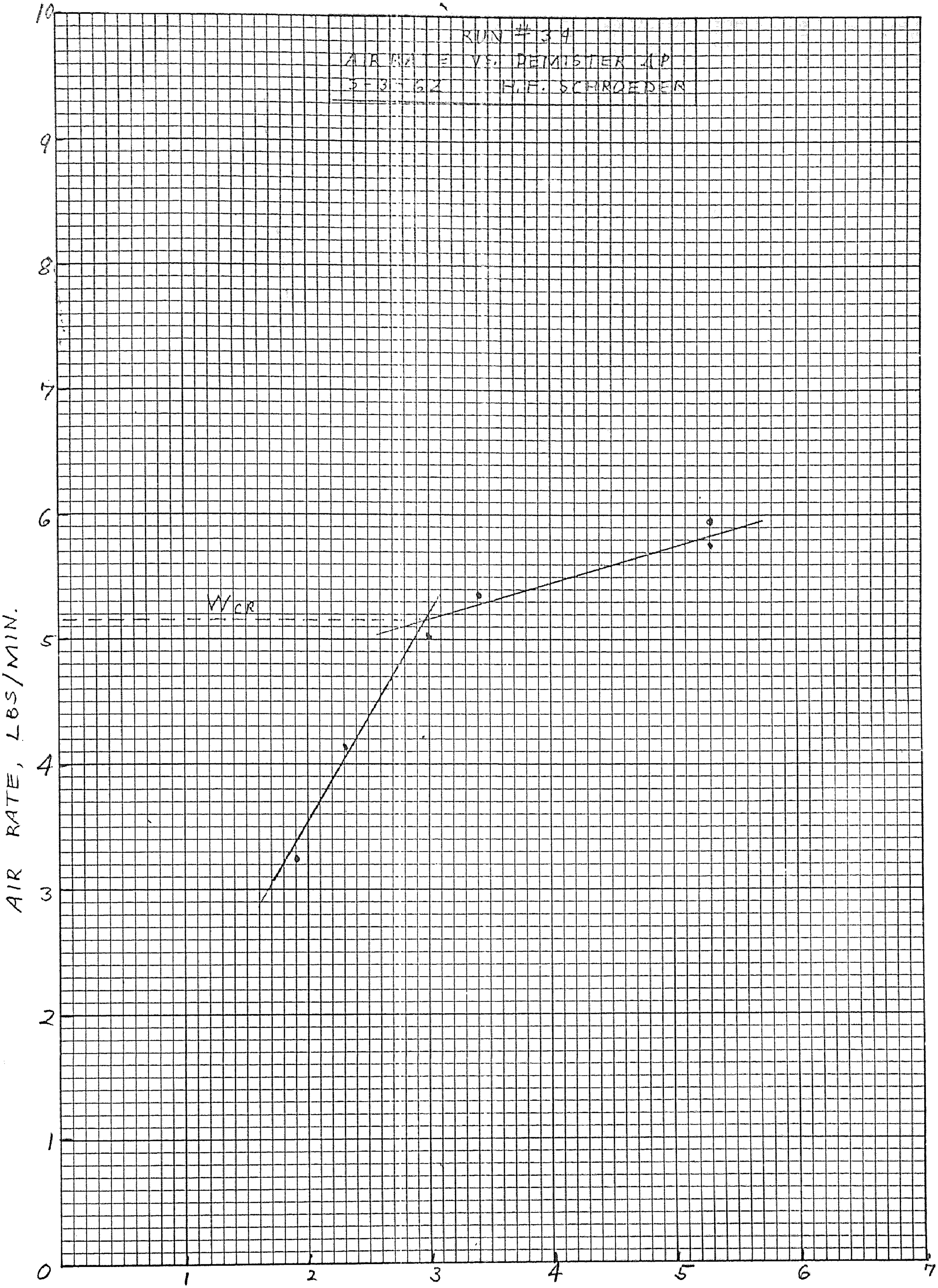
RUN # 34
AIR RATE VS. DEMISTER ΔP
5-31-62 H.F. SCHROEDER
AIR RATE, LBS/MIN.
W_{CR}
0
1
2
3
4
5
6
7
8
9
10
1
2
3
4
5
6
7

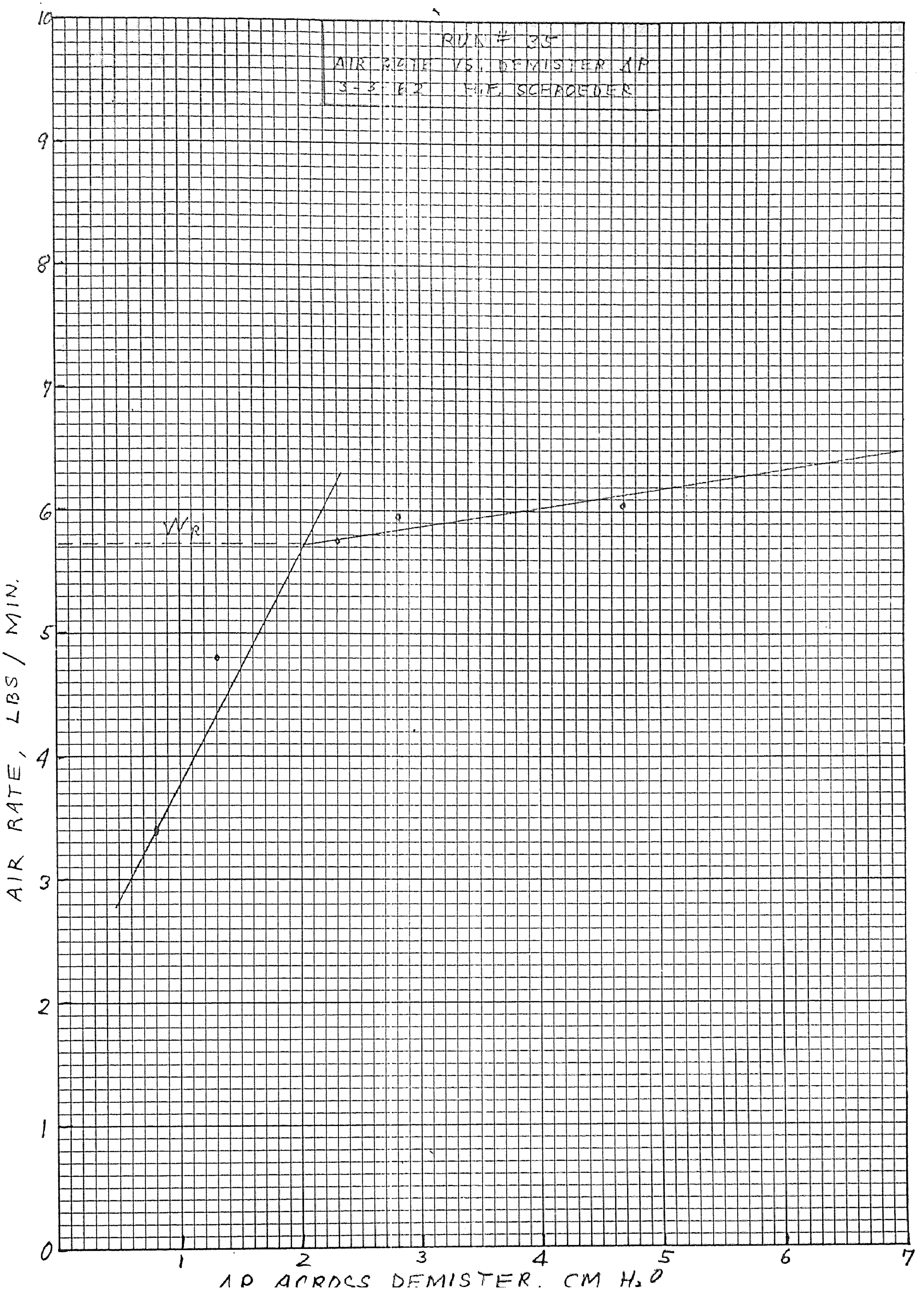
RUN # 35
AIR RATE VS. DEMISTER ΔP
3-3-62 H.E. SCHROEDER
AIR RATE, LBS / MIN.
ΔP ACROSS DEMISTER, CM H₂O
W_F
0
1
2
3
4
5
6
7
8
9
10
0
1
2
3
4
5
6
7

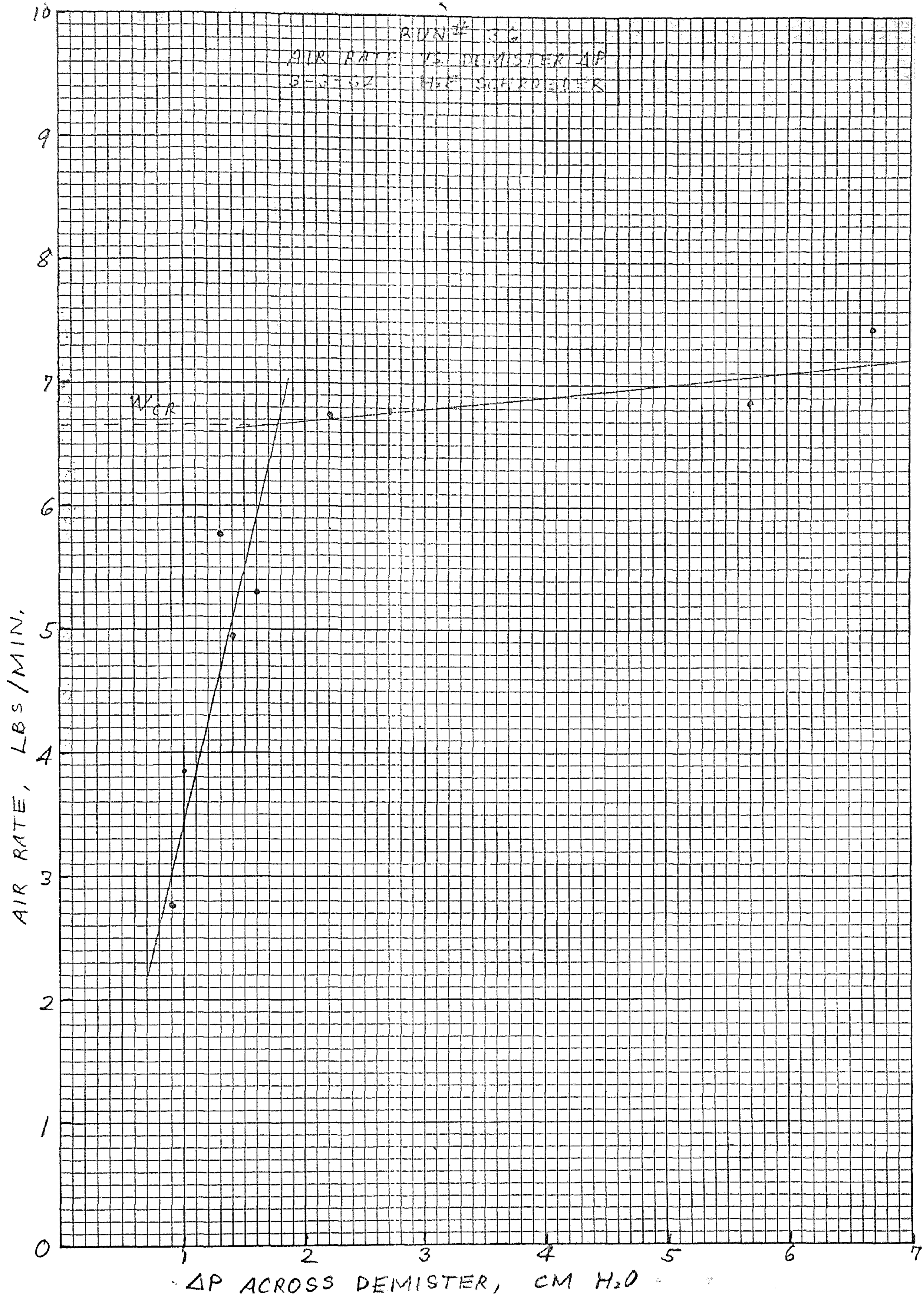
RUN # 36
AIR RATE VS. DEMISTER ΔP
W_{CR}
AIR RATE, LBS/MIN.
ΔP ACROSS DEMISTER, CM H_2O
0
1
2
3
4
5
6
7
8
9
10

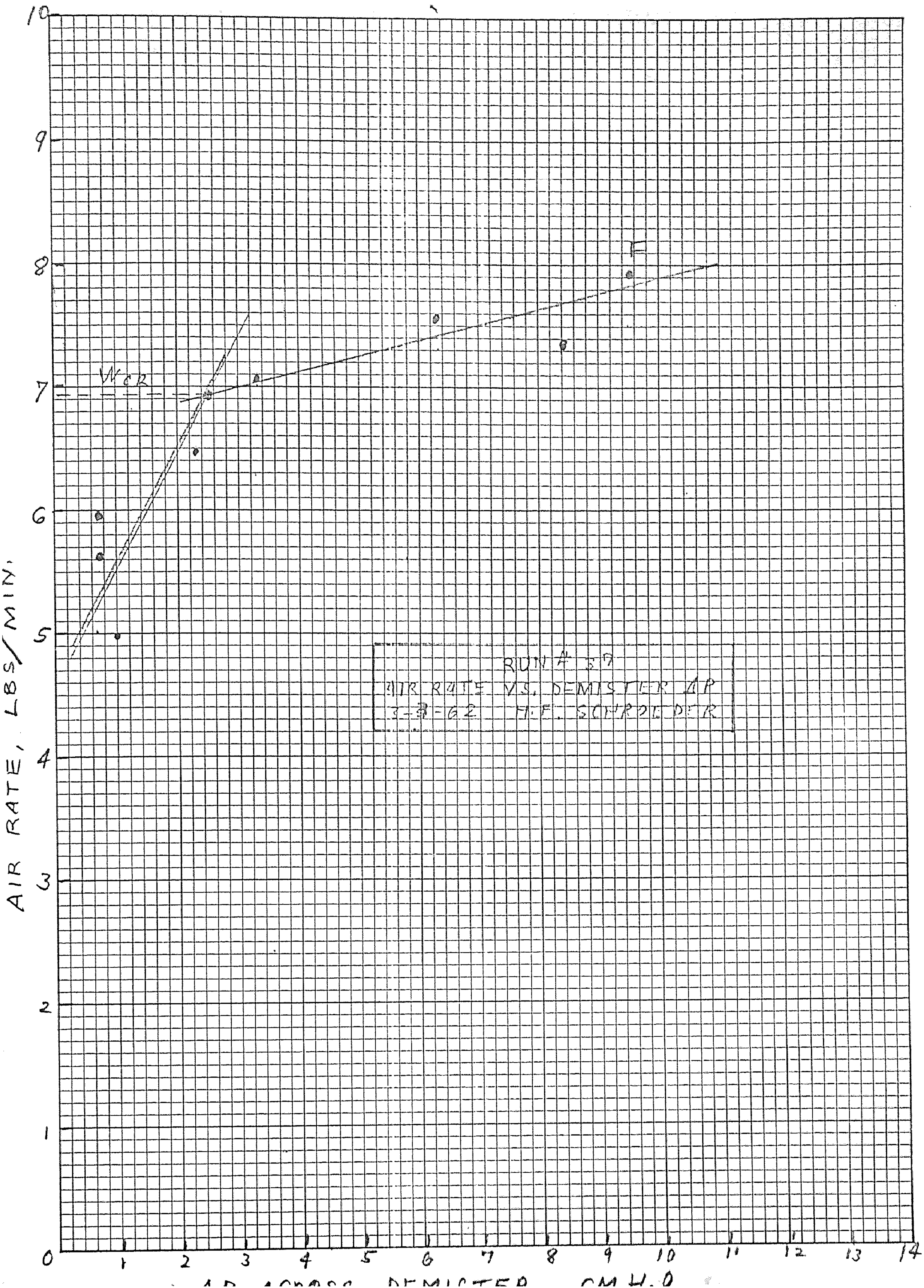
RUN # 57
AIR RATE VS. DEMISTER ΔP
3-8-62 H.F. SCHROEDER
AIR RATE, LBS/MIN.
W_CR
F
0
1
2
3
4
5
6
7
8
9
10
11
12
13
14

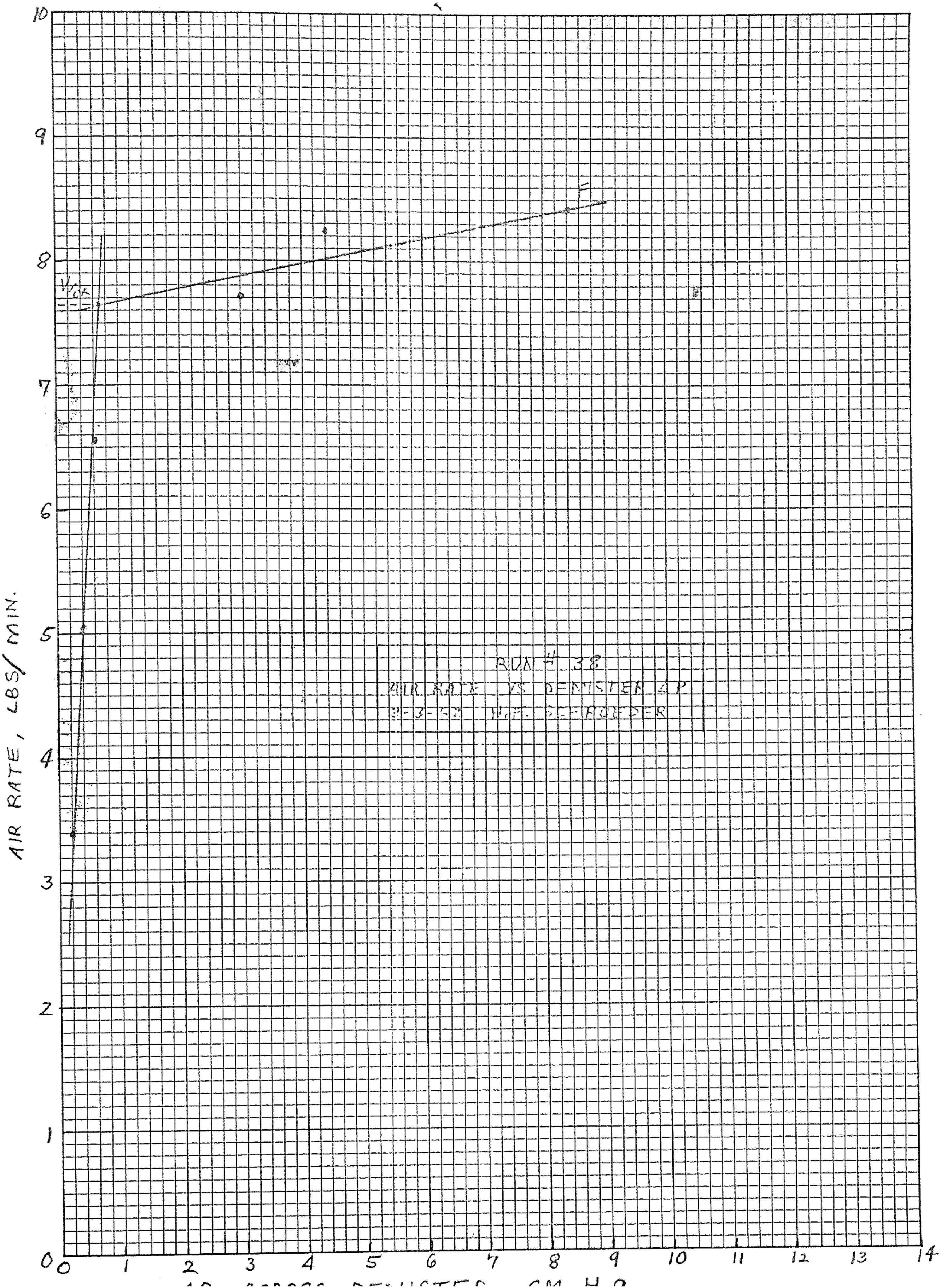
RUN # 38
AIR RATE VS DEMISTER ΔP
AIR RATE, LBS/ MIN.
0
1
2
3
4
5
6
7
8
9
10
0
1
2
3
4
5
6
7
8
9
10
11
12
13
14

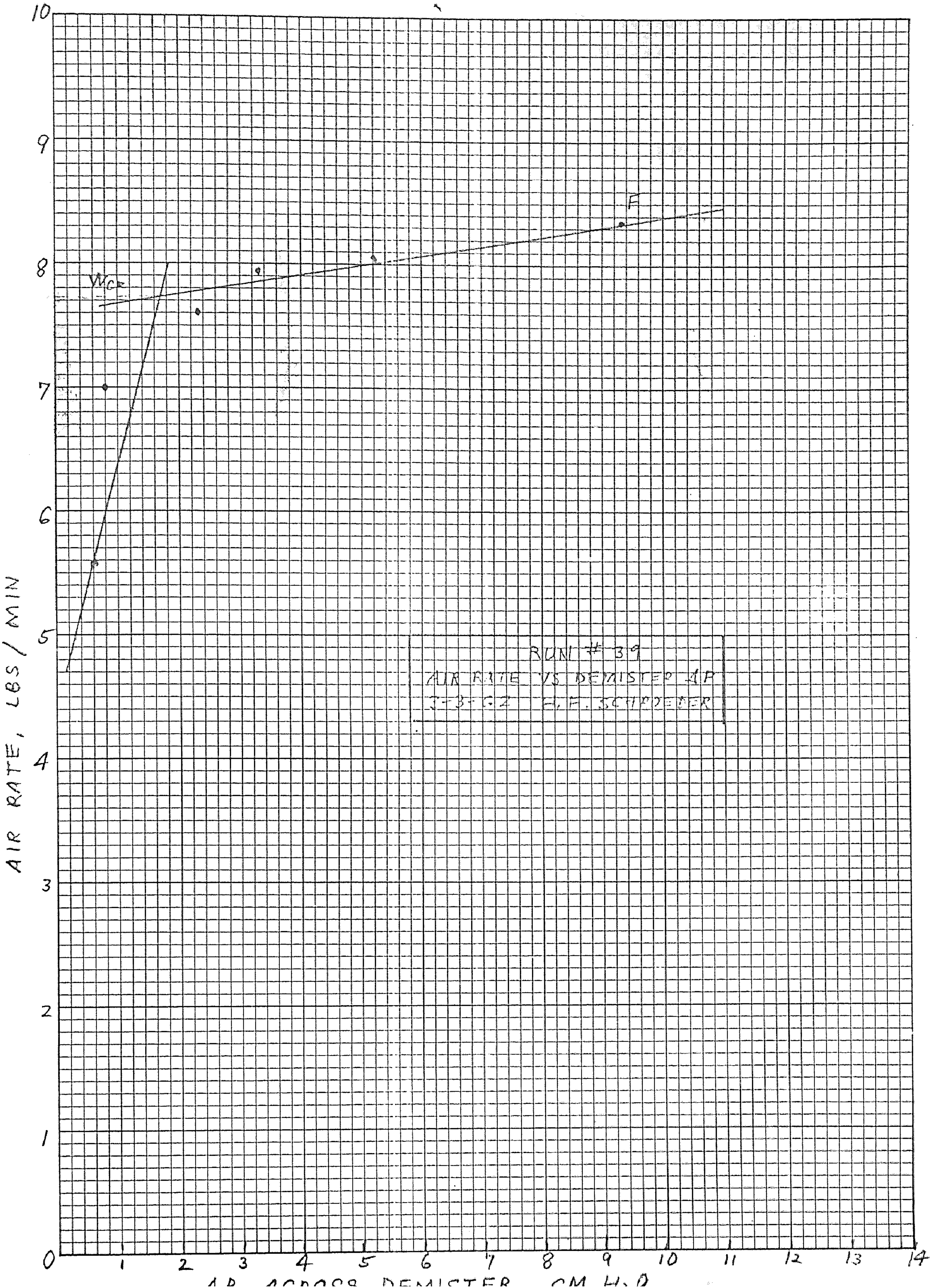
RUN # 39
AIR RATE VS DEMISTER ΔP
3-3-62 H.F. SCHROEDER
AIR RATE, LBS / MIN
ΔP ACROSS DEMISTER CM H2O
WCF
F
0
1
2
3
4
5
6
7
8
9
10
11
12
13
14

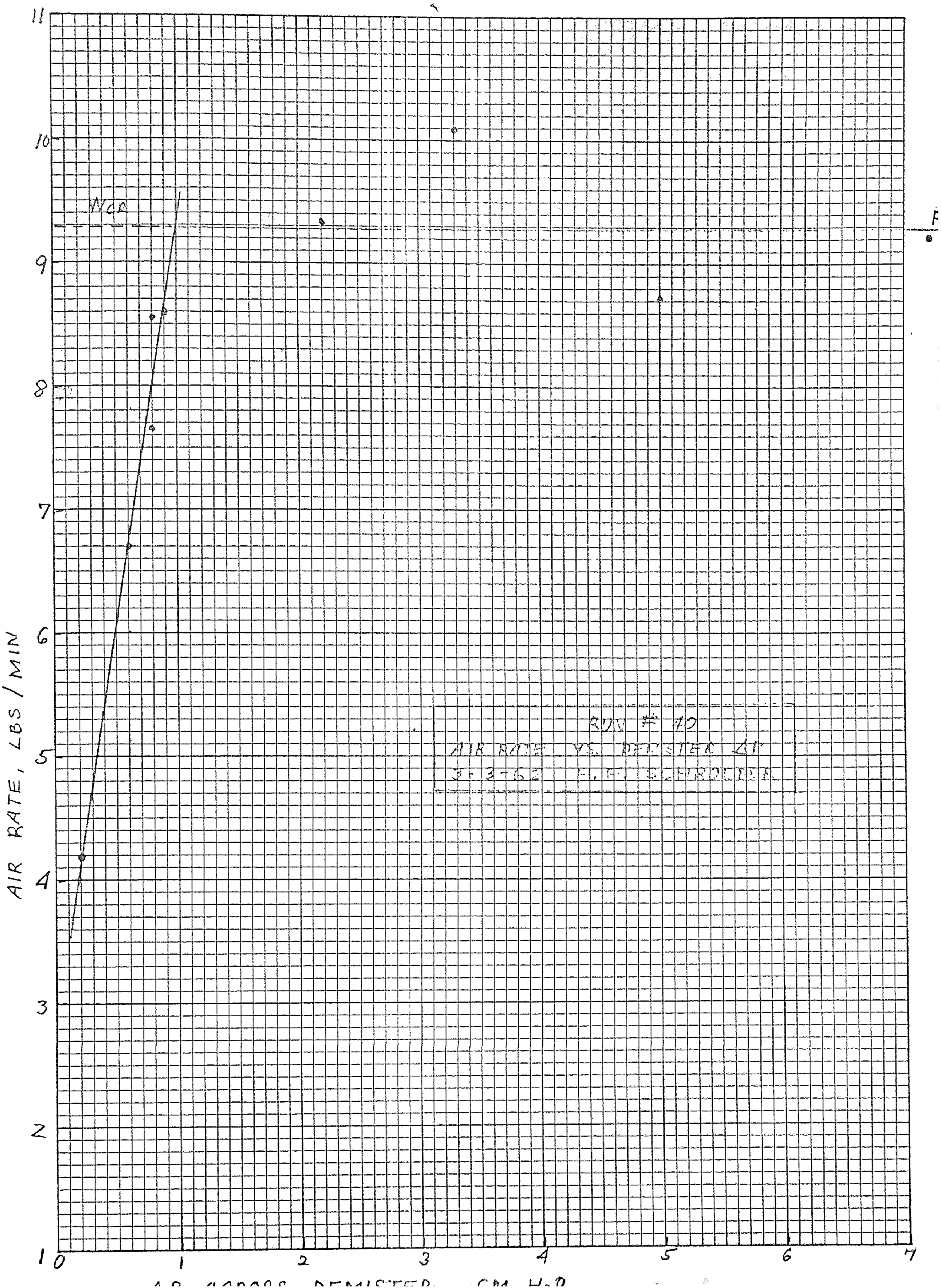

RUN # 40
AIR RATE VS. DEMISTER ΔP
3-3-62
AIR RATE, LBS / MIN
Wcr
F
ΔP ACROSS DEMISTER, CM H2O

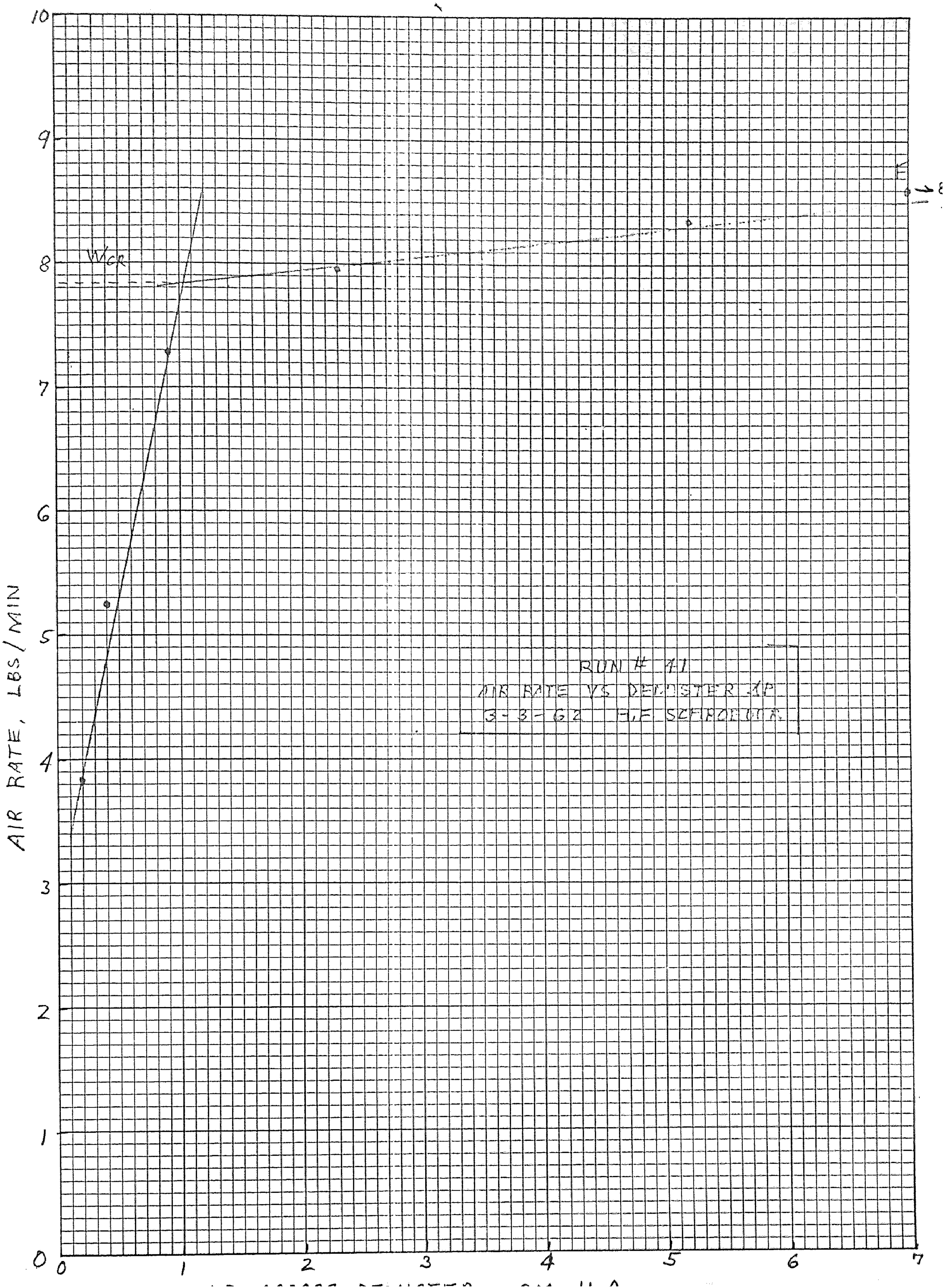

RUN # 41
AIR RATE VS DEMISTER ΔP
3-3-62
AIR RATE, LBS/MIN
W_{CR}
0
1
2
3
4
5
6
7
8
9
10

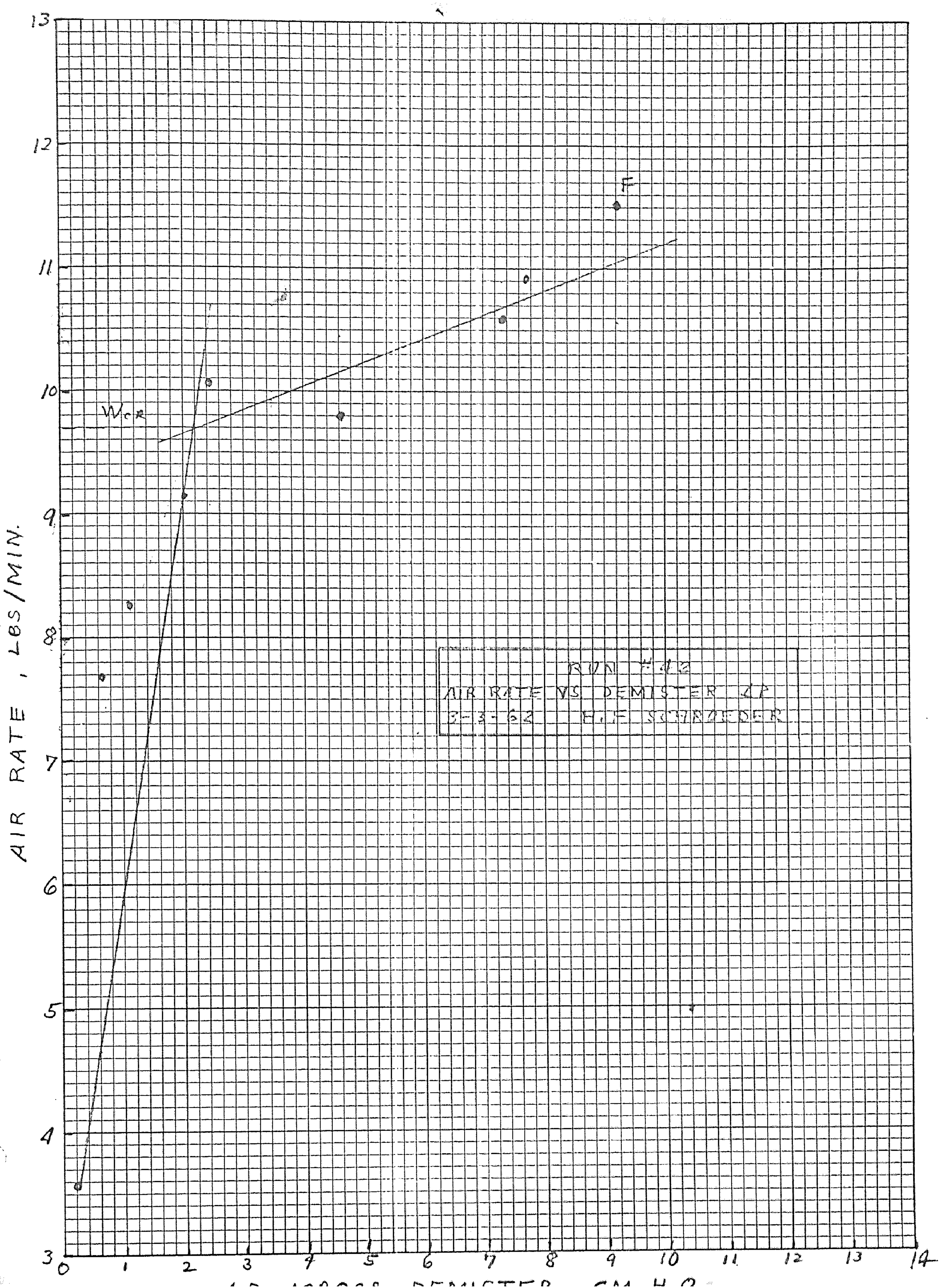

AIR RATE, LBS/MIN.
F
WCR
RUN #42
AIR RATE VS DEMISTER ΔP
3-3-62 H.F. SCHROEDER

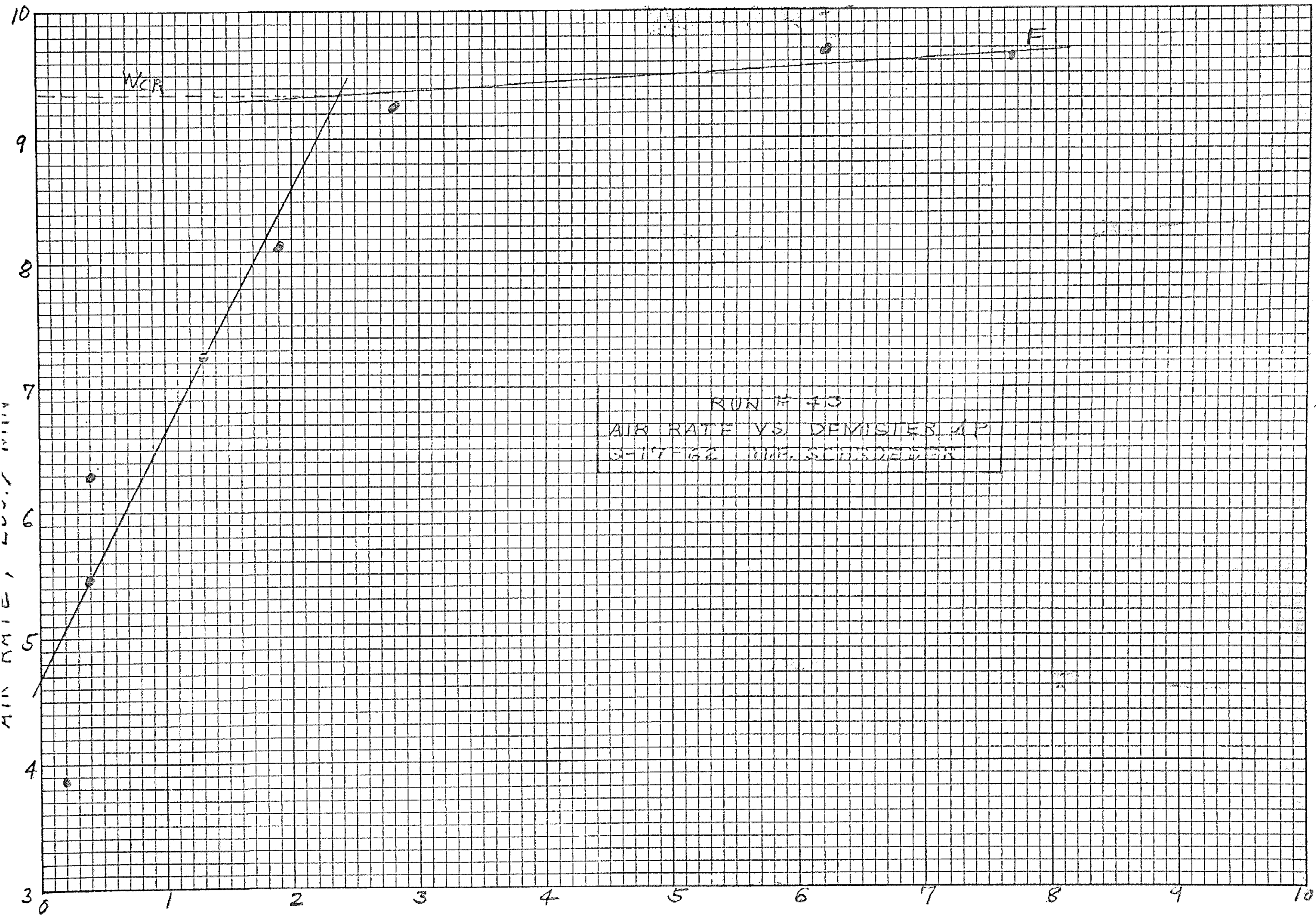
RUN # 43
AIR RATE VS DEMISTER ΔP
W CR
F
10
9
8
7
6
5
4
3
0
1
2
3
4
5
6
7
8
9
10

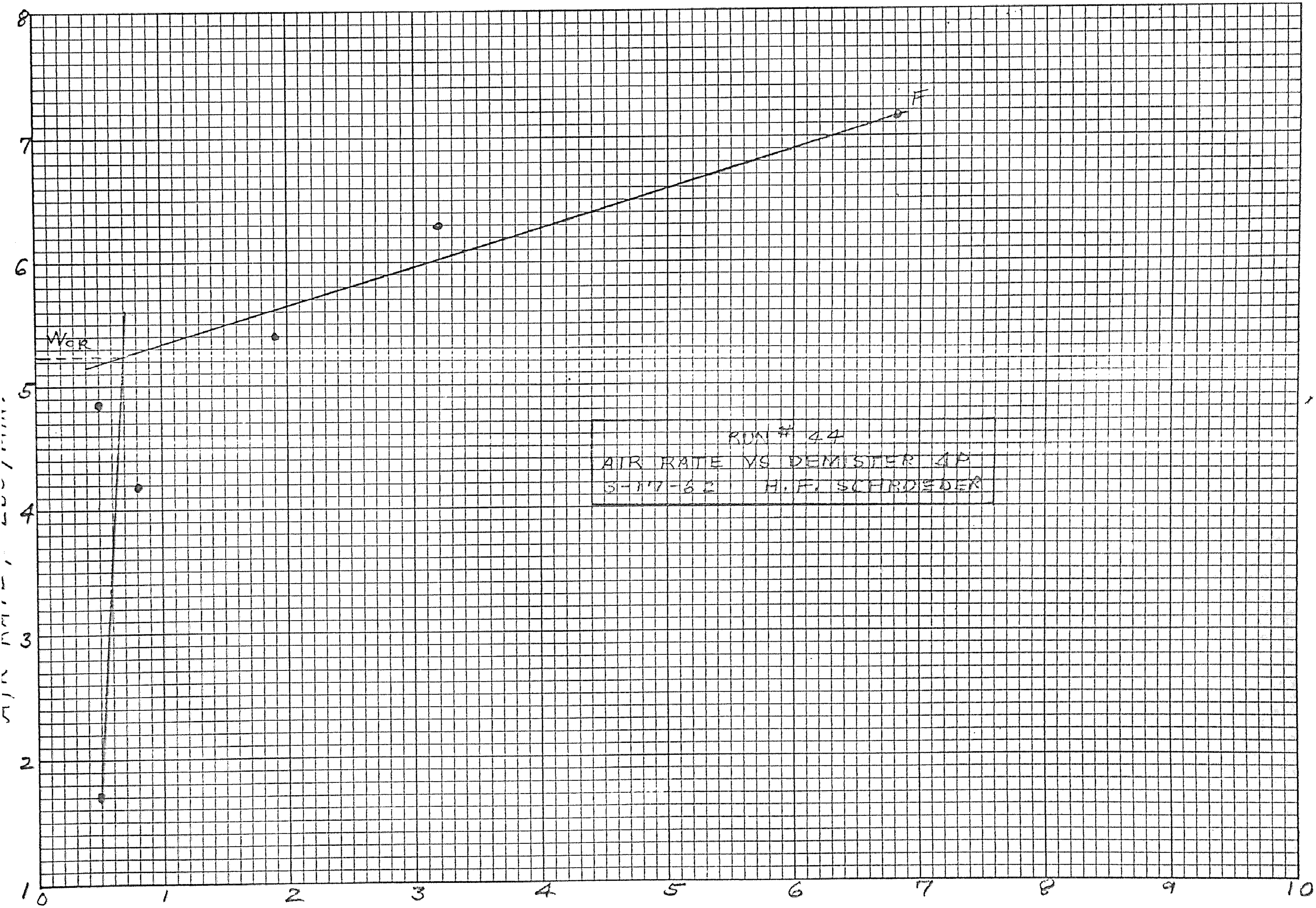
RUN # 44
AIR RATE VS DEMISTER ΔP
5-17-62 H. F. SCHROEDER
F
W CR
8
7
6
5
4
3
2
1
0
1
2
3
4
5
6
7
8
9
10

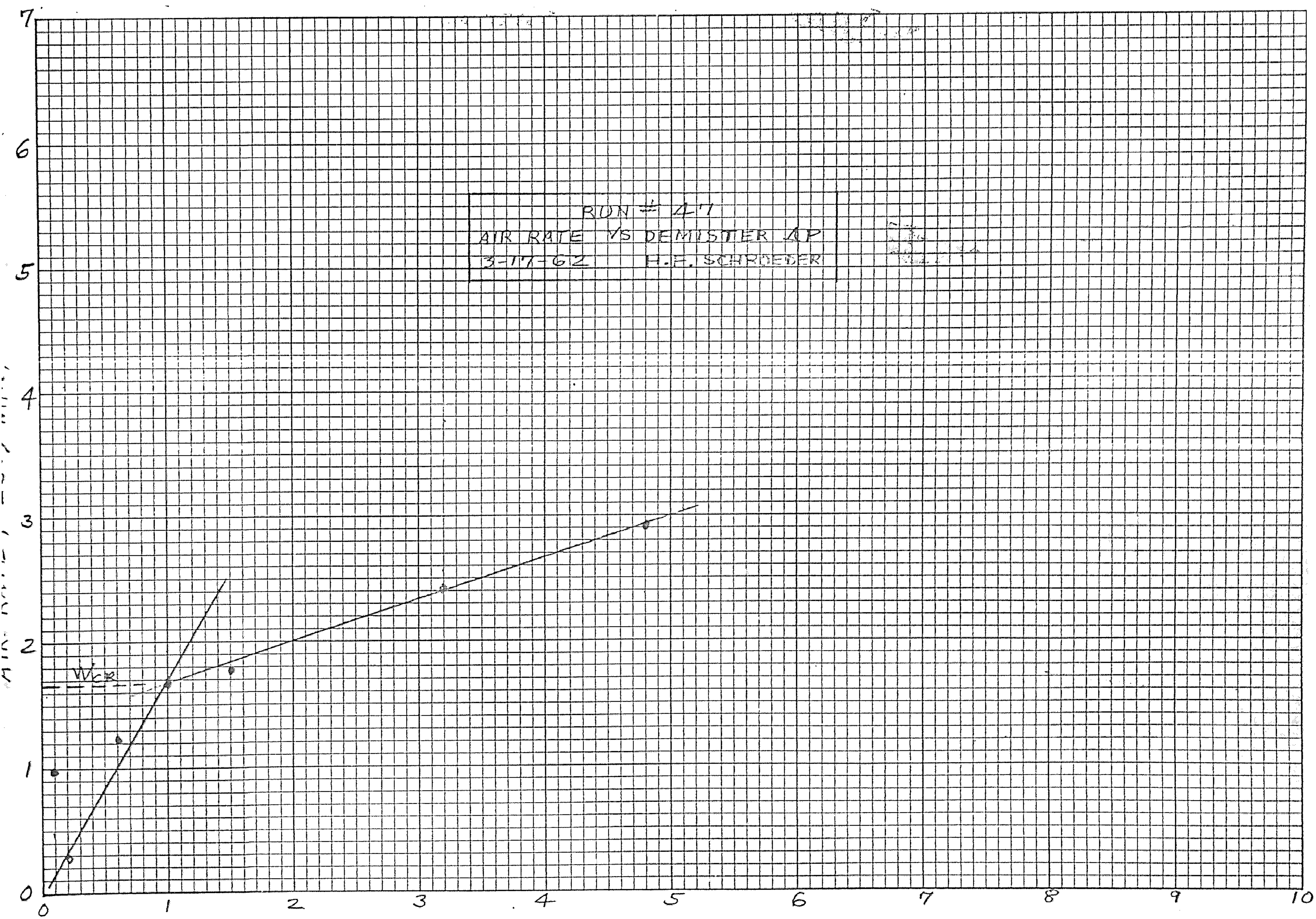
RUN # 47
AIR RATE VS DEMISTER ΔP
3-17-62 H.F. SCHROEDER
W_CR
0
1
2
3
4
5
6
7
8
9
10
0
1
2
3
4
5
6
7

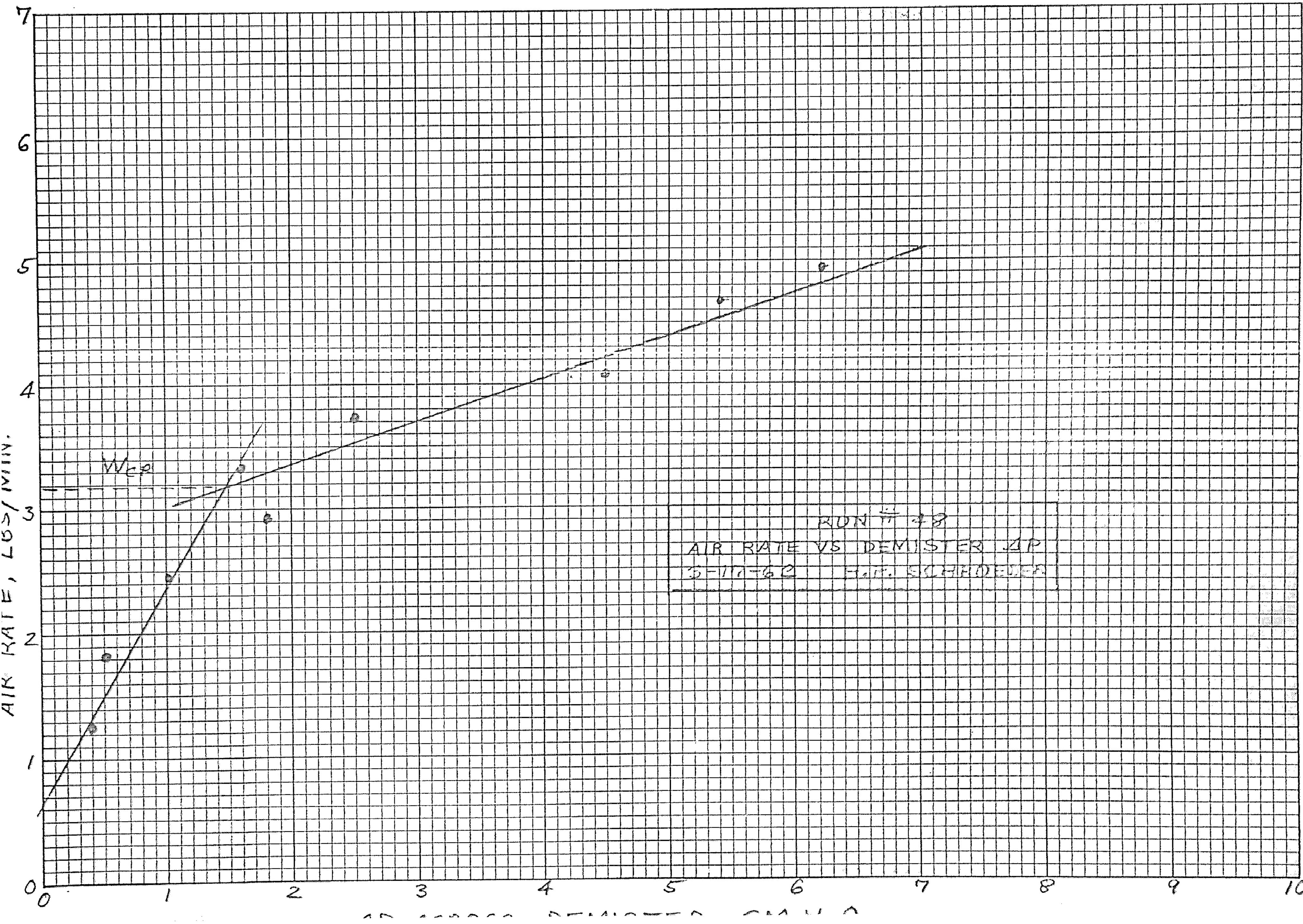
RUN # 48
AIR RATE VS DEMISTER ΔP
5-10-62
SCHROEDER
AIR RATE, LBS/MIN.
WCP
0
1
2
3
4
5
6
7
8
9
10

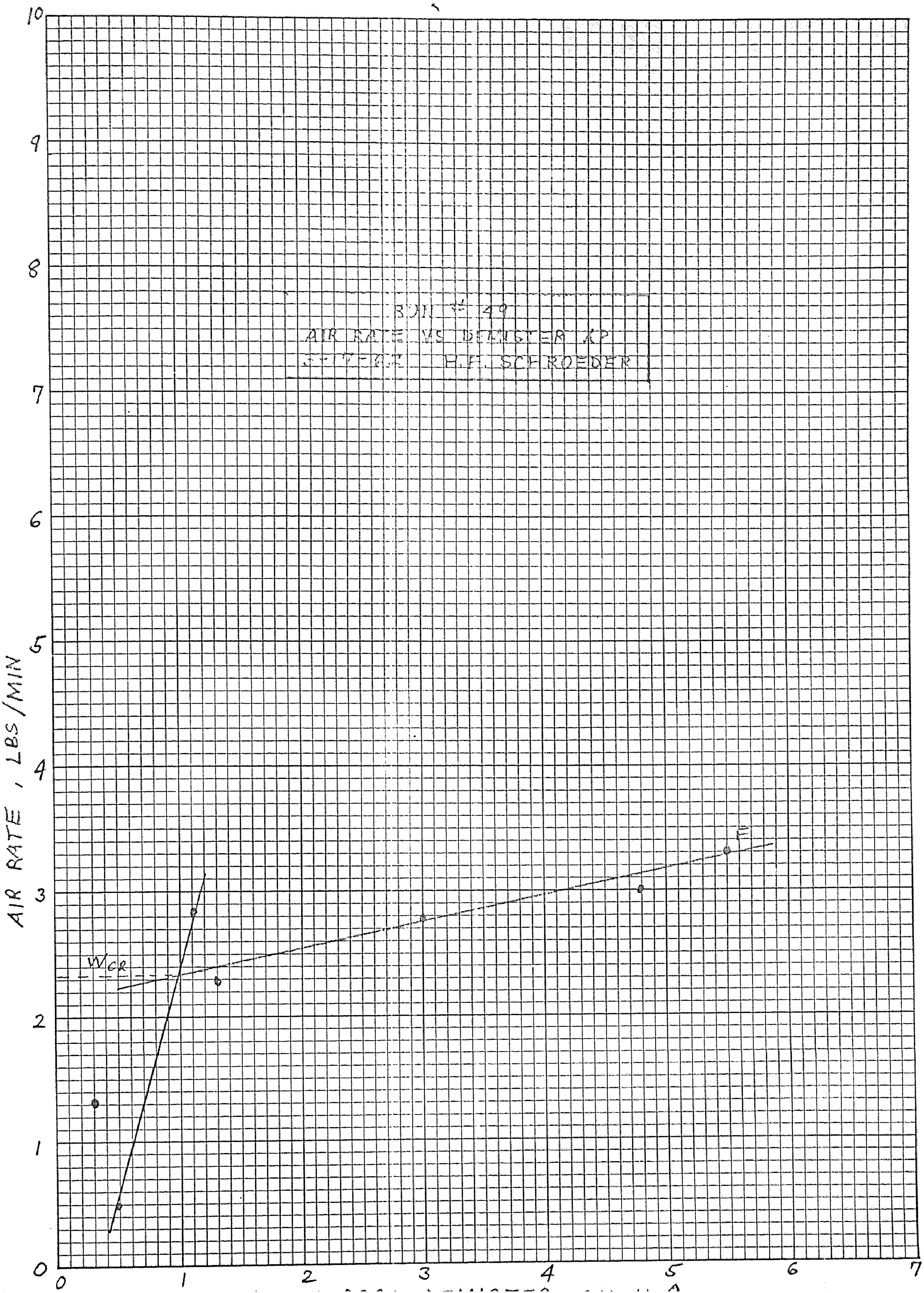
RUN # 49
AIR RATE VS DEMISTER ΔP
H.H. SCHROEDER
AIR RATE, LBS/MIN
W_CR
F
0
1
2
3
4
5
6
7
8
9
10

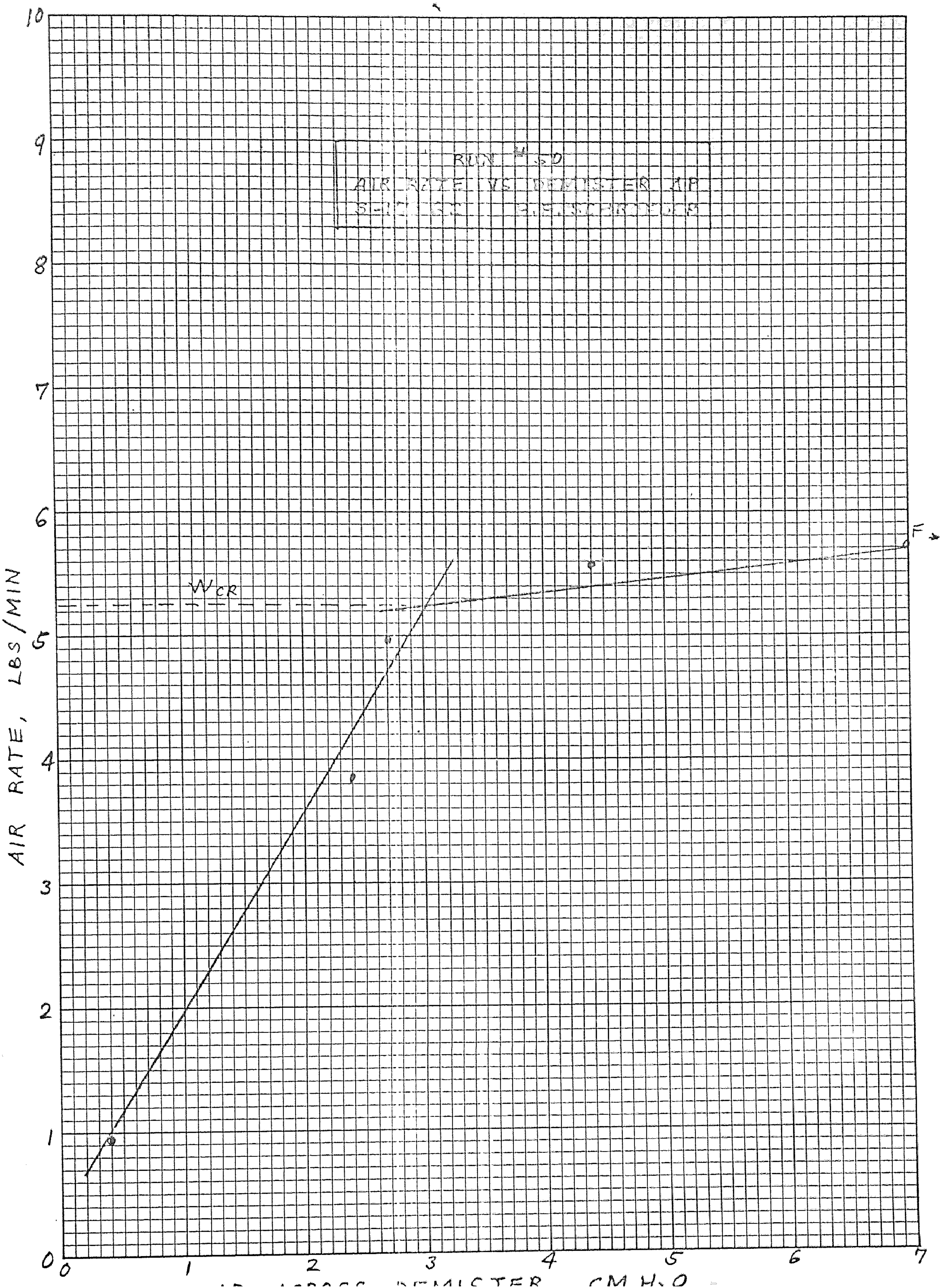
RUN # 5D
AIR RATE VS DEMISTER ΔP
AIR RATE, LBS/MIN
W_{CR}
F
0
1
2
3
4
5
6
7
8
9
10
ΔP ACROSS DEMISTER, CM H_2O

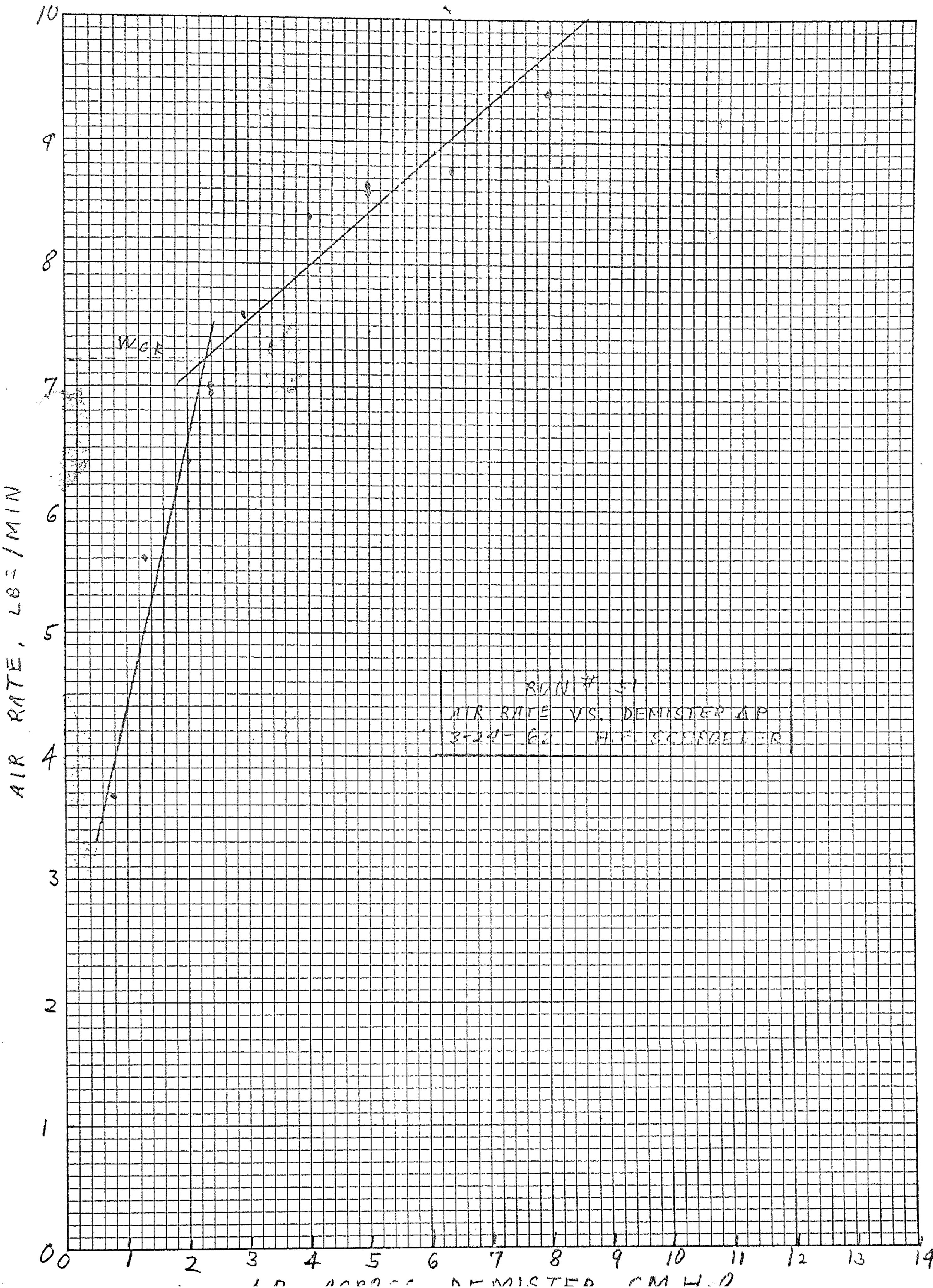
RUN # 51
AIR RATE VS. DEMISTER ΔP
AIR RATE, LBS/MIN
WCR
0 1 2 3 4 5 6 7 8 9 10 11 12 13 14
0 1 2 3 4 5 6 7 8 9 10
DEMISTER

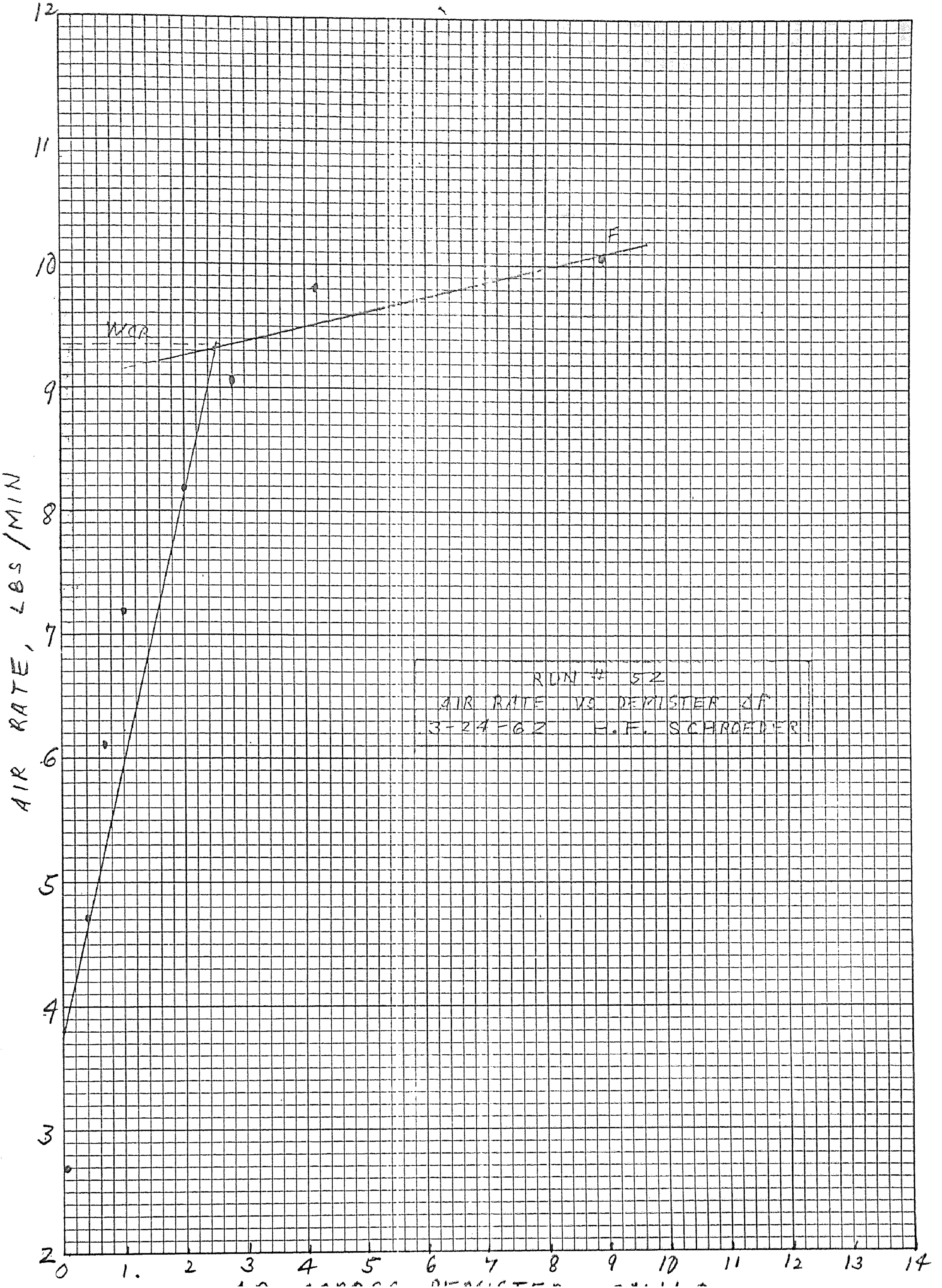
RUN # 52
AIR RATE VS DEMISTER ΔP
3-24-62 H.F. SCHROEDER
AIR RATE, LBS/MIN
WOP
F
12
11
10
9
8
7
6
5
4
3
2
0
1.
2
3
4
5
6
7
8
9
10
11
12
13
14

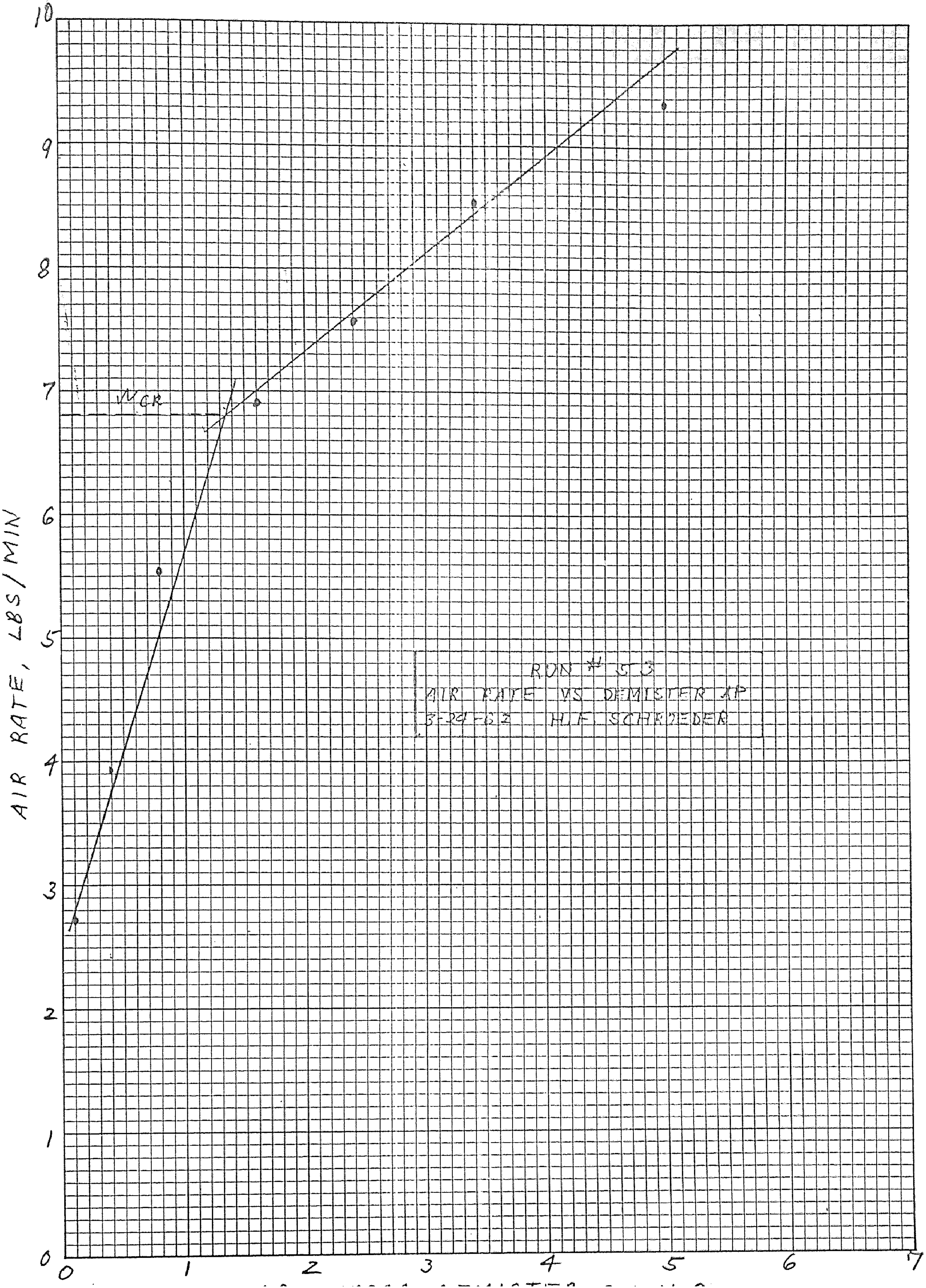
AIR RATE, LBS / MIN
0
1
2
3
4
5
6
7
8
9
10
W CR
0
1
2
3
4
5
6
7
RUN # 53
AIR RATE VS DEMISTER ΔP
3-24-62 H.F. SCHROEDER

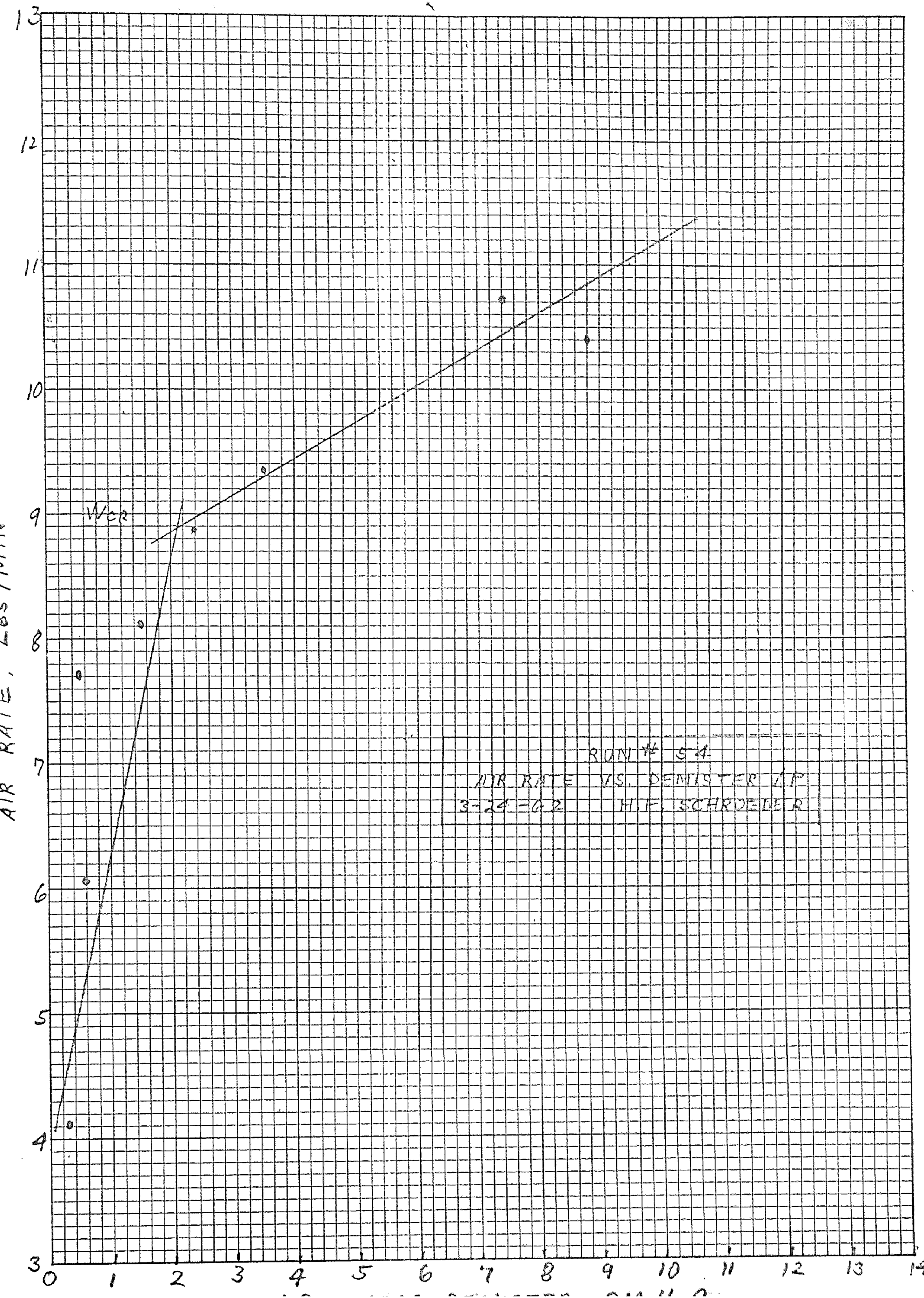
13
12
11
10
9
8
7
6
5
4
3
AIR RATE, LBS/MIN
W_{CR}
RUN # 54
AIR RATE VS. DEMISTER ΔP
3-24-62 H.F. SCHROEDER
0
1
2
3
4
5
6
7
8
9
10
11
12
13
14

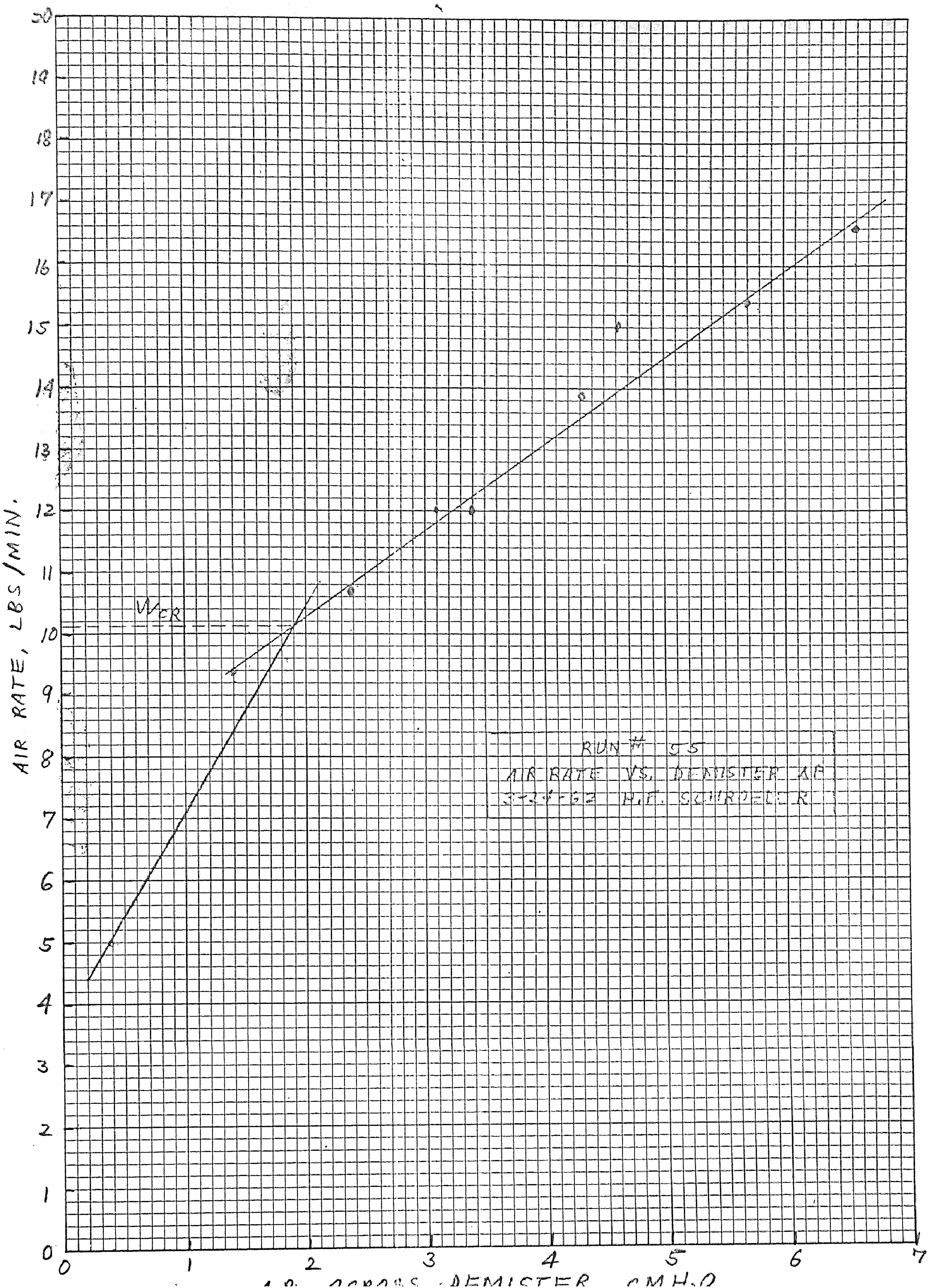
AIR RATE, LBS/MIN.
W_{CR}
RUN # 55
AIR RATE VS. DEMISTER ΔP
3-24-62 H.E. SCHROEDER
0
1
2
3
4
5
6
7
8
9
10
11
12
13
14
15
16
17
18
19
20

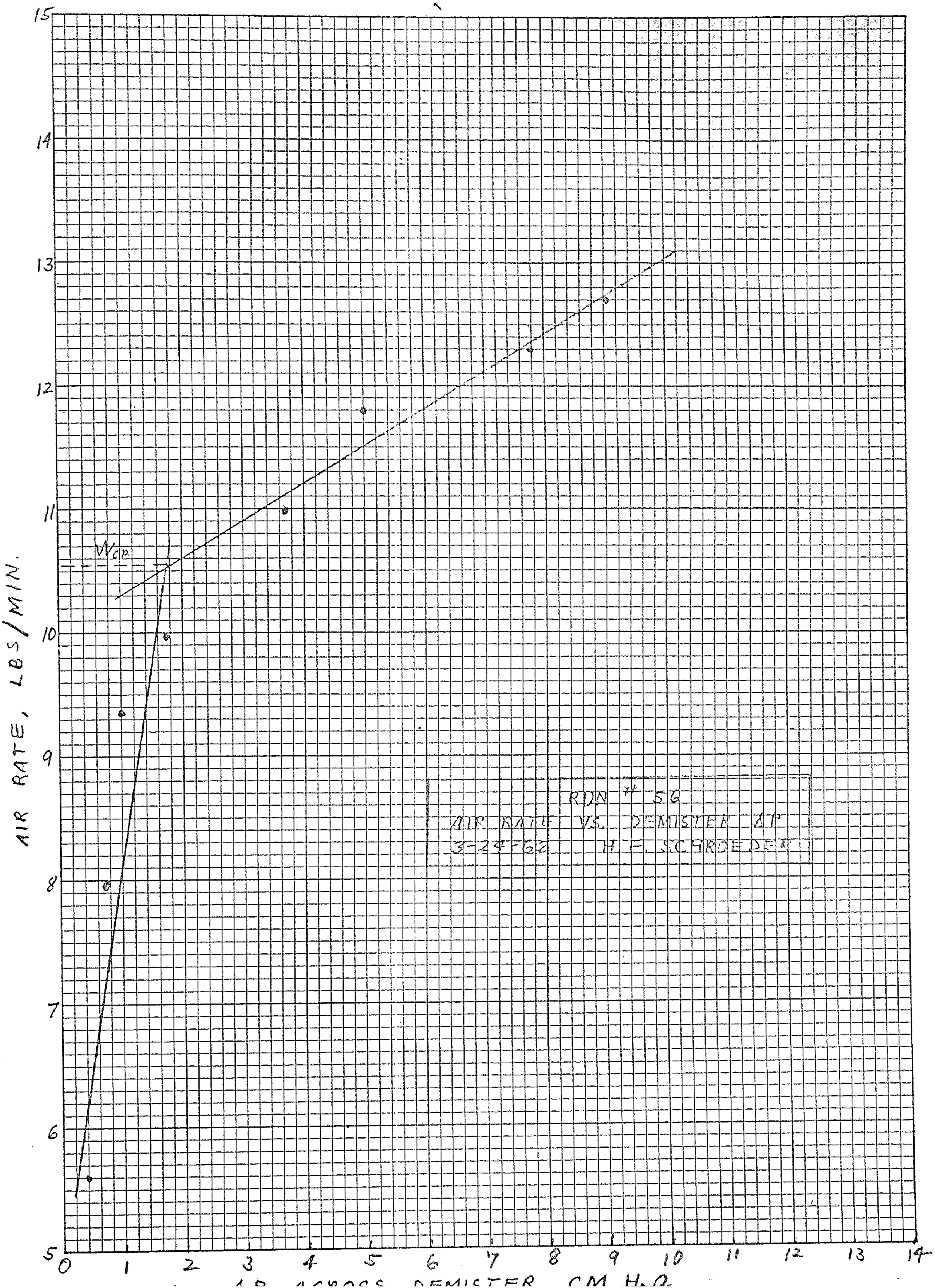
RUN # 56
AIR RATE VS. DEMISTER ΔP
3-29-62 H. E. SCHROEDER
AIR RATE, LBS/MIN.
W_cp
15
14
13
12
11
10
9
8
7
6
5
0
1
2
3
4
5
6
7
8
9
10
11
12
13
14

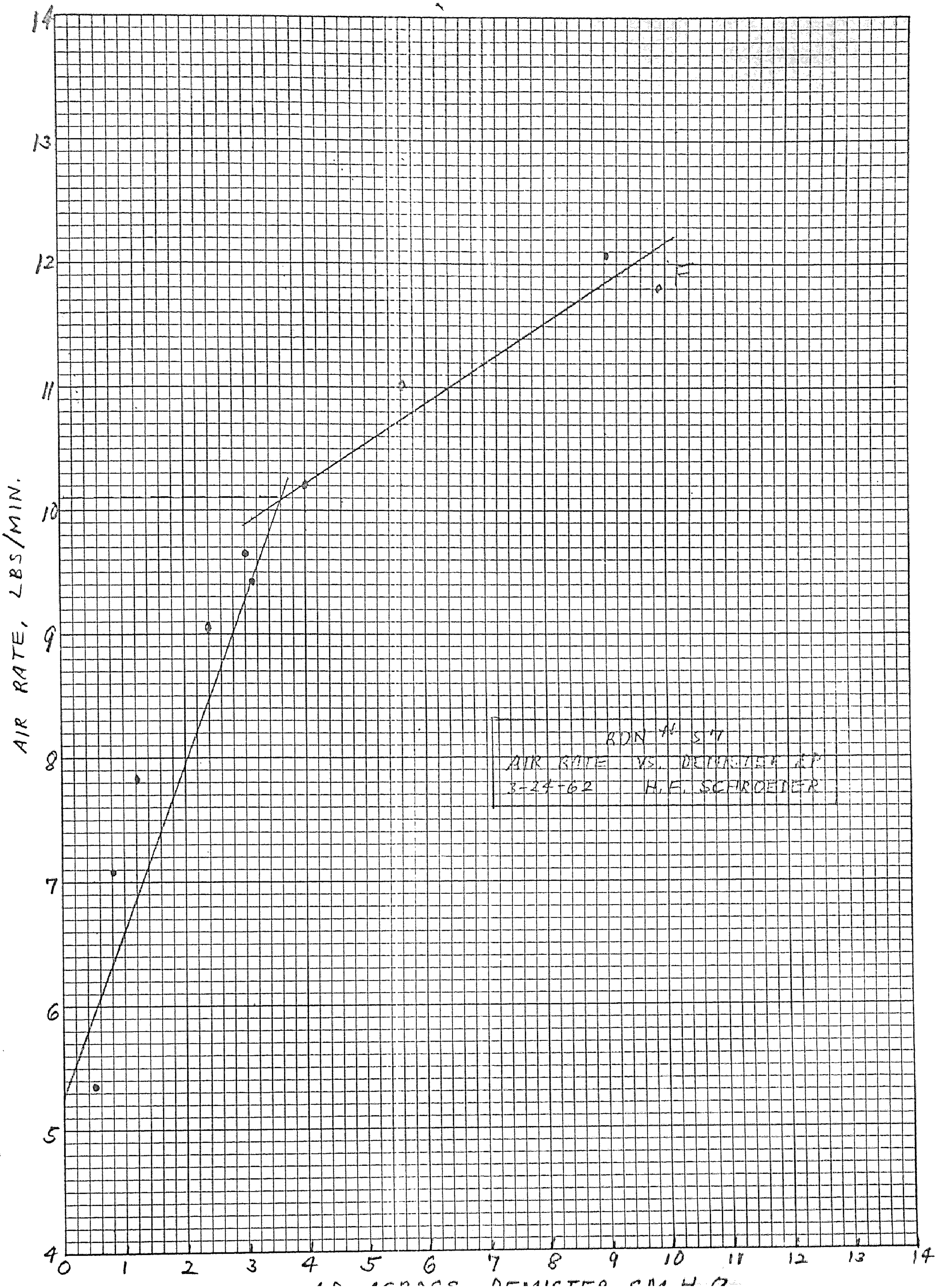
AIR RATE, LBS/MIN.
14
13
12
11
10
9
8
7
6
5
4
0
1
2
3
4
5
6
7
8
9
10
11
12
13
14
RUN # 57
AIR RATE VS. DEMISTER ΔP
3-24-62 H. F. SCHROEDER

REFERENCES

1. Wicks, M. and Dukler, A. E., Entrainment and Pressure Drop in Concurrent Gas-Liquid Flow: Air-Water in Horizontal Flow, A. I. Ch. E. Journal, Vol. 6, No. 3, Sept. 1960.

2. Anderson, G. H. and Mantzouranis, B. G., Two-Phase (Gas/Liquid) Flow Phenomena-II Liquid Entrainment, Chemical Engineering Science, Vol. XII, No. 4, July 1960.

3. Alves, G. E., Concurrent Liquid-Gas Flow in a Pipe-Line Contractor, Chemical Engineering Progress, Vol. 50, No. 9, Sept. 1954.

4. Krasjakova, L. U., Journal of Technical Physics, Vol. 22, No. 4, 1952 (U.S.S.R.).

5. Budd, J. T., Measurement of Entrainment in Two-Phase Annular Flow of Air and Water in a One Inch Horizontal Copper Tube, M. S. Ch. E. Thesis, Univ. of Deleware, 1950.

6. Fritzlen, A. F., M. S. Ch. E. Thesis, Univ. of Deleware, 1951.

7. Lane, W. R., Industrial Engineering Chemistry, Vol. 43, 1951.

8. Hughes, R. R., Evans, H. D., and Sternling, C. V., Chemical Engineering Progress, Vol. 49, 1953.

9. Souders, M., and Brown, G. G., Design of Fractionating Columns-I Entrainment and Capacity, Industrial and Engineering Chemistry, Vol. 26, No. 1, Jan. 1934.

10. Carpenter, C. L., and Othmer, D. F., Entrainment Removal by a Wire-Mesh Separator, A. I. Ch. E. Journal, Vol. I, No. 4, Dec. 1955.

11. Pollak, A. and Work, L. T., The Separation of Liquid from Vapor, Using Cyclones, Transactions of the A. S. M. E.

12. York, O. H., Chemical Engineering Progress, Vol. 50, 1954.

13. Poppele, E., M. S. Ch. E. Thesis, Newark College of Engineering, 1958.

14. Reid, M. S. Ch. E. Thesis, Newark College Of Engineering, 1960.

15. Dappert, G. F., M. Ch. E. Thesis, Polytechnic Institute of Brooklyn, 1950.

16. Marshall, W. R., Atomization and Spray Drying, Chemical Engineering Progress Monograph Series, No. 2, Vol. 50, A. I. Ch. E. 1954, N. Y.

17. Blams, J. W., High Rotational Speeds, Journal of Applied Physics, Vol. 8, Dec. 1937.

18. Parker, J. D., and Grosh, R. J., Heat Transfer to a Mist Flow, ANL-6291, Tech. Rep. No. 5, Jan. 1961.